DOI: 10.1002/cmdc.201300316

De Novo Design, Synthesis and Evaluation of Benzylpiperazine Derivatives as Highly Selective Binders of Mcl-1

Xiao Ding,[a] Yan Li,[b] Li Lv,[a] Mi Zhou,[b] Li Han,[b] Zhengxi Zhang,[b] Qian Ba,[c] Jingquan Li,[c] Hui Wang,[c] Hong Liu,*[a] and Renxiao Wang*[b]

Considerable efforts have been made to the development of small-molecule inhibitors of antiapoptotic B-cell lymphoma 2 (Bcl-2) family proteins (such as Bcl-2, Bcl-x_L, and Mcl-1) as a new class of anticancer therapies. Unlike general inhibitors of the entire family, selective inhibitors of each member protein can hopefully reduce the adverse side effects in chemotherapy treatments of cancers overexpressing different Bcl-2 family proteins. In this study, we designed four series of benzylpiperazine derivatives as plausible Bcl-2 inhibitors based on the outcomes of a computational algorithm. A total of 81 compounds were synthesized, and their binding affinities to Bcl-2, Bcl-x_L, and Mcl-1 measured. Encouragingly, 22 compounds exhibited binding affinities in the micromolar range ($K_i < 20$ μM) to at least one target protein. Moreover, some compounds were observed to be highly selective binders to Mcl-1 with no detectable binding to Bcl-2 or Bcl-x_L, among which the most potent one has a K_i value of 0.18 μM for Mcl-1. Binding modes of four selected compounds to Mcl-1 and Bcl-x_L were derived through molecular docking and molecular dynamics simulations. It seems that the binding affinity and selectivity of these compounds can be reasonably interpreted with these models. Our study demonstrated the possibility for obtaining selective Mcl-1 inhibitors with relatively simple chemical scaffolds. The active compounds identified by us could be used as lead compounds for developing even more potent selective Mcl-1 inhibitors with potential pharmaceutical applications.

Introduction

Apoptosis, or programmed cell death, is an essential physiological process required by the development and maintenance of tissue homeostasis. Disregulation of this process is known to be associated with cancer.[1–5] The B-cell lymphoma 2 (Bcl-2) family of proteins are a major group of apoptosis regulators, which includes both antiapoptotic members, such as Bcl-2, Bcl-x_L, Mcl-1, and Bcl-w, as well as proapoptotic members, such as Bak, Bax, and other BH3-only proteins.[6] Overexpression of antiapoptotic Bcl-2 family proteins contributes to the resistance to chemotherapies and ratiotherapies in various cancer cells. Therefore, targeting Bcl-2 family proteins has become an attractive approach towards the invention of new cancer therapies since the beginning of this century.[7,8]

A number of small-molecule inhibitors of Bcl-2 family proteins have been reported during the past decade.[9–30] The chemical structures and binding data of some potent Bcl-2 inhibitors are summarized in Figure 1. Interestingly, quite a number of Bcl-2 inhibitors are more potent towards Bcl-2 or Bcl-x_L than Mcl-1. For example, ABT-737 and its orally active analogue ABT-263 (Navitoclax) were found to be highly potent inhibitors of Bcl-2, Bcl-x_L and Bcl-w ($K_i < 0.001$ μM), but only modestly targeted Mcl-1 ($K_i = 0.55$ μM).[9–11] They thus lack efficacy on some types of cancer cells with Mcl-1 overexpression. Indeed, downregulation of Mcl-1 makes cancer cells sensitive to ABT-737 or other cytotoxic agents.[31–35] In contrast, identification of inhibitors of other known antiapoptotic members, such as Mcl-1, is relatively unaddressed. It is important to mention that though all antiapoptotic Bcl-2 family proteins have similar 3D structures, the sequence identities among them are only modest, typically around 30–70%, implying that they may target different types of tissues during apoptosis and could also differ in responses to different stress stimuli.[36] For example, it is known that Bcl-2 and Bcl-x_L are essential for regulating B-lymphocytes and platelet survival.[37,38] Hence, administration of anticancer drugs interacting with them might cause either lymphopaenia or thrombocytopaenia to patients in which the two proteins are not overexpressed. In contrast, Mcl-1 and Bcl-w are essential for the sustainable production of haemato-

[a] Dr. X. Ding, L. Lv, Prof. H. Liu
CAS Key Laboratory of Receptor Research
Shanghai Institute of Materia Medica
Shanghai Institutes of Biological Sciences, Chinese Academy of Sciences
555 Zu Chong Zhi Road
Shanghai 201203 (P.R. China)
E-mail: hliu@mail.shcnc.ac.cn

[b] Dr. Y. Li, M. Zhou, Dr. L. Han, Z. Zhang, Prof. R. Wang
State Key Laboratory of Bioorganic Chemistry
Shanghai Institute of Organic Chemistry, Chinese Academy of Sciences
345 Lingling Road
Shanghai 200032 (P.R. China)
E-mail: wangrx@mail.sioc.ac.cn

[c] Dr. Q. Ba, Dr. J. Li, Prof. H. Wang
Institute of Nutritional Sciences
Shanghai Institutes of Biological Sciences, Chinese Academy of Sciences
319 Yueyang Road
Shanghai 200031 (P.R. China)

Supporting information for this article is available on the WWW under http://dx.doi.org/10.1002/cmdc.201300316.

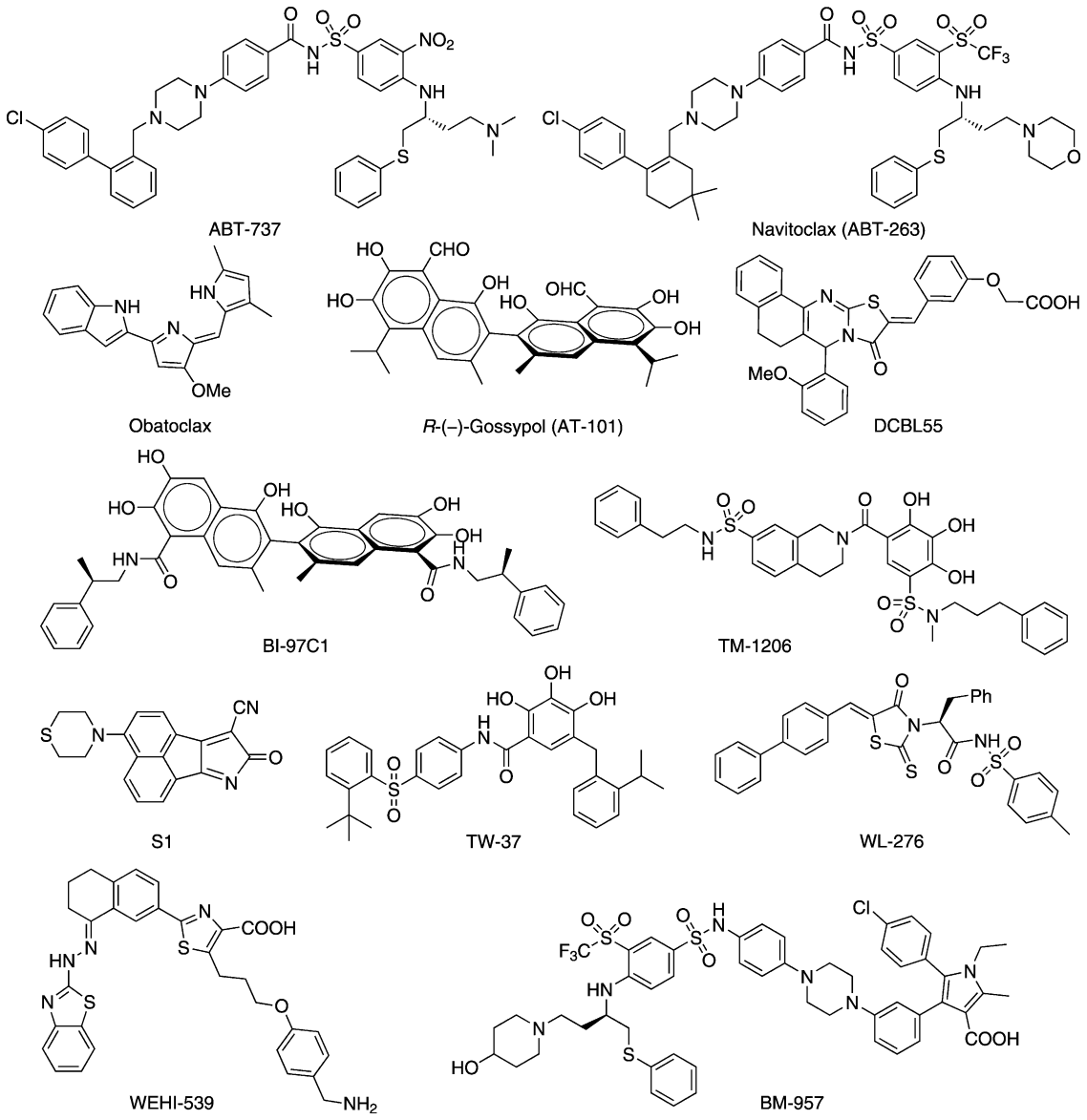

Figure 1. Known small-molecule inhibitors of antiapoptotic Bcl-2 family proteins.

poetic stem cells and sperm cells, respectively.[39,40] It is reasonable to expect that specific inhibitors of each antiapoptotic Bcl-2 family protein are able to reduce the adverse side effects in chemotherapy treatments of cancers overexpressing different Bcl-2 family proteins.

To date, some efforts have been made on targeting Mcl-1 for cancer treatment,[41] such as, downregulation of Mcl-1 by cyclin-dependent kinase inhibitors, debiquitinase inhibitors, or treatment of antisense oligonucleotides. Some small-molecule inhibitors of Bcl-2/Bcl-x_L also have decent binding affinities to Mcl-1. However, only a few selective Mcl-1 inhibitors have been reported. To the best of our knowledge, the only potent selective Mcl-1 inhibitor was reported by Friberg et al.[28] ($K_i <$ 100 nM) with roughly 100-fold selectivity over Bcl-2 or Bcl-x_L. Here, we propose that besides developing general inhibitors of Bcl-2 family proteins, developing selective Mcl-1 inhibitors represents an alternative strategy for enhancing the therapeutic efficacy of conventional anticancer chemotherapies on cancer cells with Mcl-1 overexpression. Such compounds could also be used as molecular tools to further explore the biological mechanisms of Mcl-1, which is actually not fully understood so far.

Mcl-1 as well as other Bcl-2 family proteins conduct their biological functions through protein–protein interactions with proapoptotic Bcl-2 family proteins.[6] Designing small-molecule inhibitors of protein–protein interactions is more challenging in drug discovery. A major reason is that protein–protein binding interfaces are normally wider and flatter, lacking well-defined "binding pockets".[42–45] In our previous study, we relied on structure-based virtual screening to discover lead compounds, which led to the development of more potent Bcl-2 inhibitors, for example, DCBL55.[22] In this study, we decided to adopt the de novo design strategy to generate the structural scaffolds of our lead compounds instead, since this strategy

can in principle explore a larger chemical space. It is also more convenient to incorporate human expertise during this process.

A popular approach for deriving inhibitors of protein–protein interactions is through so-called fragment-based design. Normally, the starting point of this approach is low-weight ligand molecules (MW < 300) identified by NMR screening or other experimental means. For example, a successful application of this approach has been demonstrated in the development of ABT-737/ABT-263.[9,10] In this study, we employed a computational approach to apply fragment-based design. The key idea of this approach is illustrated in Figure 2 whereas

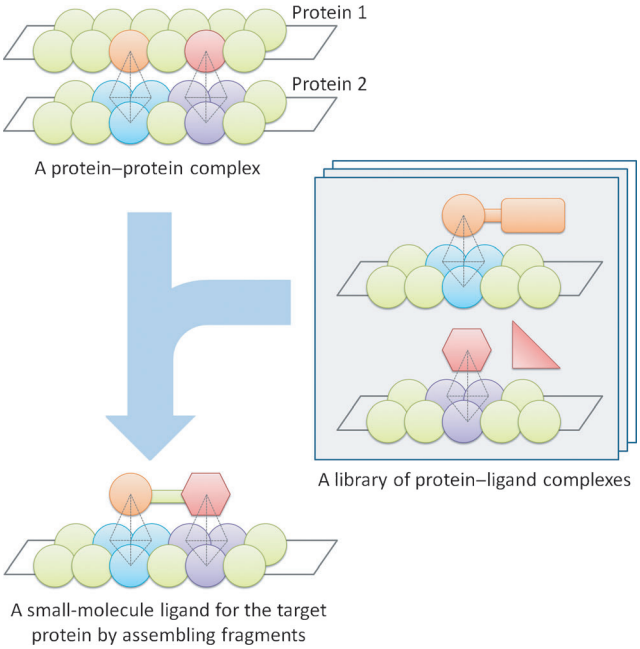

Figure 2. Illustration of a fragment-based computational approach for designing small-molecule inhibitors of protein–protein interactions. (1) Conserved residue clusters are identified on a given protein–protein binding interface. (2) A library of protein–ligand complex structures is searched for same or similar residue clusters, and chemical fragments interacting with these residue clusters are retrieved. (3) Small-molecule binders are sketched by assembling suitable chemical fragments.

detailed descriptions are given elsewhere.[46] Briefly, our assumption is that critical residues at the binding interface of protein–protein complexes exist in conserved clusters. Such residue clusters form microenvironments on the binding interface, which are able to host certain chemical fragments. Given the abundant structural information available from public domains such as the Protein Data Bank (PDB),[47] one can find suitable chemical fragments from known protein–ligand complexes by mapping the same (or similar) residue clusters. If there are multiple conserved residue clusters on a protein–protein binding interface, it is then possible to retrieve multiple chemical fragments in this way and then assemble them into complete molecules.

Following this approach, we analyzed the binding sites on Mcl-1 and Bcl-x_L with a set of in-house computer programs to identify conserved residue clusters. We then screened over 25 000 protein–ligand complexes in PDB for such residue clusters as well as the suitable chemical fragments matching them. Based on the outcomes of this analysis, four series of benzylpiperazine derivatives, in total 81 compounds, were designed and synthesized. Binding affinities of these compounds to Mcl-1, Bcl-2 and Bcl-x_L were measured in a fluorescence polarization (FP)-based binding assay. A number of obtained compounds exhibited binding to Mcl-1 with inhibition constants (K_i) ranging between 0.18–20.3 μM. Interestingly, some of them are selective binders to Mcl-1 with no detectable binding to Bcl-2 or Bcl-x_L. The structure–activity relationships (SARs) of these compounds were analyzed and further interpreted by the binding modes derived through molecular modeling. Our study provides valuable lead compounds for the development of even more potent selective Mcl-1 inhibitors. Such compounds could help to explore the biological role of Mcl-1 in normal physiology and tumor maintenance and might complement other Bcl-2 inhibitors in therapeutic applications.

Results and Discussion

Design of four compound series and their SARs

Bcl-2 family proteins are good targets for applying fragment-based design since the BH3-domain binding site on them can be divided into several subsites. As examples, the binding sites on Bcl-x_L and Mcl-1 are shown in Figure 3. In general, we divided the binding site into three subsites, P-site, Q-site, and L-site. The P-site is essentially hydrophobic, mainly consisting of Leu108, Val126 and Phe97 residues in the case of Bcl-x_L, and Met231, Leu235, Val249 residues in the case of Mcl-1. The Q-site is a more hybridized site, which mainly consists of Arg100, Asn136 and Tyr195 residues in the case of Bcl-x_L, and His224, Asn260, Phe319 residues in the case of Mcl-1. The L-site refers to the region between the P-site and the Q-site, where a linker fragment is to be placed in order to connect the chemical fragments fitting to the P-site and Q-site.

By applying a fragment-based design approach described in the Experimental Section, we obtained several types of chemical fragments from PDB that match the residue clusters at each subsite (Figure 4). It should be mentioned that in order to increase the chance for obtaining active compounds, we considered Mcl-1 as well as Bcl-x_L at this step. These fragments were then docked into each corresponding subsite to examine their fitness. A few of them are shown in Figure 3 as examples. During the next step, we selected some hydrophobic moieties, such as, phenyl, biphenyl, and piperazine groups, for the P-site, a phenyl moiety with polar substituent groups for the Q-site, and benzamide and tetrazole groups as linkers. Later, the tetrazole group was replaced by a triazole group since the latter was more convenient for synthesis through "click chemistry". These separated fragments were assembled together to form complete molecules of proper sizes for fitting to the BH3-binding groove.

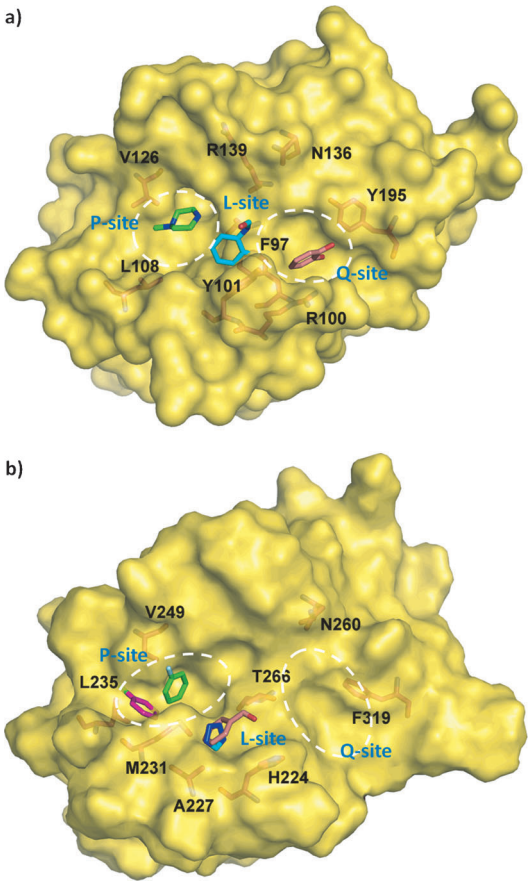

Figure 3. Illustration of the three subsites in the BH3-binding groove on a) Bcl-x_L (PDB ID: 1PQ1) and b) Mcl-1 (PDB ID: 2NL9) and some chemical fragments matching these subsites retrieved from PDB.

Synthesis

Four series (**A**–**D**), including a total of 81 compounds, were synthesized in our study (Figure 4). The synthetic routes for these compounds are illustrated in Scheme 1, 2, 3, and 4, respectively. Compounds **A1**–**A26** were synthesized through the route outlined in Scheme 1. Compound **1** was obtained from the reaction with *tert*-butoxycarbonyl (Boc)-piperazine and corresponding benzyl bromide derivatives. Benzylpiperazine **2a**–**t** were obtained from a Suzuki coupling reaction between **1** and different phenylboronic acids, followed by deprotection of the Boc group with trifluoroacetic acid (TFA). Compounds **3a**–**k** were obtained through amide coupling reaction of methyl 4-(aminomethyl)benzoate and different acids or S_N2 reactions between methyl 4-(aminomethyl)benzoate and halide compounds, which was followed by hydrolysis of the ester. Final products **A1**–**A26** were obtained by amide coupling of **2a**–**t** and **3a**–**k**.

Compounds **B1**–**B17** were synthesized through the route outlined in Scheme 2. Compounds **4a**–**g** were obtained by amide coupling reaction between methyl 3-aminobenzoate and different acids, which was followed by hydrolysis of the ester. Final products **B1**–**B17** were obtained by amide coupling of **2a**–**t** and **4a**–**g**.

Compounds **C1**–**C12** were synthesized through the route outlined in Scheme 3. Ethyl 2-bromoacetate was prepared from commercially available (3-aminophenyl)methanol or 3-(hydroxymethyl)phenol. It was followed by the bromination with *N*-bromosuccinimide (NBS) and nucleophilic displacement with azide to yield **7a**,**b**. Hydrolyzing **7a**,**b** yielded the key intermediates **8a**,**b**. Compounds **9a**–**h** were obtained by treating benzylpiperazine **2a**–**t** with 3-bromoprop-1-yne. Click reaction of azide **8a**,**b** and alkyne **9a**–**h** afforded final products **C1**–**C12**.

Scheme 4 outlines the route for the synthesis of compounds **D1**–**D26**. Amide coupling of benzylpiperazine **2a**–**t** afforded from Scheme 1 with several commercially available acids yielded compounds **D1**–**D12**. Treating benzylpiperazine **2a**–**t** with anhydride, followed by amide coupling with commercially available amines, afforded compounds **C13**–**C24**. Intermediate 11 was afforded through the reaction of phthalic anhydride with 1-(biphenyl-3-ylmethyl)piperazine. Finally, **D25** and **D26** were obtained from the amide coupling reaction between **11** and 3,4,5-trimethoxyaniline or 2,4-dimethoxyaniline, respectively.

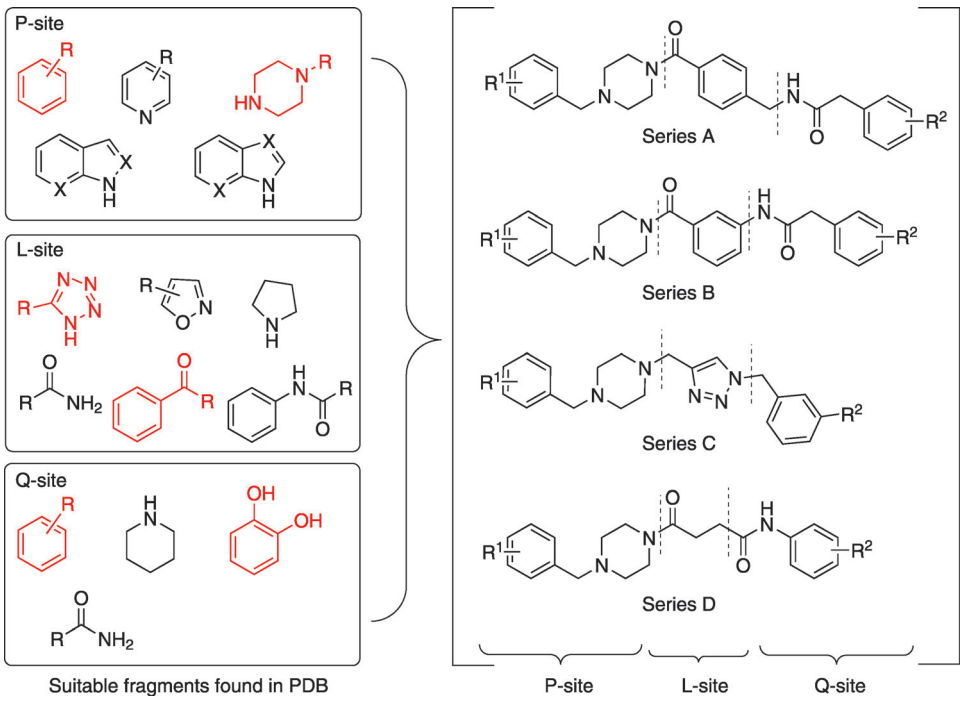

Figure 4. Fragment-based design of the compounds described in our study. The fragments actually used in our compounds are shown in red in the boxes on the left. The representative chemical structures in four series are shown on the right. Exact chemical structures of all compounds are given in Tables 1–4.

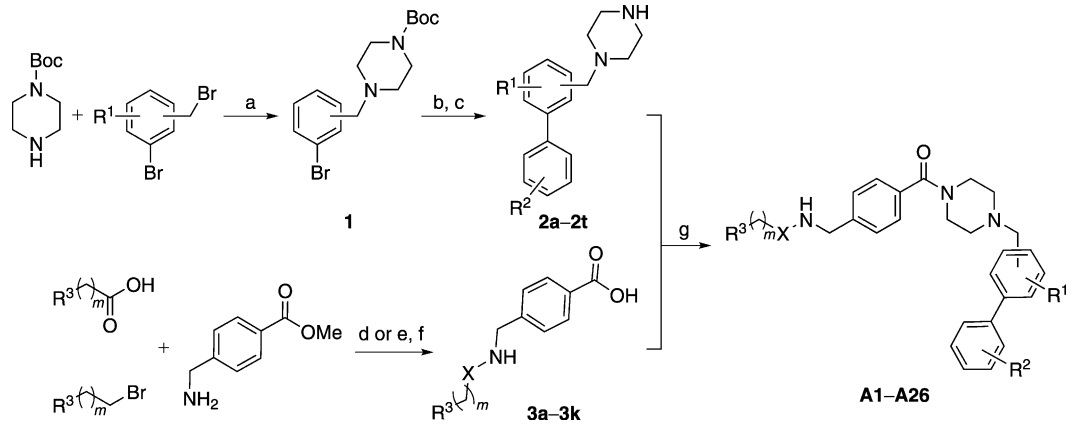

Scheme 1. *Reagents and conditions*: a) TEA, CH_2Cl_2; b) Boronic acid or ester, $Pd(PPh_3)_4$, Na_2CO_3, DME/EtOH/H_2O; c) TFA, CH_2Cl_2; d) EDCI, TEA, HOBT, CH_2Cl_2; e) TEA, CH_2Cl_2; f) NaOH, CH_3OH, H_2O; g) HATU, DIPEA, DMF.

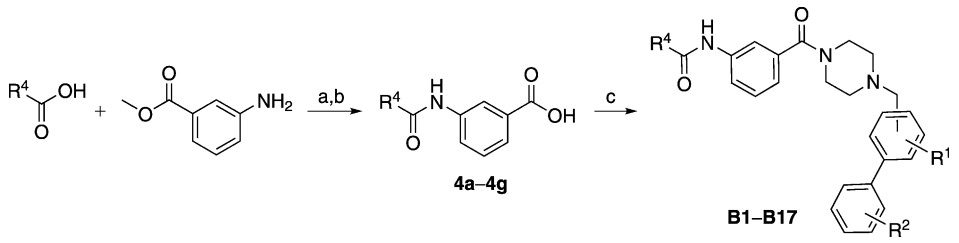

Scheme 2. *Reagents and conditions*: a) EDCI, TEA, HOBT, CH_2Cl_2; b) NaOH, CH_3OH, H2O; c) **2a–t**, HATU, DIPEA, DMF.

Chemical structures and binding affinity data of compounds **A1–A26** are summarized in Table 1. Our binding assay results indicate that a number of compounds in this series exhibited binding affinities to Mcl-1, of which six compounds (**A1**, **A7**, **A8**, **A14**, **A15** and **A17**) have K_i values below 15 μM. In particular, **A1** is the most potent compound with $K_i = 0.18$ μM. It seems that the biphenyl group is the optimal fragment for the P-site. Moving the attachment of the biphenyl group from *ortho*- (**A1**) to *meta*- (**A2**) or *para*-position (**A3**) abolishes binding affinity. This indicates that the bulky biphenyl group probably locates in a narrow cavity and thus needs to take a precise orientation. Binding affinities are also lost when some simple halogen groups are added to the *ortho*-biphenyl group (**A4–A6**), which further supports our speculation. When the *ortho*-biphenyl group is changed to a β-naphthyl (**A7**) or 3,4,5-trimethoxybenzyl group (**A8**), K_i values

Biological evaluation

All compounds were then tested in a FP-based binding assay to measure their binding affinities to three antiapoptotic Bcl-2 family proteins, including Bcl-x_L, Bcl-2, and Mcl-1. Technically, these compounds were tested first at three doses (1, 10, and 50 μM). If a compound exhibited obvious dose-dependent inhibition rates within this range and inhibited over 50% at 50 μM, it was then tested at a series of doses to derive accurate K_i values.

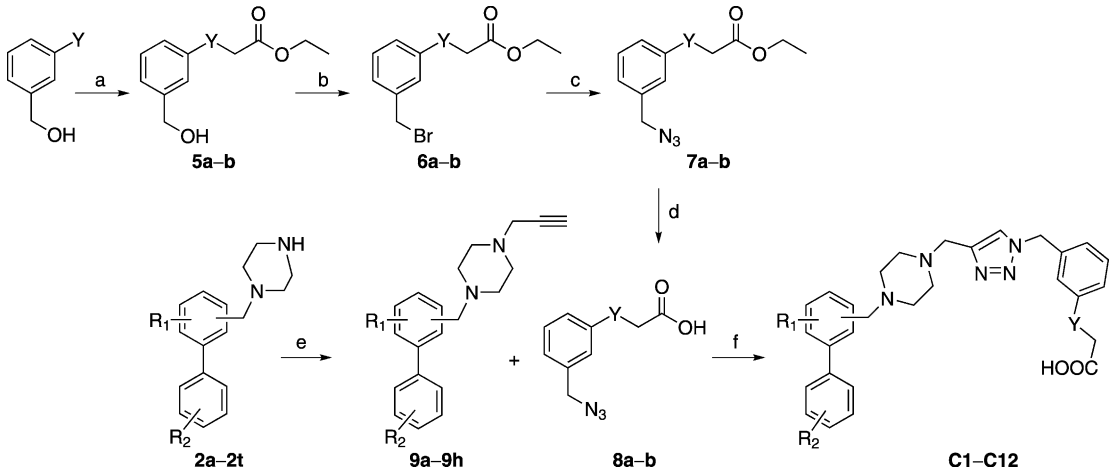

Scheme 3. *Reagents and conditions*: a) Ethyl 2-bromoacetate, K_2CO_3, acetone; b) NBS, PPh_3, THF; c) NaN_3, acetone; d) LiOH, THF/H_2O; e) 3-bromoprop-1-yne, K_2CO_3, CH_2Cl_2; f) $CuSO_4$, L-abscorbic acid, *tert*-butyl alcohol/H_2O.

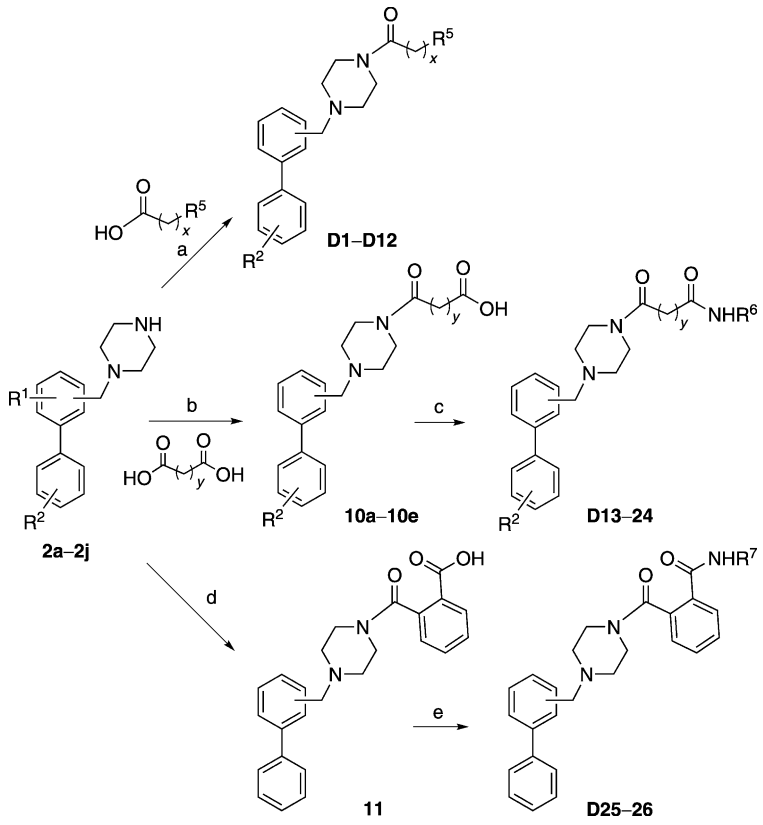

Scheme 4. *Reagents and conditions*: a) HATU, DIPEA, DMF; b) CH_2Cl_2, 40 °C; c) Amines, HATU, DIPEA, DMF; d) CH_2Cl_2, 40 °C; e) Amines, HATU, DIPEA, DMF.

increase significantly to 14.5 and 4.9 μM, respectively. As for the fragment occupying the Q-site, a wider range of chemical groups were attempted since this subsite is relatively open. However, as indicated in Table 1, most of them were not successful. Binding affinities to Mcl-1 are only observed when this fragment is either a 2-(3,4,5-trimethoxyphenyl)acetic group (**A1**, **A7**, **A8**, **A17**) or 3-carboxylbenzyl group (**A14**, **A15**). This observation suggests that a phenyl group with appropriate hydrogen-bond-acceptor substituent groups is desired for this subsite. Interestingly, the selective Mcl-1 binders in this series (**A1** and **A7)** have no detectable binding to Bcl-x_L or Bcl-2. There are also general binders of Bcl-2 family proteins (**A8**, **A14**, and **A15)** that do not have obvious selectivities among all three tested proteins.

Chemical structures and binding affinity data of compounds **B1**–**B17** and **C1**–**C12** are summarized in Table 2 and Table 3, respectively. No compound in these two series exhibits an obvious binding affinity to any of the three Bcl-2 family proteins. Note that in these two series, the P-groups and Q-groups are similar to their counterparts in series A. Thus, the 3-aminobenzyl group as well as the triazole group is not a good linker to connect the chemical moieties that are supposed to fit into the P- and Q-site. Compared to the effective linker group in series A, we speculate that the 3-aminobenzyl group lacks the desired conformational flexibility due to the absence of one critical methylene unit, whereas the triazole group is simply too short. It is true that although the computational approach employed in our study is able to retrieve plausible chemical fragments for each well-defined subsite (Figure 1), it does not automatically suggest how these fragments can be connected appropriately. Thus, linker groups were still chosen manually by chemists in our study. In the case of series B and C, our choices of the linker were unfortunately not successful.

Chemical structures and binding affinity data of compounds **D1**–**D26** are summarized in Table 4. Structures in this series are actually similar

Table 1. Chemical structures and binding data of compounds **A1**–**A26**.

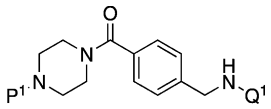

Compd	P^1	Q^1	Mcl-1 Inhibition [%][a]	Mcl-1 K_i [μM][b]	Bcl-x_L Inhibition [%][a]	Bcl-x_L K_i [μM][b]	Bcl-2 Inhibition [%][a]	Bcl-2 K_i [μM][b]
A1	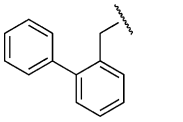	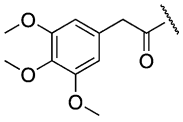	66	0.18 ± 0.05	−6	N.A.	40	N.A.
A2	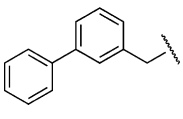	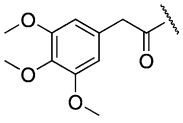	54	N.A.	−15	N.A.	47	N.A.
A3	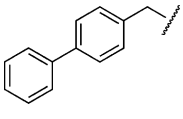	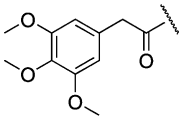	52	N.A.	−15	N.A.	32	N.A.
A4	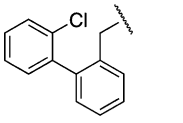	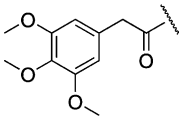	48	N.A.	1	N.A.	31	N.A.
A5	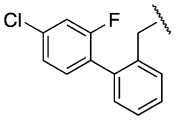	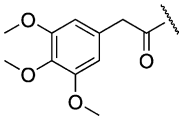	9	N.A.	−6	N.A.	15	N.A.

Table 1. (Continued)

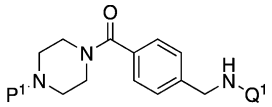

Compd	P^1	Q^1	Mcl-1 Inhibition [%][a]	Mcl-1 K_i [μM][b]	Bcl-x_L Inhibition [%][a]	Bcl-x_L K_i [μM][b]	Bcl-2 Inhibition [%][a]	Bcl-2 K_i [μM][b]
A6	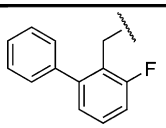	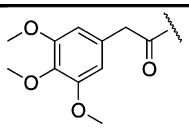	43	N.A.	−12	N.A.	22	N.A.
A7	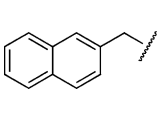	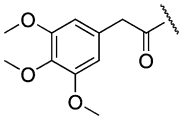	66	14.5 ± 2.3	−2	N.A.	39	N.A.
A8	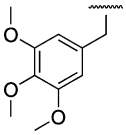	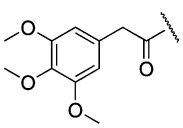	78	4.9 ± 1.2	78	2.1 ± 0.4	59	4.0 ± 1.1
A9	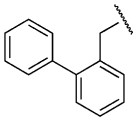	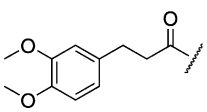	10	N.A.	−41	N.A.	48	N.A.
A10	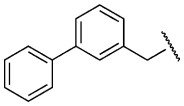	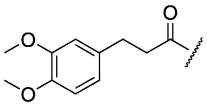	36	N.A.	−30	N.A.	42	N.A.
A11	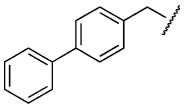	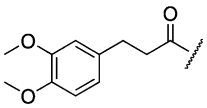	49	N.A.	−8	N.A.	32	N.A.
A12	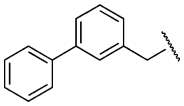	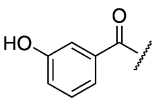	22	N.A.	−9	N.A.	8	N.A.
A13	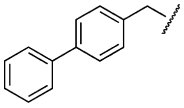	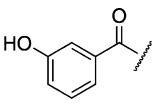	29	N.A.	−35	N.A.	19	N.A.
A14	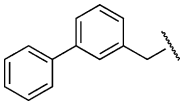	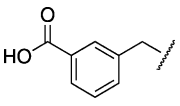	90	3.3 ± 1.3	67	9.0 ± 3.1	50	3.8 ± 0.3
A15	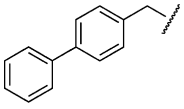	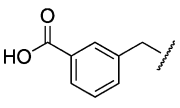	83	2.9 ± 0.5	75	5.9 ± 0.6	50	3.1 ± 0.8
A16	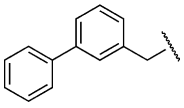	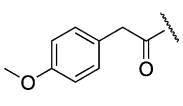	44	N.A.	−19	N.A.	41	N.A.
A17	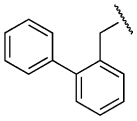	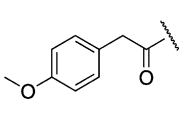	60	3.2 ± 2.0	−12	N.A.	44	N.A.
A18	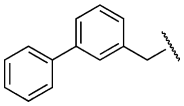	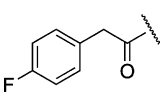	16	N.A.	6	N.A.	2	N.A.

to those in series A. The major difference is that the phenyl moiety for the linker was replaced by a short hydrocarbon chain, that is, $-(CH_2)_2-$ or $-(CH_2)_3-$, in series D. It is thus not surprising to observe that 16 compounds in this series also exhibited obvious binding affinities to Mcl-1, with K_i values lower than 20 μM. The most potent compounds are **D14** (K_i = 0.32 μM) and **D16** (K_i = 0.35 μM), suggesting that it is a reasonable design where the linker group is connected to the substituent phenyl ring through an additional amide group. Generally speaking, the compounds in this series are selective binders to Mcl-1, which are basically inactive on Bcl-x_L or Bcl-2. The only exception is **D11**, which exhibited roughly 12-fold selectivity towards Bcl-x_L (K_i = 0.26 μM) over Mcl-1 (K_i = 3.2 μM).

Analysis of the binding modes of the active compounds with Mcl-1 protein

The compounds tested in this study were designed using a fragment-based computational approach plus intuitive modifications. It is encouraging to observe that at least some of them actually have promising binding affinities to Bcl-2 family proteins, demonstrating that our de novo design was effective. In order to derive the binding modes for the active compounds, we selected compound **D11** to monitor the chemical shift

Table 1. (Continued)

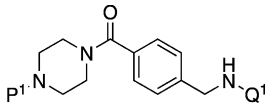

Compd	P^1	Q^1	Mcl-1 Inhibition [%][a]	Mcl-1 K_i [μM][b]	Bcl-x_L Inhibition [%][a]	Bcl-x_L K_i [μM][b]	Bcl-2 Inhibition [%][a]	Bcl-2 K_i [μM][b]
A19	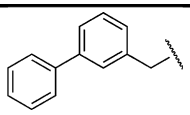	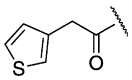	20	N.A.	−9	N.A.	33	N.A.
A20	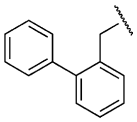	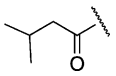	14	N.A.	−19	N.A.	28	N.A.
A21	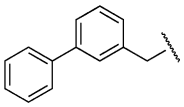	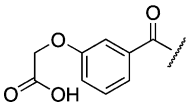	24	N.A.	4	N.A.	31	N.A.
A22	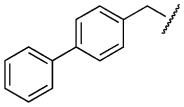	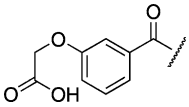	34	N.A.	14	N.A.	38	N.A.
A23	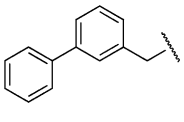	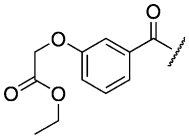	−2	N.A.	−35	N.A.	−5	N.A.
A24	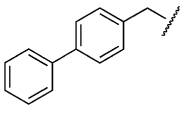	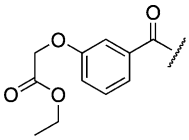	5	N.A.	0	N.A.	13	N.A.
A25	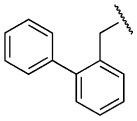	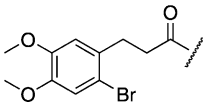	11	N.A.	6	N.A.	−3	N.A.
A26	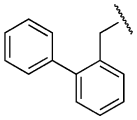	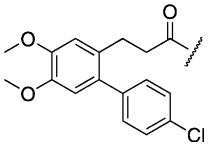	8	N.A.	2	N.A.	2	N.A.

[a] Inhibition at 50 μM test compound. [b] Data represent the mean ± SD and are derived from three parallel measurements. N.A.: No activity, that is, obvious binding was not observed in the initial screening or not confirmed in the subsequent measurements using multiple doses.

changes upon its complexation with Bcl-x_L through ^{15}N-HSQC NMR experiment. **D11** was chosen for this experiment because it was the most potent compound (K_i = 0.26 μM) on Bcl-x_L. Besides, good solubility of this compound in dichloromethane made it suitable for NMR measurements. The same ^{15}N-HSQC NMR experiment was not performed using Mcl-1 in our study because ^{15}N-labeled Mcl-1 protein was not available to us at that time.

The ^{15}N-HSQC spectrum of **D11** is shown in Figure 5a. ABT-737 was used as a positive control, and its ^{15}N-HSQC spectrum is given in the Supporting Information. One can see that many residues on Bcl-x_L exhibited apparent chemical shifts upon the addition of **D11**. More importantly, an overall similarity can be observed between the chemical shift patterns between **D11** and ABT-737 (Figure 5b), which is a strong indication that **D11** binds to Bcl-x_L at the same site as ABT-737. To illustrate this point further, the nine residues associated with the highest Ω values upon the addition of **D11** are shown on the Bcl-x_L structure in Figure 5c. Most of them indeed scatter around the BH3-binding pocket, suggesting that **D11** binds to Bcl-x_L in the expected manner. Because Mcl-1 and Bcl-x_L shares a certain level of structural similarity, it is reasonable to assume that the Mcl-1 binders obtained in our study also bind to Mcl-1 resembling the binding mode of **D11** to Bcl-x_L.

We then employed molecular modeling to derive the binding modes at the atomic level for the active compounds obtained in our study. Two compounds from series A (**A1** and **A15**) and two from series D (**D11** and **D12**) were considered for this purpose. These compounds include selective Mcl-1 binders (**A1** and **D12**) as well as general binders to all three tested proteins (**A15** and **D11**). The predicted binding modes of these four compounds in complex with Mcl-1 and Bcl-x_L are shown in Figure 6 and Figure 7. It is naive to expect that every binding data obtained in our study can be explained perfectly by these predicted binding modes. Instead, we hope to interpret the overall trends in the SARs as well as the selectivities of our compounds.

In order to fit the P-site, which is essentially hydrophobic, we chose a biphenyl group for most of our compounds. Such a moiety was among the general suggestion given by our computational approach (Figure 4). The choice of this particular group was inspired by the molecular structure of ABT-737 (Figure 1). One can see in Figure 6 and 7 that this group has the right size and shape to fit the P-site. The Q-site, however,

Table 2. Chemical structures and binding data of compounds **B1**–**B17**.

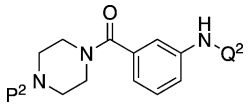

Compd	P^2	Q^2	Inhibition [%][a] Mcl-1	Bcl-x_L	Bcl-2
B1	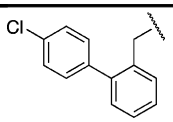	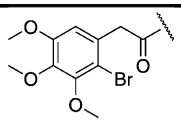	15	−8	5
B2	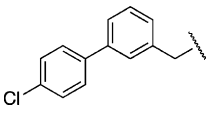	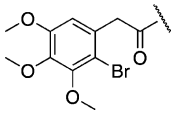	0	−4	−2
B3	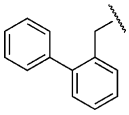	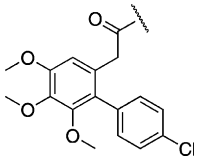	32	−10	10
B4	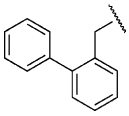	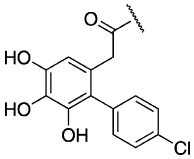	5	16	13
B5	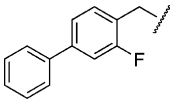	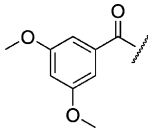	14	−8	−8
B6	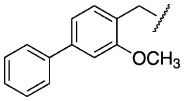	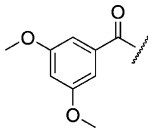	−1	−27	−3
B7	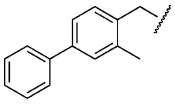	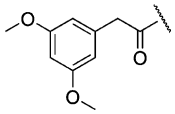	30	−13	4
B8	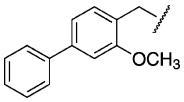	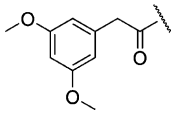	−5	−20	−4
B9	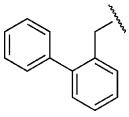	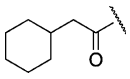	1	−15	7
B10	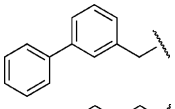	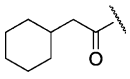	−8	−31	−3
B11	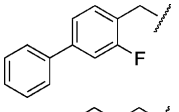	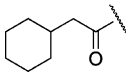	−4	−32	−4
B12	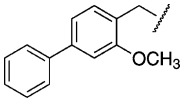	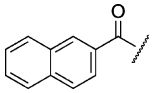	5	−19	−1
B13	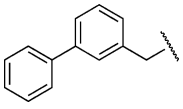	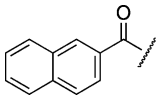	2	−14	7

Table 2. (Continued)

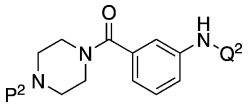

Compd	P^2	Q^2	Inhibition [%][a] Mcl-1	Bcl-x_L	Bcl-2
B14	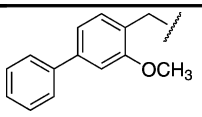	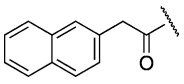	22	−2	−6
B15	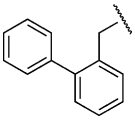	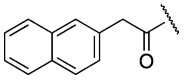	−1	−23	7
B16	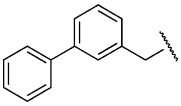	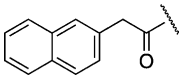	8	−17	−7
B17	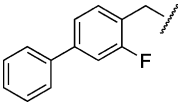	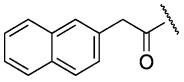	11	−31	−10

[a] Inhibition at 50 μM test compound.

is hybridized in nature, consisting of nonpolar as well as polar residues. We mainly chose a phenyl group decorated with hydrogen-bond donor or acceptor substituent groups for fitting this site. The most notable difference among series A–D is the linker moiety connecting these two parts in the molecular structure. Note that all of the active compounds observed in our study belong to series A or D, whereas no compound has obvious binding affinities to any of the three proteins in series B or C. This indicates that the linker in series B or C is not suitable (Figure 4). In series C, the linker is obviously too short to allow the chemical fragments at both sides to reach the P- and the Q-site on the target protein simultaneously. In series B, the linker is a phenyl ring with two amide groups attached at the *meta*-position, which is about the same length as the linkers in series A or D. Nevertheless, due to the conjugation between the two amide groups and the phenyl ring, the linker in series B is essentially flat, lacking the conformational flexibility to allow the chemical fragments at both sides to fit comfortably into the P- and the Q-site.

Our predicted binding modes suggest that the linker moiety does not merely fill up the space between the P- and the Q-site. They could also be involved in critical interactions with the target protein. In the complex of Mcl-1 with **A1** for example, one amide group on the linker moiety forms a C=O···H–N hydrogen bond with Arg263 above the binding groove on Mcl-1; whereas the other amide group on the linker moiety forms a N–H···O hydrogen bond with Thr266 at the bottom of the binding groove. The occupancy of both hydrogen bonds was above 50% during molecular dynamics (MD) simulation. This probably explains why **A1** is the most potent compound for Mcl-1 among all compounds. **A15** has the same hydrogen-bond donor/acceptor groups on its linker moiety as **A1**. However, due to the different connection between the biphenyl

Table 3. Chemical structures and binding data of compounds **C1**–**C12**.

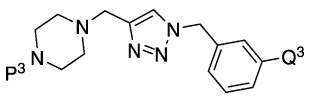

Compd	P^3	Q^3	Inhibition [%][a] Mcl-1	Bcl-x_L	Bcl-2
C1	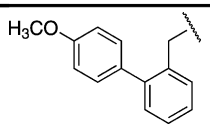	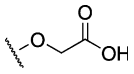	1	−6	7
C2	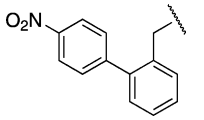	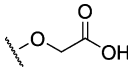	13	−5	6
C3	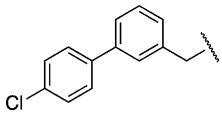	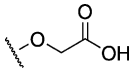	5	−19	12
C4	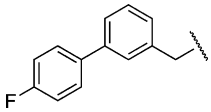	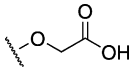	26	−10	16
C5	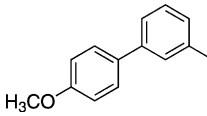	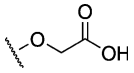	3	−27	−12
C6	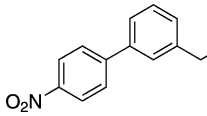	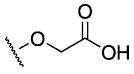	−27	−29	−15
C7	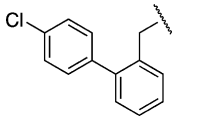	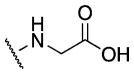	−4	−29	8
C8	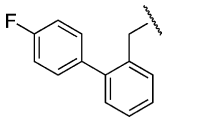	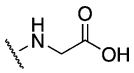	8	6	−14
C9	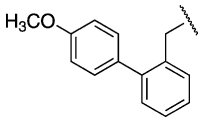	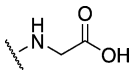	7	−4	−8
C10	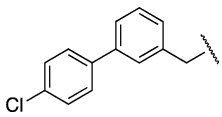	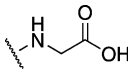	32	−43	27
C11	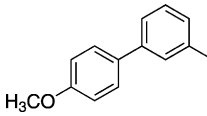	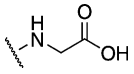	11	−28	5
C12	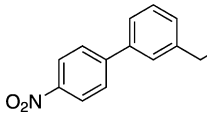	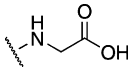	−5	10	14

[a] Inhibition at 50 μM test compound.

group and the piperazine ring in **A15**, the binding pose of **A15** to Mcl-1 is very different from that of **A1** (Figure 6). Consequently, **A15** is not able to maintain the hydrogen bonds with Arg263 and Thr266. In fact, the occupancy of both hydrogen bonds was below 20% during MD simulation. But when the target protein is Bcl-x_L, the carboxyl group on the substituent phenyl ring on **A15** can form a charged hydrogen bond (i.e., salt bridge) with Arg100 at the Q-site in the binding groove. This critical interaction is missing in the case of **A1** because there is no negatively charged, strong hydrogen acceptor group at the equivalent part on **A1**. Besides, our predicted binding mode of **A1** with Bcl-x_L indicates that the relatively bulky Q-moiety on **A1**, which is a phenyl ring plus three methoxy groups, is actually not well accommodated at this part of the binding groove. The binding modes shown in both Figure 6 and 7 are the outcomes after 3 ns-long MD simulations. We assume that one would observe the dissociation of **A1** from Bcl-x_L if a much longer MD simulation was performed.

Compound **D11** is a general binder to all three proteins, while **D12** is a selective binder to Mcl-1. Note that the only difference between the chemical structures of these two compounds lies in the substituent groups on the phenyl ring fitting the Q-site: In the case of **D11**, the substituent groups are two hydroxy groups, which can act as hydrogen-bond donors or acceptors; while in the case of **D12**, the substituent groups are two methoxy groups, which can act only as weak hydrogen-bond acceptors. Our predicted binding mode of **D11** with Mcl-1 suggests that it forms an O–H···O=C hydrogen bond with the terminal amide group on the side chain of residue Asn260 (Figure 7). **D12** also forms an O···H–N hydrogen bond with the terminal amide group on the same residue. But this hydrogen bond was observed to be unstable during MD simulation and is not seen in the final binding mode shown in Figure 7. This observation is consistent with the fact that **D11** has a stronger affinity to Mcl-1 (K_i = 3.2 μM) than **D12** (K_i = 9.4 μM).

When the target protein is Bcl-x_L, our predicted binding mode of **D11** reveals certain similarities to that of ABT-737. This is not surprising because these two compounds both have a benzyl substituted piperazine moiety at the center of their chemical structures (Figure 1 and 7). Superimposed binding modes of **D11** and ABT-737 to Bcl-x_L are given in Figure S5 in the Supporting Information. One can see there that (1) the terminal biphenyl moiety on both compounds occupies the hydrophobic P-site, and (2) the substituted piperazine moiety on both compounds bridges the P-site and the L-site. However, the Q-moieties on **D11** and ABT-737 are totally different. ABT-737 has a more complicated and branched structure fitting this subsite, which extends further to the C terminus of Bcl-x_L. In contrast, **D11** has a simple substituted phenol moiety fitting to this subsite, which forms an O–H···O=C hydrogen bond with the terminal carboxylic group on the side chain of residue Glu96. The Q-moiety on **D12** cannot form any hydrogen bond with the residues at the Q-site since the hydroxy groups are blocked on this molecule. In theory, the Q-moiety on **D12** has only dispersed hydrophobic contacts with the surrounding residues. But the Q-site on Bcl-x_L is much less hydrophobic as compared with Mcl-1. Thus, the hydrophobic Q-moiety on **D12** loses its advantage here, which explains why

Table 4. Chemical Structures and binding data of compounds **D1**–**D26**.

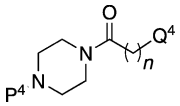

Compd	P^4	Q^4	*n*	Mcl-1 Inhibition [%][a]	Mcl-1 K_i [μM][b]	Bcl-x_L Inhibition [%][a]	Bcl-x_L K_i [μM][b]	Bcl-2 Inhibition [%][a]	Bcl-2 K_i [μM][b]
D1	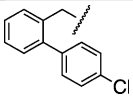	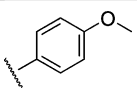	2	13	N.A.	−7	N.A.	25	N.A.
D2	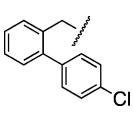	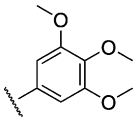	2	69	2.5 ± 0.7	20	N.A.	34	N.A.
D3	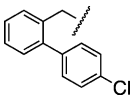	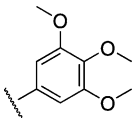	1	0	N.A.	6	N.A.	11	N.A.
D4	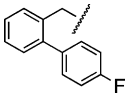	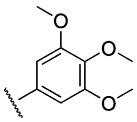	2	63	18.2 ± 6.0	−14	N.A.	43	N.A.
D5	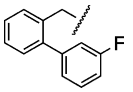	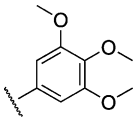	2	52	20.0 ± 4.9	−7	N.A.	35	N.A.
D6	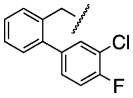	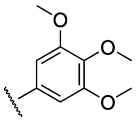	2	65	12.6 ± 3.7	−14	N.A.	36	N.A.
D7	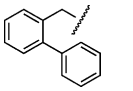	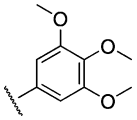	2	35	N.A.	1	N.A.	32	N.A.
D8	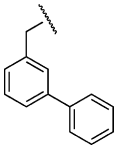	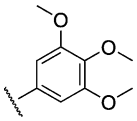	2	49	N.A.	−12	N.A.	46	N.A.
D9	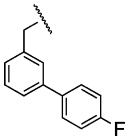	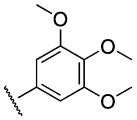	2	65	1.2 ± 0.9	11	N.A.	42	N.A.
D10	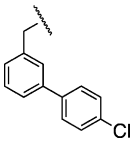	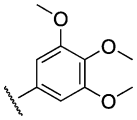	2	59	11.6 ± 1.8	16	N.A.	37	N.A.
D11	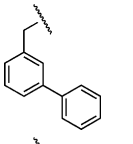	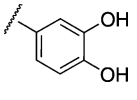	2	49	3.2 ± 1.4	52	0.26 ± 0.15	74	3.6 ± 1.7
D12	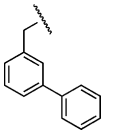	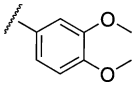	2	55	9.4 ± 4.0	−15	N.A.	37	N.A.

D12 is essentially inactive on Bcl-x_L. This is actually similar to the case of **A1**.

It is known that the BH3-binding groove on Bcl-2 family proteins undergoes notable conformational changes upon ligand binding. Such difference can be observed on the predicted complex structures of several selected compounds even though our MD simulations were not extensive. Our predicted binding modes suggest that the selective binding of **A1** and **D12** to Mcl-1 can be explained by their specific interactions with certain residues on Mcl-1. They have the right structural scaffolds, which favor such interactions upon binding to Mcl-1 but not Bcl-x_L.

As mentioned in above, Friberg and coworkers recently reported a class of potent selective Mcl-1 inhibitors,[28] which is to our knowledge the only work of this kind so far. Several most potent compounds reported in their study are given in Figure 8. One can see that their compounds are structurally quite different from ours, implying that Mcl-1 is a molecular target that allows ligands in versatile chemotypes. The most potent compounds obtained in our study (e.g., **A1**, **D14**, and **D16**) are es-

Table 4. (Continued)

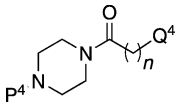

Compd	P^4	Q^4	n	Mcl-1 Inhibition [%][a]	Mcl-1 K_i [μM][b]	Bcl-x_L Inhibition [%][a]	Bcl-x_L K_i [μM][b]	Bcl-2 Inhibition [%][a]	Bcl-2 K_i [μM][b]
D13	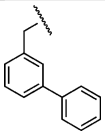	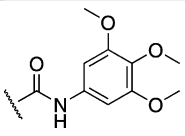	2	56	7.4 ± 1.3	−4	N.A.	40	N.A.
D14	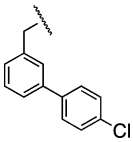	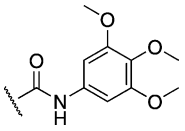	2	61	0.32 ± 0.14	9	N.A.	48	N.A.
D15	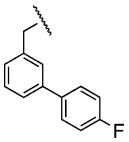	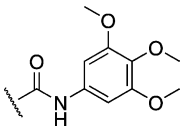	2	59	0.95 ± 0.25	20	N.A.	42	N.A.
D16	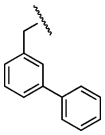	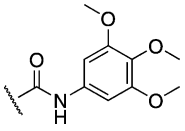	3	51	0.35 ± 0.18	1	N.A.	38	N.A.
D17	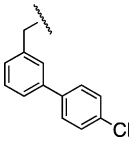	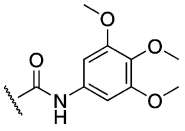	3	64	1.8 ± 0.3	9	N.A.	42	N.A.
D18	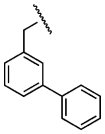	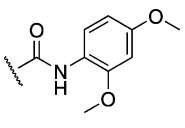	3	49	N.A.	15	N.A.	30	N.A.
D19	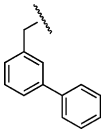	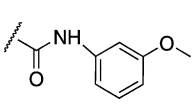	3	31	N.A.	−23	N.A.	33	N.A.
D20	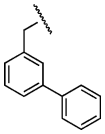	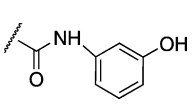	2	40	N.A.	−10	N.A.	41	N.A.
D21	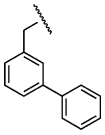	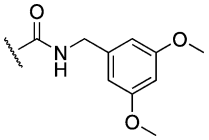	2	49	10.6 ± 5.2	−18	N.A.	39	N.A.
D22	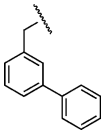	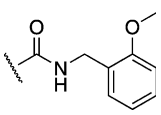	2	50	15.9 ± 8.8	−32	N.A.	40	N.A.
D23	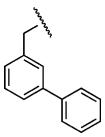	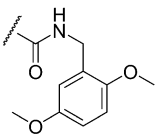	3	43	N.A.	4	N.A.	33	N.A.

sentially on the same level as theirs in terms of binding affinities to Mcl-1. Besides, these compounds seem to be selective Mcl-1 binders since they do not show detectable binding to Bcl-2 or Bcl-x_L. In terms of ligand efficiency (LE), which is computed as $-\log K_i$ divided by the number of nonhydrogen atoms in the ligand molecule, our most potent compounds on Mcl-1 (**A1**, **D14**, and **D16**) have LE values of 0.15, 0.17, and 0.17, respectively; whereas Friberg's compounds **53**, **57**, and **60** have LE values of 0.28, 0.24, and 0.26, respectively. Therefore, our compounds are less "efficient" compared to Friberg's compounds. There is still plenty of room for improving the potency of our compounds through structural optimization.

In order to understand the ligand efficiency gap between our compounds and Friberg's compounds, we compared their binding modes to Mcl-1. The crystal structure of Friberg's compound **53** in complex with Mcl-1 is shown in Figure 9. A remarkable feature of this complex structure is the conformational change upon ligand binding at the P-site, especially in the helical region between Val243 to Phe254.

Table 4. (Continued)

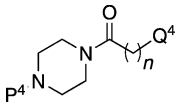

Compd	P^4	Q^4	n	Mcl-1 Inhibition [%][a]	Mcl-1 K_i [μM][b]	Bcl-x_L Inhibition [%][a]	Bcl-x_L K_i [μM][b]	Bcl-2 Inhibition [%][a]	Bcl-2 K_i [μM][b]
D24	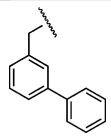	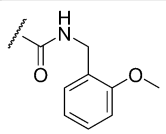	3	−34	N.A.	−30	N.A.	−2	N.A.
D25	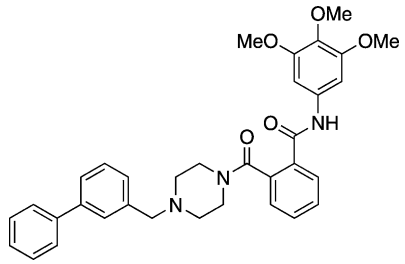			9	N.A.	−26	N.A.	18	N.A.
D26	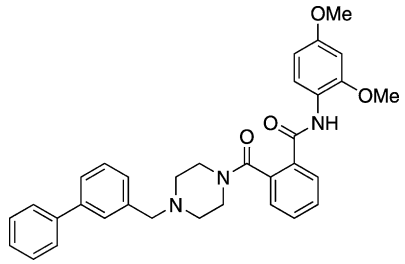			53	2.0 ± 1.3	−51	N.A.	39	N.A.

[a] Inhibition at 50 μM test compound. [b] Data represent the mean ± SD and are derived from three parallel measurements. N.A.: No activity, that is, obvious binding was not observed in the initial screening or not confirmed in the subsequent measurements using multiple doses.

This phenomenon is quite unique among other known Mcl-1 complex structures. An associated consequence is that there is not a typical Q-site inside the binding groove on this Mcl-1 structure. In fact, **53** does not stretch into that part of the binding groove at all. The substituted phenoxyl moiety on **53** and part of the connecting chain fill up the hydrophobic P-site, which is equivalent to the terminal biphenyl moiety on our compound **A1**. The indole ring on **53** resides at the L-site. Notably, the carboxylic group on this indole ring forms a salt bridge with the side chain of Arg263, a conserved residue among all antiapoptotic Bcl-2 family proteins. This important interaction with Arg263 is missing in all of our compounds, which accounts for the higher ligand efficiencies of Friberg's compounds. Comparison of the binding modes of our compounds and Friberg's compounds suggests that the L-moiety on our compounds needs further optimization, and the Q-moiety can be much simplified.

Our work and Friberg's work collectively demonstrate that development of small-molecule selective inhibitors of Mcl-1 is possible. Such molecules do not need to be as sophisticated as ABT-737 or ABT-263. Relatively simple molecules may fulfill this goal. Of course, a panel of mechanism-based studies is still needed to determine if the active compounds obtained in our study can antagonize the biological functions of overexpressed Mcl-1 in cells or even in vivo. These compounds could serve as lead compounds for the development of potent Mcl-1 inhibitors with pharmaceutical applications.

Conclusions

In this study, we attempted to obtain small-molecule inhibitors of Bcl-2 family proteins by de novo design. We divided the BH3-binding groove on Bcl-x_L and Mcl-1 into three subsites, and then sketched molecules that consist of suitable fragments fitting these subsites. Our design was aided by the use of a computational algorithm, which was developed to analyze the critical residue clusters on protein–protein binding interface and retrieve suitable chemical fragments matching them. A total of 81 compounds were synthesized, and their binding affinities to Bcl-2, Bcl-x_L, and Mcl-1 were measured. Twenty-two compounds exhibited binding affinities at the micromolar level ($K_i < 20$ μM) for at least one target protein, indicating that our design strategy was successful. Interestingly, though it was not our original aim, some of our compounds were observed to be selective binders to Mcl-1. For example, the most potent one (**A1**) has an inhibition constant (K_i) of 0.18 μM for Mcl-1 and virtually no binding to Bcl-x_L or Bcl-2. Molecular modeling was employed to derive the binding modes of several selected compounds, including selective binders of Mcl-1 and general binders of all three tested proteins. It seems that the selectivity to Mcl-1 can be explained by their different interaction patterns with Mcl-1 and Bcl-x_L. Nevertheless, our study provides a proof-of-concept demonstration that it is possible to obtain highly selective inhibitors of Mcl-1 with relatively simple chemical structures.

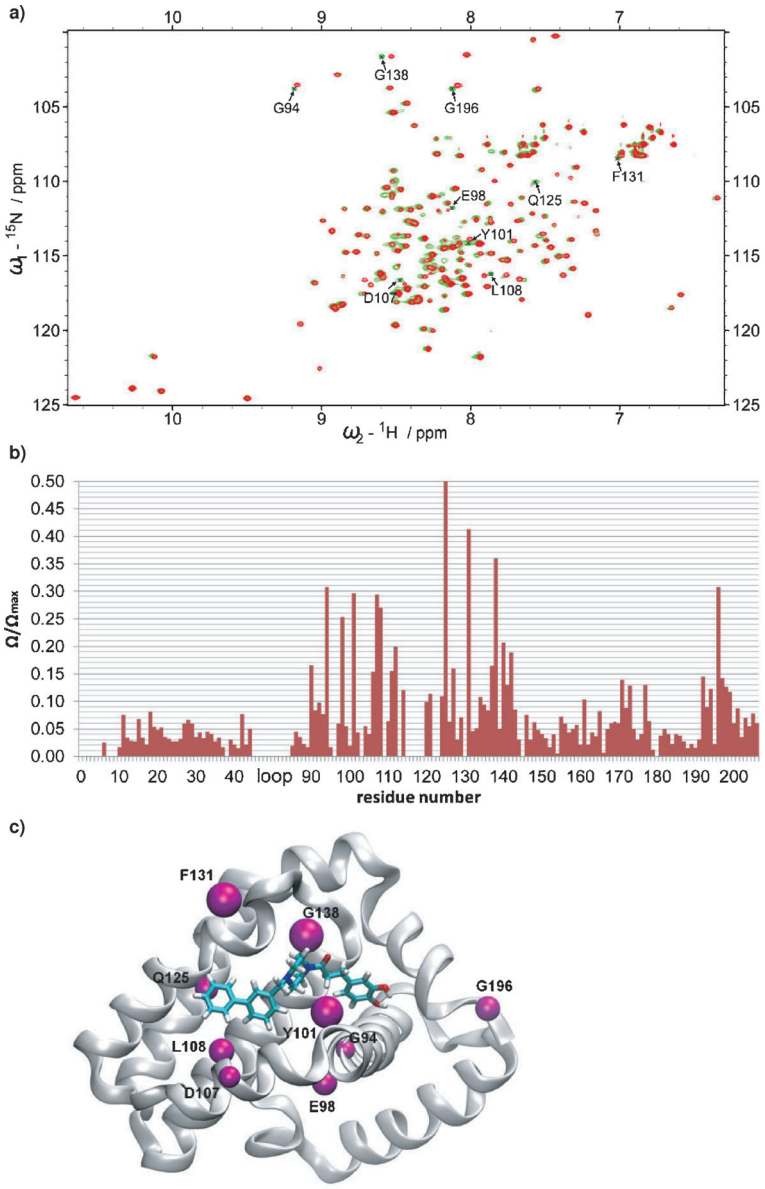

Figure 5. a) Superimposed ^{1}H-^{15}N-HSQC spectra of free Bcl-x_L (in green) and Bcl-x_L in complex with **D11** (in red). The nine residues with the highest Ω values are labeled explicitly. b) Refined chemical shift perturbation maps for all backbone amide nitrogen atoms on Bcl-x_L in complex with **D11**. c) A binding mode of **D11** derived through molecular modeling. **D11** is shown in the stick model. The backbone of Bcl-x_L is shown as gray ribbons, where locations of the nine residues with the highest Ω values are indicated by purple spheres.

Experimental Section

Synthesis

All reagents were purchased from Lancaster, Acros, and Shanghai Chemical Reagent, and were used without further purification. Analytical thin-layer chromatography (TLC) was performed with HSGF 254 (150–200 μm thickness; Yantai Huiyou, China). NMR spectroscopy was performed on a Bruker AMX-400 and AMX-300 (TMS as internal standard). Chemical shifts are reported in parts per million (ppm, δ) downfield from TMS. Proton coupling patterns are described as singlet (s), doublet (d), triplet (t), quartet (q), multiplet (m), and broad (br). Low- and high-resolution mass spectra (LRMS and HRMS) are given with electric, electrospray, and matrix-assisted laser desorption ionization (EI, ESI, and MALDI) produced by a Finnigan MAT-95, LCQ-DECA spectrometer and IonSpec 4.7 T. The purity of final compounds was assessed with analytical HPLC and observed to be > 95%. An Agilent 1100 series HPLC with an Agilent Zorbax Eclipse SB-C18 (4.6×150 mm, 5 μm particle sizes) reversed-phase column was used for analytical HPLC analyses. The eluent was an A/B gradient, where A = H_2O and B = CH_3OH. Retention time and relative purity of all compounds are given in the Supporting Information.

General procedure I for the synthesis of 2a–t: 1-(Biphenyl-2-ylmethyl)piperazine (2a): 1-*tert*-butoxycarbonyl (Boc)-piperazine (4.0 mmol) and Et_3N (6.0 mmol) were added to a solution of 2-bromobenzyl bromide (4.0 mmol) in CH_2Cl_2 (60 mL). After heating at reflux for 6 h, the reaction mixture was diluted with H_2O (100 mL) and extracted with CH_2Cl_2. The organic phase was washed with H_2O and brine, dried over Na_2SO_4, filtered and concentrated in vacuo. The residue was purified by chromatography with *n*-pentane/EtOAc (8:1 *v/v*) to obtain the intermediate *tert*-butyl 4-(2-bromobenzyl) piperazine-1-carboxylate (LC-MS: 355 $[M+H]^+$), which was then dissolved in dimethoxyethane (DME)/EtOH/H_2O (1:1:1 *v/v/v*, 3 mL), followed by addition of phenylboronic acid (2.1 mmol), $Pd(PPh_3)_4$ (0.028 mmol) and anhyd Na_2CO_3 (5.4 mmol). The reaction mixture was stirred at 100 °C for 30 min under microwave irradiation. The solvent was evaporated in vacuo and the residue was purified by chromatography with *n*-pentane/EtOAc (8:1, *v/v*) to get *tert*-butyl 4-([1,1′-biphenyl]-2-ylmethyl)piperazine-1-carboxylate (LC-MS: 353 $[M+H]^+$). After dissolution in CH_2Cl_2, trifluoroacetic acid (TFA; 15.5 mmol) was added and the mixture was heated at reflux for 2 h. The reaction mixture was diluted with saturated $NaHCO_3$ (100 mL) and extracted with CH_2Cl_2. The combined organic phases were washed with H_2O, brine, dried over Na_2SO_4. The solvent was evaporated in vacuo to obtain **2a** as a yellow oil (440 mg, 62%): ^{1}H NMR (300 Hz, $CDCl_3$): δ = 7.88 (d, J = 7.2 Hz, 1H), 7.70–7.62 (m, 2H), 7.48 (m, 1H), 7.40–7.29 (m, 4H), 7.19 (d, J = 7.4 Hz, 1H), 3.62 (s, 2H), 2.75 (br s, 4H), 2.45 ppm (br s, 4H); MS (ESI): *m/z* 253 $[M+H]^+$.

1-(Biphenyl-3-ylmethyl)piperazine (2b): Prepared according to general procedure I from 3-bromobenzyl bromide (455 mg, 63%): ^{1}H NMR (300 Hz, $CDCl_3$): δ = 7.58 (s, 1H), 7.45 (d, J = 7.4 Hz, 2H), 7.40–7.31 (m, 4H), 7.20 (d, J = 6.8 Hz, 2H), 3.56 (s, 2H), 2.55 (br s, 4H), 2.48 (br s, 2H), 2.38 ppm (br s, 2H); MS (ESI): *m/z* 253 $[M+H]^+$.

1-(Biphenyl-4-ylmethyl)piperazine (2c): Prepared according to general procedure I from 4-bromobenzyl bromide (426 mg, 60%): ^{1}H NMR (300 Hz, $CDCl_3$): δ = 7.82 (d, J = 7.8 Hz, 1H), 7.67–7.58 (m, 2H), 7.40–7.29 (m, 5H), 7.19 (d, J = 6.8 Hz, 1H), 3.68 (s, 2H), 2.78 (br s, 4H), 2.45 (br s, 2H), 2.26 ppm (br s, 2H); MS (ESI): *m/z* 253 $[M+H]^+$.

1-((2′-Chlorobiphenyl-2-yl)methyl)piperazine (2d): Prepared according to general procedure I from 2-bromobenzyl bromide and 2-chlorophenylboronic acid (517 mg, 64%):^{1}H NMR (300 Hz, [D_6]DMSO): δ = 7.89 (d, J = 7.5 Hz, 1H), 7.47–7.35 (m, 6H), 7.30–7.29

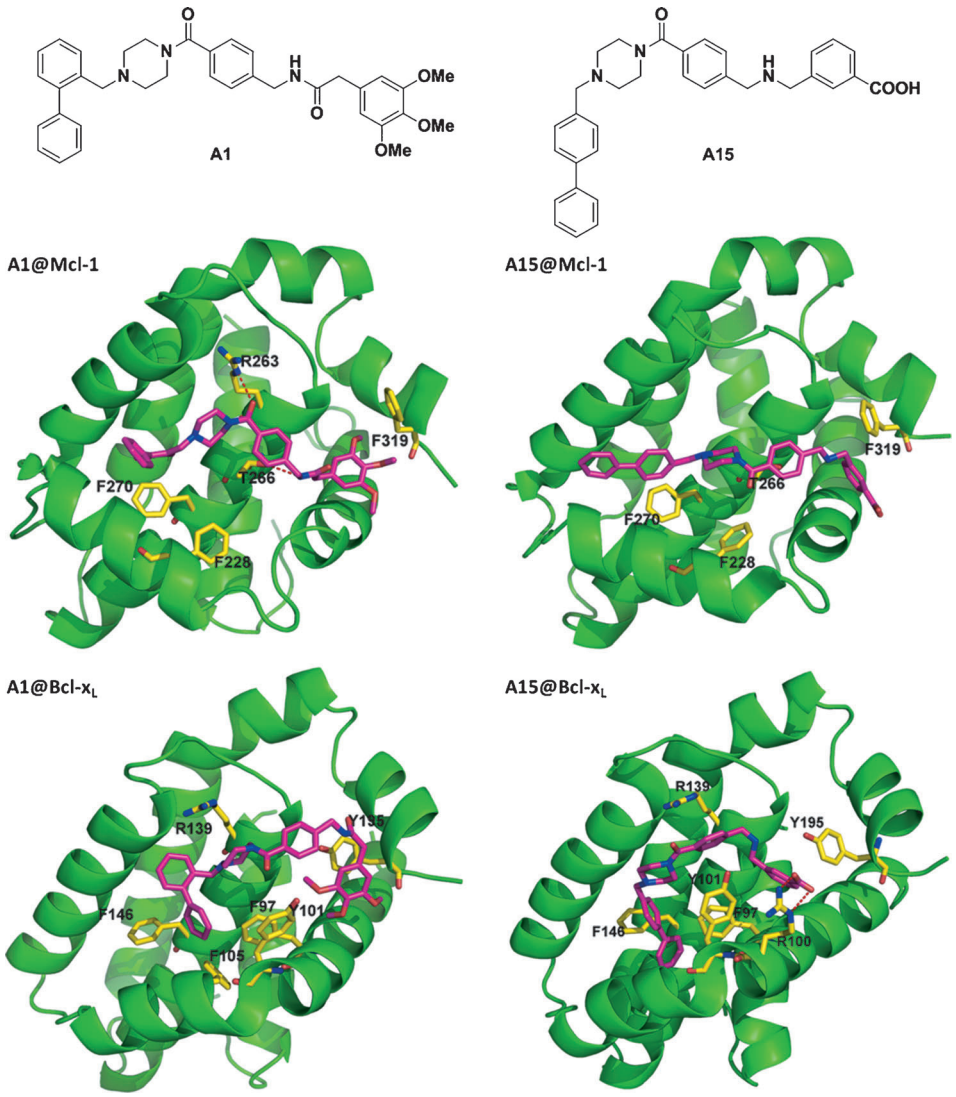

Figure 6. Chemical structures of **A1** and **A15** and their binding modes to Mcl-1 and Bcl-x_L derived through molecular modeling.

(100 mL) and extracted with CH_2Cl_2. The organic phase was washed with H_2O, brine, dried over Na_2SO_4, filtered and concentrated in vacuo. The intermediate (LC-MS: 327 $[M+H]^+$; 3.1 mmol), purified by chromatography with *n*-pentane/EtOAc (8:1 *v/v*), was dissolved in CH_2Cl_2. TFA (15.5 mmol) was added, and the solution was heated at reflux for 2 h. The reaction mixture was diluted with saturated $NaHCO_3$ (100 mL) and extracted with CH_2Cl_2. The combined organic phases were washed with H_2O, brine and dried over Na_2SO_4 and concentrated in vacuo. Compound **2g** was afforded as a white solid (769 mg, 85%): ^{1}H NMR (300 Hz, [D$_6$]DMSO): $\delta = 8.27$ (d, $J =$ 7.5 Hz, 1H), 7.86–7.83 (m, 2H), 8.94–7.83 (m, 4H), 3.84 (s, 2H), 2.52 (brs, 4H), 2.38 ppm (brs, 4H); MS (ESI): *m/z* 227 $[M+H]^+$.

1-((4′-Chlorobiphenyl-2-yl)methyl)piperazine (2h): Prepared according to general procedure I from 4-chlorophenylboronic acid (532 mg, 66%): ^{1}H NMR (300 Hz, $CDCl_3$): $\delta = 7.73$ (d, $J = 7.8$ Hz, 2H), 7.54 (m, 4H), 7.30 (m, 2H), 3.66 (s, 2H), 2.85 (brs, 4H), 2.45 ppm (brs, 4H); MS (ESI): *m/z* 287 $[M+H]^+$.

1-((4′-Chlorobiphenyl-3-yl)methyl)piperazine (2i): Prepared according to general procedure I from 3-bromobenzyl bromide and 4-chlorophenylboronic acid (524 mg, 65%): ^{1}H NMR (300 Hz, $CDCl_3$): $\delta = 8.01$ (d, $J = 7.8$ Hz, 1H), 7.95 (d, $J = 7.6$ Hz, 1H), 7.80 (s, 1H), 7.45 (t, $J = 7.4$ Hz, 2H), 7.25–7.39 (m, 3H), 3.63 (s, 2H), 2.51 (brs, 4H), 2.43 ppm (brs, 4H); MS (ESI): *m/z* 287 $[M+H]^+$.

(m, 1H), 3.26 (s, 2H), 2.67 (brs, 4H), 2.24 ppm (brs, 4H); MS (ESI): *m/z* 287 $[M+H]^+$.

1-((3′-Chloro-4′-fluorobiphenyl-2-yl)methyl)piperazine (2e): Prepared according to general procedure I from 2-bromobenzyl bromide and 3-chloro-4-fluorophenylboronic acid (566 mg, 66%): ^{1}H NMR (300 Hz, [D$_6$]DMSO): $\delta = 7.54$–7.51 (m, 1H), 7.41–7.36 (m, 3H), 7.34–7.28 (m, 2H), 7.13–7.11 (m, 1H), 3.13 (s, 2H), 2.54 (brs, 4H), 2.01 ppm (brs, 4H); MS (ESI): *m/z* 305 $[M+H]^+$.

1-((3-Fluorobiphenyl-2-yl)methyl)piperazine (2f): Prepared according to general procedure I from 2-fluoro-6-bromobenzyl bromide and phenylboronic acid (471 mg, 62%): ^{1}H NMR (300 Hz, [D$_6$]DMSO): $\delta = 7.72$–7.70 (m, 2H), 7.53–7.46 (m, 5H), 7.42–7.40 (m, 1H), 3.58 (s, 2H), 2.51 (brs, 4H), 2.48 ppm (brs, 4H); MS (ESI): *m/z* 271 $[M+H]^+$.

1-(Naphthalen-2-ylmethyl)piperazine (2g): 1-Boc-piperazine (4.0 mmol) and Et_3N (6.0 mmol) was added to a solution of 2-(bromomethyl)naphthalene (4.0 mmol) in CH_2Cl_2 (60 mL). After heating at reflux for 6 h, the reaction mixture was diluted with H_2O

1-((3-Fluorobiphenyl-4-yl)methyl)piperazine (2j): Prepared according to general procedure I from 2-fluoro-4-bromobenzyl bromide (58%): ^{1}H NMR (300 Hz, $CDCl_3$): $\delta = 7.65$ (d, $J = 7.4$ Hz,1H), 7.60 (s, 1H),7.67–7.60 (m, 2H), 7.55 (d, $J = 7.2$ Hz,1H), 7.40–7.32 (m, 3H), 3.65 (s, 2H), 2.98 (brs, 4H), 2.65 (brs, 2H), 2.50 ppm (brs, 2H); MS (ESI): *m/z* 271 $[M+H]^+$.

1-((3-Methoxybiphenyl-4-yl)methyl)piperazine (2k): Prepared according to general procedure I from 2-methoxy-4-bromobenzyl bromide (66%): ^{1}H NMR (300 Hz, $CDCl_3$): $\delta = 7.78$ (d, $J = 7.6$ Hz,1H), 7.70 (s, 1H), 7.68–7.60 (m, 2H), 7.49 (d, $J = 7.2$ Hz, 2H), 7.45–7.38 (m, 2H), 3.98 (s, 3H), 3.65 (s, 2H), 2.78 (brs, 4H), 2.45 (brs, 2H), 2.28 ppm (brs, 2H); MS (ESI): *m/z* 283 $[M+H]^+$.

1-((3-Methylbiphenyl-4-yl)methyl)piperazine (2l): Prepared according to general procedure I from 2-methyl-4-bromobenzyl bromide (62%): ^{1}H NMR (300 Hz, $CDCl_3$): $\delta = 7.85$ (s, 1H), 7.82 (d, $J =$ 7.6 Hz,1H), 7.67–7.60 (m, 2H), 7.40–7.32 (m, 3H), 7.19 (d, $J =$

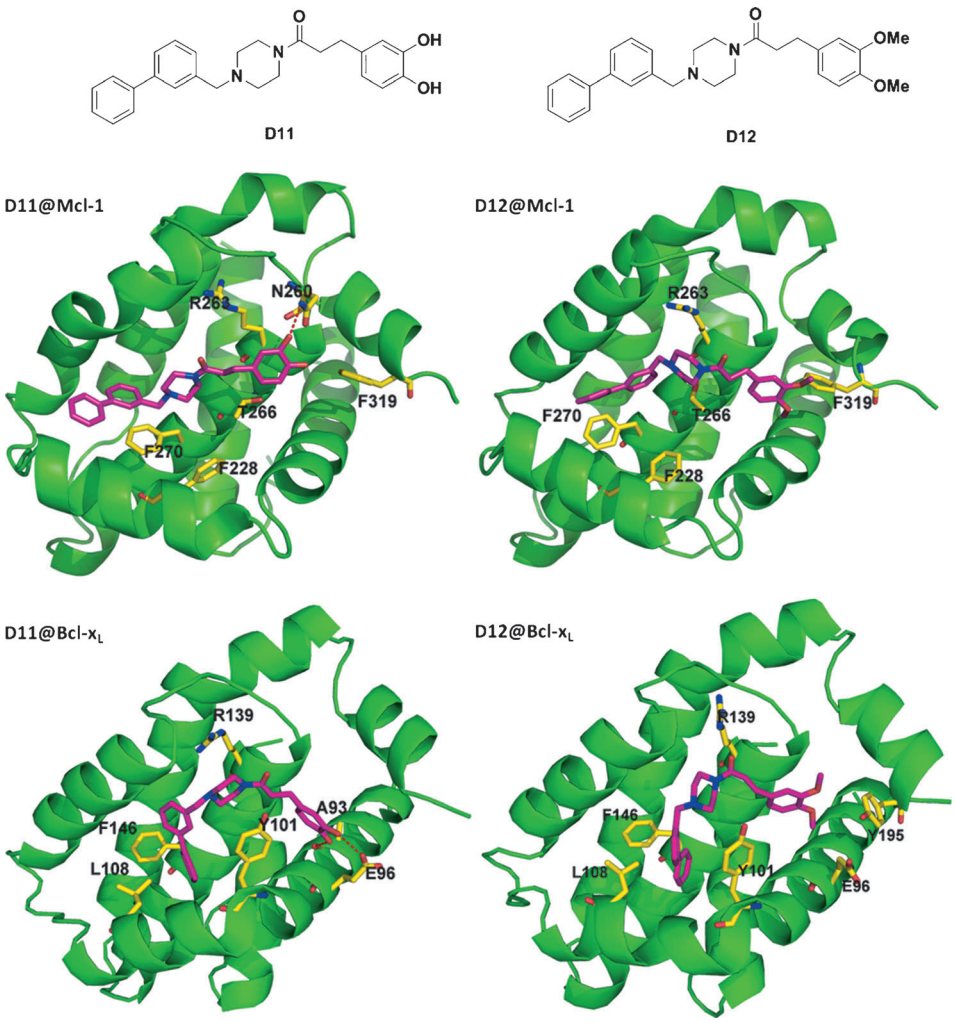

Figure 7. Chemical structures of **D11** and **D12** and their binding modes to Mcl-1 and Bcl-x_L derived through molecular modeling.

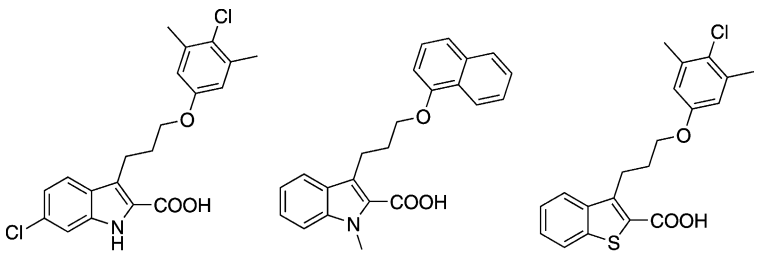

Figure 8. Chemical structures and binding data of several most potent Mcl-1 inhibitors recently reported by Friberg et al.[28]

7.2 Hz,1H), 3.65 (s, 2H), 2.80 (brs, 4H), 2.50 (brs, 2H), 2.38 (s, 3H), 2.26 ppm (brs, 2H); MS (ESI): *m/z* 267 $[M+H]^+$.

1-((4′-Methoxybiphenyl-2-yl)methyl)piperazine (2m): Prepared according to general procedure I from 2-bromobenzyl bromide and 4-methoxyphenylboronic acid (60%): ^{1}H NMR (300 Hz, $CDCl_3$): δ = 7.68 (d, J = 8.1 Hz, 2H), 7.50 (t, J = 7.8 Hz, 2H), 7.05–7.15 (m, 4H), 3.99 (s, 3H), 3.68 (s, 2H), 2.55 (brs, 4H), 2.24(brs, 2H), 2.18 ppm (brs, 2H); MS (ESI): *m/z* 283 $[M+H]^+$.

1-((4′-Nitrobiphenyl-2-yl)methyl)-piperazine (2n): Prepared according to general procedure I from 2-bromobenzyl bromide and 4-nitrophenylboronic acid (55%): ^{1}H NMR (300 Hz, $CDCl_3$): δ = 8.29 (d, J = 8.0 Hz, 2H), 7.82 (d, J = 7.8 Hz, 2H), 7.57–7.46 (m, 4H), 3.66 (s, 2H), 2.79 (brs, 4H), 2.55 ppm (brs, 4H); MS (ESI): *m/z* 298 $[M+H]^+$.

1-((4′-Chlorobiphenyl-3-yl)methyl)piperazine (2o): Prepared according to general procedure I from 3-bromobenzyl bromide and 4-chlorophenylboronic acid (54%): ^{1}H NMR (300 Hz, $CDCl_3$): δ = 8.01 (d, J = 7.8 Hz, 1H), 7.95 (d, J = 7.6 Hz, 1H), 7.80 (s, 1H), 7.45 (t, J = 7.4 Hz, 2H), 7.25–7.39 (m, 3H), 3.63 (s, 2H), 2.51 (brs, 4H), 2.43 ppm (brs, 4H); MS (ESI): *m/z* 287 $[M+H]^+$.

1-((4′-Fluorobiphenyl-3-yl)methyl)piperazine (2p): Prepared according to general procedure I from 3-bromobenzyl bromide and 4-fluorophenylboronic acid (56%): ^{1}H NMR (300 Hz, $CDCl_3$): δ = 7.81 (s, 1H), 7.68–7.58 (m, 4H), 7.29 (t, J = 7.8 Hz, 1H), 7.18 (d, J = 7.4 Hz, 2H), 3.59 (s, 2H), 2.47 (brs, 2H), 2.38 (brs, 2H), 2.29 ppm (brs, 4H); MS (ESI): *m/z* 271 $[M+H]^+$.

1-((4′-Methoxybiphenyl-3-yl)methyl)piperazine (2q): Prepared according to general procedure I from 3-bromobenzyl bromide and 4-methoxyphenylboronic acid (57%): ^{1}H NMR (300 Hz, $CDCl_3$): δ = 7.70 (s, 1H), 7.40–7.36 (m, 2H), 7.30 (d, J = 7.6 Hz, 1H), 7.20–7.12 (m, 4H), 3.89 (s, 3H), 3.68 (s, 2H), 2.82 (brs, 2H), 2.75 (brs, 2H), 2.38 (brs, 2H), 2.29 ppm (brs, 2H); MS (ESI): *m/z* 283 $[M+H]^+$.

1-((4′-Nitrobiphenyl-3-yl)methyl)piperazine (2r): Prepared according to general procedure I from 3-bromobenzyl bromide and 4-nitrophenylboronic acid (53%): ^{1}H NMR (300 Hz, $CDCl_3$): δ = 8.22 (d, J = 7.8 Hz, 2H), 7.85 (s, 1H), 7.76 (d, J = 7.9 Hz, 2H), 7.26–7.35 (m, 3H), 3.69 (s, 2H), 2.71 (brs, 4H), 2.45 (brs, 2H), 2.38 ppm (brs, 2H); MS (ESI): *m/z* 298 $[M+H]^+$.

1-((4′-Fluorobiphenyl-2-yl)methyl)piperazine (2s): Prepared according to general procedure I from 2-bromobenzyl bromide and 4-fluorophenylboronic acid (59%): ^{1}H NMR (300 Hz, $CDCl_3$): δ = 7.70 (d, J = 7.9 Hz, 1H), 7.30–7.37 (m, 4H), 7.29–7.33 (m, 2H), 7.21 (d, J = 7.6 Hz, 1H), 3.58 (s, 2H), 2.65 (brs, 2H), 2.57 (brs, 2H), 2.49 ppm (brs, 4H); MS (ESI): *m/z* 271 $[M+H]^+$.

1-((3′-Fluorobiphenyl-2-yl)methyl)piperazine (2t): Prepared according to general procedure I from 2-bromobenzyl bromide and

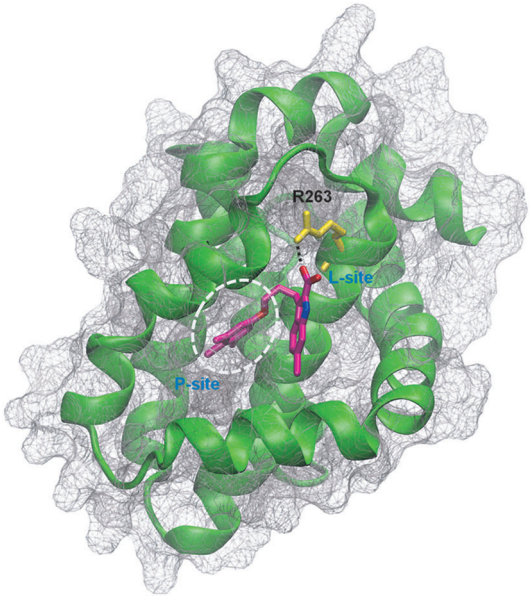

Figure 9. Crystal structure of Mcl-1 in complex with Friberg's compound **53** (PDB ID 4HW2) where the backbone of Mcl-1 is represented by green ribbons and **53** is shown in the stick model.

3-fluorophenylboronic acid (76%): ^{1}H NMR (400 Hz, $CDCl_3$): $\delta=$ 7.41–7.44 (m, 1H), 7.36–7.38 (m, 1H), 7.34–7.35 (m, 1H), 7.31–7.34 (m, 1H), 7.25–7.27 (m, 1H), 7.14–7.18 (m, 1H), 7.10–7.12 (m, 1H), 7.02–7.08 (m, 1H), 6.26 (s, 1H), 3.43 (s, 2H), 3.03 (t, $J=4.8$ Hz, 4H), 2.55 ppm (br s, 4H); MS (ESI): m/z 271 $[M+H]^+$.

General procedure II for the synthesis of 3a–l: **4-((2-(3,4,5-Trimethoxyphenyl)acetamido)methyl)benzoic acid (3a):** Et_3N (2.6 mmol) was added to a solution of 2-(3,4,5-trimethoxyphenyl)-acetic acid (1.7 mmol), 1-ethyl-3-(3-dimethylaminopropyl)carbodiimide (EDCI; 2.6 mmol) and hydroxybenzotriazole (HOBt; 1.7 mmol) in CH_2Cl_2 (60 mL), followed by methyl 4-(aminomethyl)benzoate (1.4 mmol). After heating at reflux for 4 h, the reaction mixture was diluted with H_2O (100 mL) and extracted with CH_2Cl_2. The organic phase was washed with saturated $NaHCO_3$ and brine, dried over Na_2SO_4, filtered and concentrated in vacuo. The crude compound (LC-MS: 373 $[M+H]^+$) was then dissolved in CH_3OH (20 mL), and 10% NaOH solution (20 mL) was added. The mixture was stirred at 60 °C for 2 h. CH_3OH was evaporated in vacuo, the reaction mixture was diluted with H_2O (100 mL) and extracted with CH_2Cl_2 (3×). The water layer was acidified with 6 N HCl. The formed precipitate was collected by filtration, washed with H_2O, and dried on the sintered glass to yield **3a** as a white solid (728 mg, 74%): ^{1}H NMR (300 Hz, $[D_6]$DMSO): $\delta=8.01$ (d, $J=7.8$ Hz,1H), 7.89 (d, $J=7.8$ Hz, 1H), 7.80–7.72 (m, 2H), 6.55 (s, 2H), 4.12 (s, 2H), 3.98 (s, 9H), 3.88 ppm (s, 2H); MS (ESI): m/z 358 $[M-H]^-$.

4-((3-(2,3-Dimethoxyphenyl)propanamido)methyl)benzoic acid (3b): Prepared according to general procedure II from 3-(3,4-dimethoxyphenyl)propanoic acid (420 mg, 72%): ^{1}H NMR (300 Hz, $[D_6]$DMSO): $\delta=8.09$ (d, $J=7.8$ Hz,1H), 7.89 (s, 1H), 7.62–7.55 (m, 3H), 6.85 (m, 2H), 4.32 (s, 2H), 3.97 (s, 6H), 3.12 (t, $J=7.6$ Hz, 2H), 2.49 ppm (t, $J=7.6$ Hz, 2H); MS (ESI): m/z 342 $[M-H]^-$.

4-((3-Hydroxybenzamido)methyl)benzoic acid (3c): Prepared according to general procedure II from 3-hydroxybenzoic acid (142 mg, 62%): ^{1}H NMR (300 Hz, $[D_6]$DMSO): $\delta=8.10$ (d, $J=$ 7.8 Hz,1H), 7.92 (s, 1H), 7.75–7.63 (m, 4H), 7.23 (d, $J=7.6$ Hz, 2H), 5.52 (s, 1H), 4.35 ppm (s, 2H); MS (ESI): m/z 270 $[M-H]^-$.

4-((3-(Methoxycarbonyl)benzylamino)methyl)benzoic acid (3d): Prepared according to general procedure II from methyl 3-(bromomethyl)benzoate (315 mg, 62%): ^{1}H NMR (300 Hz, $[D_6]$DMSO): $\delta=$ 8.10 (d, $J=7.8$ Hz, 1H),8.01 (s, 1H), 7.92 (d, $J=8.1$ Hz, 1H), 7.78 (s, 1H), 7.45–7.36 (m, 4H), 3.99 (s, 3H), 3.75 (s, 2H), 3.52 ppm (s, 2H); MS (ESI): m/z 299 $[M-H]^-$.

4-((2-(4-Methoxyphenyl)acetamido)methyl)benzoic acid (3e): Prepared according to general procedure II from 2-(4-methoxyphenyl)acetic acid (740 mg, 78%): ^{1}H NMR (300 Hz, $[D_6]$DMSO): $\delta=8.44$ (s, 1H), 7.75 (d, $J=7.5$ Hz, 2H), 7.20 (d, $J=8.1$ Hz, 2H), 7.08 (d, $J=$ 8.4 Hz, 2H), 6.87 (d, $J=8.7$ Hz,2H), 4.24 (s, 2H), 3.74 (s, 3H), 1.40 ppm (s, 2H); MS (ESI): m/z 298 $[M-H]^-$.

4-((2-(4-Fluorophenyl)acetamido)methyl)benzoic acid (3f): Prepared according to general procedure II from 2-(4-fluorophenyl)-acetic acid (366 mg, 75%): ^{1}H NMR (300 Hz, $[D_6]$DMSO): $\delta=8.48$ (s, 1H), 7.78 (d, $J=7.2$ Hz, 2H), 7.31 (d, $J=7.2$ Hz, 2H), 7.14 (m, $J=$ 7.2 Hz, 4H), 4.28 (s, 2H), 3.48 ppm (s, 2H); MS (ESI): m/z 286 $[M-H]^-$.

4-((2-(Thiophen-2-yl)acetamido)methyl)benzoic acid (3g): Prepared according to general procedure II from 2-(thiophen-3-yl)acetic acid (322 mg, 69%): ^{1}H NMR (300 Hz, $[D_6]$DMSO): $\delta=8.69$ (s, 1H), 7.89 (d, $J=7.8$ Hz, 2H), 7.36 (m, 3H), 6.96 (m, 2H), 4.35 (s, 2H), 3.82 ppm (s, 2H); MS (ESI): m/z 274 $[M-H]^-$.

4-((3-Methylbutanamido)methyl)benzoic acid (3h): Prepared according to general procedure II from 3-methylbutanoic acid (300 mg, 75%): ^{1}H NMR (300 Hz, $[D_6]$DMSO): $\delta=8.39$ (s, 1H), 7.88 (d, $J=8.1$ Hz, 2H), 7.34 (d, $J=7.8$ Hz, 2H), 4.32 (s, 2H), 2.03 (br s, 3H), 1.06 ppm (br s, 6H); MS (ESI): m/z 234 $[M-H]^-$.

4-((3-(2-Ethoxy-2-oxoethoxy)benzamido)methyl)benzoic acid (3i): Prepared according to general procedure II from 3-(2-ethoxy-2-oxoethoxy)benzoic acid (314 mg, 70%): ^{1}H NMR (300 Hz, $[D_6]$DMSO): $\delta=8.12$ (d, $J=7.8$ Hz, 1H), 8.01 (s, 1H), 7.82–7.71 (m, 3H), 7.18 (d, $J=8.0$ Hz, 2H),6.91 (s, 1H), 4.85 (s, 2H), 4.11 (q, $J=$ 6.9 Hz, 2H), 3.58 (s, 2H), 1.26 ppm (t, $J=6.9$ Hz, 3H); MS (ESI): m/z 356 $[M-H]^-$.

4-((3-(2-Bromo-4,5-dimethoxyphenyl)propanamido)methyl) benzoic acid (3j): Prepared according to general procedure II from 3-(2-bromo-4,5-dimethoxyphenyl)propanoic acid (536 mg, 72%): ^{1}H NMR (300 Hz, $[D_6]$DMSO): $\delta=8.10$ (d, $J=8.1$ Hz, 1H), 7.91 (s, 1H), 7.57–7.48 (m, 2H), 7.05 (d, $J=7.8$ Hz, 1H), 6.85 (s, 1H), 4.25 (s, 2H), 3.98 (s, 6H), 3.01 (t, $J=7.2$ Hz, 2H), 2.58 ppm (t, $J=7.2$ Hz, 2H); MS (ESI): m/z 420 $[M-H]^-$.

4-((3-(4′-Chloro-4,5-dimethoxybiphenyl-2-yl)propanamido)methyl) benzoic acid (3k): Prepared according to general procedure II from 3-(4′-chloro-4,5-dimethoxybiphenyl-2-yl)propanoic acid (591 mg, 74%): ^{1}H NMR (300 Hz, $CDCl_3$): $\delta=8.11$ (d, $J=7.8$ Hz, 1H), 7.90 (s, 1H), 7.62–7.51 (m, 4H), 7.12 (s, 1H), 7.03–6.85 (m, 3H), 4.32 (s, 2H), 3.97 (s, 6H), 3.12 (t, $J=7.6$ Hz, 2H), 2.49 ppm (t, $J=7.6$ Hz, 2H); MS (ESI): m/z 452 $[M-H]^-$.

General procedure III for the synthesis of 4a–g: **3-(2-(6-Bromo-2,3,4-trimethoxyphenyl)acetamido)benzoic acid (4a)**: Et_3N (2.6 mmol) was added to a solution of 2-(2-bromo-3,4,5-trimethoxyphenyl)acetic acid (1.7 mmol), EDCI (2.6 mmol) and HOBt (1.7 mmol), followed by methyl 3-aminobenzoate (1.4 mmol). After heating at reflux for 4 h, the reaction mixture was diluted with H_2O (100 mL) and extracted with CH_2Cl_2. The combined organic phases were washed with saturated $NaHCO_3$ and brine, dried over Na_2SO_4, filtered and concentrated in vacuo. The crude compound (LC-MS: 438 $[M+H]^+$) was dissolved in CH_3OH (20 mL), and 10% NaOH so-

lution (20 mL) was added. The mixture was stirred at 60 °C for 2 h. After CH_3OH was evaporated in vacuo, the reaction mixture was diluted with H_2O (100 mL) and extracted with CH_2Cl_2 (3×). The water layer was acidified with 6 N HCl. The formed precipitate was collected by filtration, washed with H_2O, and dried on the sintered glass to yield **4a** as a white solid (504 mg, 70%): ^{1}H NMR (300 Hz, $CDCl_3$): δ = 8.10 (s, 1H), 7.98–7.81 (m, 3H), 6.55 (s, 1H), 4.01 (s, 9H), 3.78 ppm (s, 2H); MS (ESI): *m/z* 422 $[M-H]^-$.

3-(2-(4′-Chloro-3,4,5-trimethoxy-[1,1′-biphenyl]-2-yl)acetamido)-benzoic acid (4b): Prepared according to general procedure III from 2-(4′-chloro-4,5,6-trimethoxy-3-methylbiphenyl-2-yl)acetic acid (504 mg, 62%): ^{1}H NMR (300 Hz, $CDCl_3$): δ = 8.36 (s, 1H), 7.98 (d, *J* = 8.0 Hz, 2H), 7.75 (d, *J* = 7.8 Hz, 2H), 7.68–7.56 (m, 3H), 6.58 (s, 1H), 3.98 (s, 9H), 3.78 ppm (s, 2H); MS (ESI): *m/z* 454 $[M-H]^-$.

3-(3,5-Dimethoxybenzamido)benzoic acid (4c): Prepared according to general procedure III from 3,5-dimethoxybenzoic acid (394 mg, 77%): ^{1}H NMR (300 Hz, $CDCl_3$): δ = 8.35 (s, 1H), 7.95–7.84 (m, 3H), 6.87 (s, 1H), 6.59 (s, 2H), 3.98 ppm (s, 6H); MS (ESI): *m/z* 300 $[M-H]^-$.

3-(2-(3,5-Dimethoxyphenyl)acetamido)benzoic acid (4d): Prepared according to general procedure III from 2-(3,5-dimethoxyphenyl)acetic acid (397 mg, 74%): ^{1}H NMR (300 Hz, $CDCl_3$): δ = 8.35 (s, 1H), 7.85–7.76 (m, 3H), 6.65 (s, 1H), 6.52 (s, 2H), 4.01 (s, 2H), 3.89 ppm (s, 6H); MS (ESI): *m/z* 314 $[M-H]^-$.

3-(2-Cyclohexylacetamido)benzoic acid (4e): Prepared according to general procedure III from 2-cyclohexylacetic acid (320 mg, 72%): ^{1}H NMR (300 Hz, $CDCl_3$): δ = 8.45 (s, 1H), 7.95 (d, *J* = 7.8 Hz, 2H), 7.84–7.76 (m, 1H), 2.35 (d, *J* = 6.5 Hz, 2H), 2.09–1.94 (m, 1H), 1.19–1.14 (m, 4H), 1.07–0.98 ppm (m, 6H); MS (ESI): *m/z* 260 $[M-H]^-$.

3-(2-Naphthamido)benzoic acid (4f): Prepared according to general procedure III from 2-naphthoic acid (366 mg, 74%): ^{1}H NMR (300 Hz, $CDCl_3$): δ = 8.56 (s, 1H), 8.23 (s, 2H), 8.01 (d, *J* = 7.8 Hz, 2H), 7.64–7.59 (m, 3H), 7.48–7.39 ppm (m, 3H); MS (ESI): *m/z* 290 $[M-H]^-$.

3-(2-(Naphthalen-2-yl)acetamido)benzoic acid (4g): Prepared according to general procedure III from 2-(naphthalen-2-yl)acetic acid (389 mg, 75%): ^{1}H NMR (300 Hz, $CDCl_3$): δ = 8.45 (s, 1H), 8.18 (s, 2H), 8.00 (d, *J* = 8.0 Hz, 2H), 7.70–7.61 (m, 3H), 7.45–7.36 (m, 3H), 4.10 ppm (s, 2H); MS (ESI): *m/z* 304 $[M-H]^-$.

General procedure IV for the synthesis of 8a,b: **2-(3-(Azidomethyl)phenoxy)acetic acid (8a)**: K_2CO_3 (16.2 mmol) and ethyl bromoacetate (8.1 mmol) was added to a solution of 3-hydroxybenzyl alcohol (8.1 mmol) in acetone (40 mL). After heating at reflux for 12 h, the reaction mixture was diluted with H_2O (100 mL) and extracted with EtOAc. The combined organic phases were washed with H_2O and brine, dried over Na_2SO_4, filtered and concentrated in vacuo. The crude compound was purified by chromatography with *n*-pentane/EtOAc (4:1 *v/v*) to afford **5a** as a white solid (LC-MS: 197 $[M+H]^+$). Ph_3P (4.2 mmol) was added to a solution of **5a** (3.8 mmol) in dry tetrahydrofuran (THF; 50 mL) under a nitrogen atmosphere. N-bromosuccinimide (NBS; 4.2 mmol) was added to the reaction mixture 5 min later. After stirring at RT for 2 h, the solvent was evaporated in vacuo. H_2O (50 mL) was added, and the aqueous layer was back-extracted with CH_2Cl_2. The combined organic phases were washed with H_2O and brine, dried over Na_2SO_4, filtered and concentrated in vacuo. The crude compound was purified by chromatography with *n*-pentane/EtOAc (8:1 *v/v*) to afford **6a** as a white solid (LC-MS: 259 $[M+H]^+$). NaN_3 (5.5 mmol) was added to a solution of **6a** (3.7 mmol) in acetone (40 mL). The reaction mixture was stirred at 60 °C for 2 h. After filtration, the solvent was evaporated in vacuo. The crude compound (LC-MS: 222 $[M+H]^+$) was dissolved in THF (20 mL), followed by the addition of H_2O (20 mL) and LiOH (18.5 mmol). The reaction mixture was stirred at RT for 12 h. 1 N HCl solution was added, and the formed precipitate was collected by filtration, washed with H_2O, and dried on the sintered glass to yield **8a** as white solid (390 mg, 73%): ^{1}H NMR (300 Hz, $CDCl_3$): δ = 7.35 (m, 1H), 7.21 (s, 1H), 7.10 (d, *J* = 7.4 Hz, 2H), 4.56 (s, 2H), 2.98 ppm (s, 2H); MS (ESI): *m/z* 206 $[M-H]^-$.

2-(3-(Azidomethyl)phenylamino)acetic acid (8b): Prepared according to general procedure IV from 3-aminobenzyl alcohol (61%): ^{1}H NMR (300 Hz, $CDCl_3$): δ = 7.25 (m, 1H), 7.12 (d, *J* = 7.8 Hz, 2H), 7.01 (s, 1H), 4.21 (s, 2H), 2.87 ppm (s, 2H); MS (ESI): *m/z* 205 $[M-H]^-$.

General procedure V for the synthesis of 9a–h: **1-((4′-Methoxybiphenyl-2-yl)methyl)-4-(prop-2-ynyl)piperazine (9a)**: K_2CO_3 (3.50 mmol) and 3-bromo-1-propyne (1.75 mmol) was added to a mixture **2m** (1.75 mmol) in CH_2Cl_2 (40 mL). After heating at reflux for 12 h, the reaction mixture was diluted with H_2O (100 mL) and extracted with CH_2Cl_2. The combined organic phases were washed with H_2O and brine, dried over Na_2SO_4, filtered and concentrated in vacuo. The crude compound was purified by chromatography with *n*-pentane/EtOAc (8:1 *v/v*) to afford **9a** as a white solid (510 mg, 90%): ^{1}H NMR (300 Hz, $CDCl_3$): δ = 7.67 (d, *J* = 7.8 Hz, 2H), 7.51 (t, *J* = 8.0 Hz, 2H), 7.05–7.15 (m, 4H), 3.99 (s, 3H), 3.68 (s, 2H), 3.52 (s, 2H), 2.55 (br s, 4H), 2.24 (br s, 2H), 2.18 (br s, 2H), 2.02 ppm (m, 1H); MS (ESI): *m/z* 321 $[M+H]^+$.

1-((4′-Nitrobiphenyl-2-yl)methyl)-4-(prop-2-ynyl)piperazine (9b): Prepared according to general procedure V from **2n** (91%): ^{1}H NMR (300 Hz, $CDCl_3$): δ = 8.31 (d, *J* = 8.0 Hz, 2H), 7.92 (d, *J* = 7.8 Hz, 2H), 7.60–7.46 (m, 4H), 3.66 (s, 2H), 3.58 (s, 2H), 2.79 (br s, 4H), 2.68 (m, 1H), 2.50 (br s, 2H), 2.39 ppm (br s, 2H); MS (ESI): *m/z* 336 $[M+H]^+$.

1-((4′-Chlorobiphenyl-3-yl)methyl)-4-(prop-2-ynyl)piperazine (9c): Prepared according to general procedure V from **2o** (89%): ^{1}H NMR (300 Hz, $CDCl_3$): δ = 8.10 (d, *J* = 7.8 Hz, 1H), 7.85 (d, *J* = 7.6 Hz, 1H), 7.78 (s, 1H), 7.45 (t, *J* = 7.4 Hz, 1H), 7.25–7.39 (m, 4H), 3.90 (s, 2H), 3.63 (s, 2H), 2.51 (br s, 4H), 2.43 (m, 2H), 2.56 (m, 1H), 2.32 ppm (m, 2H); MS (ESI): *m/z* 325 $[M+H]^+$.

1-((4′-Fluorobiphenyl-3-yl)methyl)-4-(prop-2-ynyl)piperazine (9d): Prepared according to general procedure V from **2p** (92%): ^{1}H NMR (300 Hz, $CDCl_3$): δ = 7.90 (s, 1H), 7.68–7.58 (m, 4H), 7.31 (t, *J* = 8.1 Hz, 1H), 7.20 (d, *J* = 7.8 Hz, 2H), 4.00 (s, 2H), 3.59 (s, 2H), 2.61 (m, 1H), 2.47 (br s, 4H), 2.38 (br s, 2H), 2.29 ppm (br s, 2H); MS (ESI): *m/z* 309 $[M+H]^+$.

1-((4′-Methoxybiphenyl-3-yl)methyl)-4-(prop-2-ynyl)piperazine (9e): Prepared according to general procedure V from **2q** (90%): ^{1}H NMR (300 Hz, $CDCl_3$): δ = 7.65 (s, 1H), 7.42–7.38 (m, 4H), 7.28 (d, *J* = 7.6 Hz, 1H), 7.20–7.12 (m, 2H), 3.89 (s, 3H), 3.68 (s, 2H), 3.59 (s, 2H), 2.82 (br s, 2H), 2.75 (br s, 2H), 2.38 (br s, 2H), 2.29 (br s, 2H), 2.34 ppm (m, 1H); MS (ESI): *m/z* 321 $[M+H]^+$.

1-((4′-Nitrobiphenyl-3-yl)methyl)-4-(prop-2-ynyl)piperazine (9f): Prepared according to general procedure V from **2r** (87%): ^{1}H NMR (300 Hz, $CDCl_3$): δ = 8.29 (d, *J* = 7.8 Hz, 2H), 7.98 (s, 1H), 7.86 (d, *J* = 7.9 Hz, 2H), 7.58–7.43 (m, 3H), 3.78 (s, 2H), 3.69 (s, 2H), 2.71 (br s, 4H), 2.45 (br s, 2H), 2.38 (br s, 2H), 2.28 ppm (m, 1H); MS (ESI): *m/z* 336 $[M+H]^+$.

1-((4′-Chlorobiphenyl-2-yl)methyl)-4-(prop-2-ynyl)piperazine (9g): Prepared according to general procedure V from **2h** (90%):

^{1}H NMR (300 Hz, $CDCl_3$): δ = 7.73 (d, J = 7.8 Hz, 2H), 7.54 (m, 4H), 7.30 (m, 2H), 3.89 (s, 2H), 3.66 (s, 2H), 2.85 (brs, 4H), 2.65 (m, 1H), 2. 35 (brs, 2H), 2.24 ppm (brs, 2H); MS (ESI): m/z 325 $[M+H]^+$.

1-((4′-Fluorobiphenyl-2-yl)methyl)-4-(prop-2-ynyl)piperazine (9h): Prepared according to general procedure V from **2s** (93%): ^{1}H NMR (300 Hz, $CDCl_3$): δ = 7.67 (d, J = 7.9 Hz, 1H), 7.37–7.29 (m, 4H), 7.33–7.19 (m, 2H), 7.02 (d, J = 7.6 Hz, 1H), 3.76 (s, 2H), 3.58 (s, 2H), 2.65 (brs, 4H), 2.58 (m, 1H), 2.49 (brs, 2H), 2.38 ppm (brs, 2H); MS (ESI): m/z 309 $[M+H]^+$.

General procedure VI for the synthesis of 10a–e: **4-(4-{[3-(4-Fluorophenyl)phenyl]methyl}piperazin-1-yl)-4-oxobutanoic acid (10a)**: Dihydrofuran-2,5-dione (0.47 mmol) was added to a mixture of **2p** (0.39 mmol) in CH_2Cl_2 (2 mL). After heating to 40 °C for about 1.5 h, the starting material disappeared as monitored by TLC. The reaction mixture was diluted with H_2O (20 mL) and extracted with CH_2Cl_2. The combined organic phases were washed with brine, dried over Na_2SO_4, filtered and concentrated in vacuo. The crude compound was purified by chromatography with CH_2Cl_2/MeOH (20:1 *v/v*) to afford **10a** as a yellow oil (76 mg, 52%): ^{1}H NMR (400 Hz, $CDCl_3$): δ = 7.55–7.57 (m, 1H), 7.54 (m, 1H), 7.51 (s, 1H), 7.47 (d, J = 7.6 Hz, 1H), 7.38–7.42 (t, J = 7.2 Hz, 1H), 7.29–7.31 (d, J = 7.6 Hz, 1H), 7.11–7.15 (t, J = 8.8 Hz, 2H), 3.82 (s, 2H), 3.66 (m, 4H), 3.53–3.55 (t, J = 4.2 Hz, 2H), 2.62–2.67 (m, 4H), 2.53–2.56 ppm (m, 4H); MS (ESI): m/z 371 $[M+H]^+$.

4-(4-{[3-(4-Chlorophenyl)phenyl]methyl}piperazin-1-yl)-4-oxobutanoic acid (10b): Prepared according to general procedure VI from **2o** (80%): ^{1}H NMR ($CDCl_3$): δ = 7.56 (s, 1H), 7.54 (m, 1H), 7.53 (m, 1H), 7.49–7.51 (d, J = 7.6 Hz, 1H), 7.40–7.44 (m, 3H), 7.33–7.35 (d, J = 7.6 Hz, 1H), 3.70 (s, 4H), 3.59 (s, 2H), 2.59–2.69 ppm (m, 8H); MS (ESI): m/z 387 $[M+H]^+$.

4-Oxo-4-{4-[(3-phenylphenyl)methyl]piperazin-1-yl}butanoic acid (10c): Prepared according to general procedure VI from **2b** (91%): ^{1}H NMR ($CDCl_3$): δ = 8.45 (s, 1H), 7.58 (s, 1H), 7.57 (s, 1H), 7.54 (s, 1H), 7.50 (d, J = 8.0 Hz, 1H), 7.42 (t, J = 8.0 Hz, 2H), 7.37 (d, J = 7.6 Hz, 1H), 7.32 (t, J = 7.6 Hz, 1H), 7.28 (d, J = 7.6 Hz, 1H), 3.63 (s, 2H), 3.61 (brs, 2H), 3.48 (brs, 2H), 2.50–2.56 ppm (m, 8H); MS (ESI): m/z 353 $[M+H]^+$.

5-Oxo-5-{4-[(3-phenylphenyl)methyl]piperazin-1-yl}pentanoic acid (10d): Prepared according to general procedure VI from **2b** and dihydro-2*H*-pyran-2,6(3*H*)-dione (89%): ^{1}H NMR ($CDCl_3$): δ = 9.90 (s, 1H), 7.59–7.60 (m, 1H), 7.58 (s, 1H), 7.55 (m, 2H), 7.43–7.46 (m, 2H), 7.40–7.42 (t, J = 6.8 Hz, 1H), 7.33–7.37 (m, 1H), 7.29–7.31 (d, J = 7.7 Hz, 1H), 3.70–3.74 (m, 4H), 3.56 (s, 2H), 2.62 (s, 4H), 2.37–2.42 (m, 4H), 1.88–1.95 ppm (m, 2H); MS (ESI): m/z 367 $[M+H]^+$.

5-(4-{[3-(4-Chlorophenyl)phenyl]methyl}piperazin-1-yl)-5-oxopentanoic acid (10e): Prepared according to general procedure VI from **2o** and dihydro-2*H*-pyran-2,6(3*H*)-dione (75%): ^{1}H NMR ($CDCl_3$): δ = 7.52 (m, 1H), 7.50–7.51 (m, 2H), 7.47–7.49 (m, 1H), 7.42 (d, J = 3.2 Hz, 1H), 7.40–7.41 (m, 1H), 7.38–7.39 (d, J = 3.2 Hz, 1H), 7.29–7.31 (d, J = 7.6 Hz, 1H), 3.65 (m, 4H), 3.50–3.53 (t, J = 4.8 Hz, 2H), 2.51–2.56 (m, 4H), 2.37–2.41 (m, 4H), 1.89–1.96 ppm (m, 2H); MS (ESI): m/z 401 $[M+H]^+$.

General procedure VII for the synthesis of A1–A27, B1–B3, B5–B17: ***N*-(4-(4-(biphenyl-2-ylmethyl)piperazine-1-carbonyl)benzyl)-2-(3,4,5-trimethoxyphenyl)acetamide (A1)**: 1-[Bis(dimethylamino)-methylene]-1*H*-1,2,3-triazolo[4,5-*b*]pyridinium 3-oxid hexafluorophosphate (HATU; 1.2 mmol) and *N*,*N*-diisopropylethylamine (DIPEA; 1.5 mmol) was added to a solution of **3a** (1.0 mmol) in dry DMF (10 mL). After stirring at −10 °C for 30 min, **2a** (0.8 mmol) was added, and the reaction mixture was stirred at −10 °C for 2 h and then warmed to RT and stirred overnight. The solvent was evaporated in vacuo, and the mixture was diluted with H_2O (100 mL) and extracted with CH_2Cl_2. The organic phases were washed with saturated $NaHCO_3$ and brine, dried over Na_2SO_4, filtered and concentrated in vacuo. The crude compound was purified by chromatography with CH_2Cl_2/CH_3OH (20:1 *v/v*) to afford **A1** as a white solid (114 mg, 80%): HPLC: 96.16%, t_R = 1.462 min; ^{1}H NMR ($CDCl_3$): δ = 7.51–7.49 (m, 1H), 7.39–7.32 (m, 6H), 7.31–7.27 (m, 2H), 7.17 (d, J = 8.4 Hz,2H), 6.48 (d, J = 7.5 Hz,4H), 4.00 (s, 2H), 3.84 (s, 3H), 3.82 (s, 6H), 3.73 (t, J = 6.3 Hz, 2H), 3.55 (s, 2H), 3.44 (s, 2H), 3.26 (t, J = 6.3 Hz, 2H), 2.39–2.24 ppm (br, 4H); MS (ESI): m/z 594 $[M+H]^+$; HRMS (ESI): m/z $[M+H]^+$ calcd for $C_{36}H_{39}N_3O_5$: 594.2890, observed: 594.2979.

***N*-(4-(4-(Biphenyl-3-ylmethyl)piperazine-1-carbonyl)benzyl)-2-(3,4,5-trimethoxyphenyl)acetamide (A2)**: Prepared according to general procedure VII from **2b** and **3a** (115 mg, 81%): HPLC: 97.60%, t_R = 1.331 min; ^{1}H NMR (300 Hz, [D$_6$]DMSO): δ = 8.65 (m, 1H), 7.71–7.68 (m, 3H), 7.53–7.48 (m, 3H), 7.43-.30 (m, 6H), 6.59 (s, 2H), 4.32 (d, J = 5.4 Hz, 2H), 3.74 (s, 6H), 3.63 (s, 3H), 3.42 (brs, 4H), 3.34 (brs, 4H), 2.51 (brs, 2H), 2.02 ppm (brs, 2H); MS (ESI): m/z 594 $[M+H]^+$; HRMS (ESI): m/z $[M+H]^+$ calcd for $C_{36}H_{40}N_3O_5$: 594.2890, observed: 594.2995.

***N*-(4-(4-(Biphenyl-4-ylmethyl)piperazine-1-carbonyl)benzyl)-2-(3,4,5-trimethoxyphenyl)acetamide (A3)**: Prepared according to general procedure VII from **2c** and **3a** (120 mg, 84%): HPLC: 95.06%, t_R = 1.323 min; ^{1}H NMR (300 Hz, [D$_6$]DMSO): δ = 8.57–8.54 (m, 1H), 7.70–7.67 (m, 3H), 7.51–7.30 (m, 9H), 6.59 (s, 2H), 4.32 (d, J = 5.4 Hz, 2H), 3.74 (s, 6H), 3.63 (s, 3H), 3.52–3.47 (m, 4H), 3.43 (brs, 2H), 2.52 (brs, 2H), 2.01 ppm (brs, 2H); MS (ESI): m/z 594 $[M+H]^+$; HRMS (ESI): m/z $[M+H]^+$calcd for $C_{36}H_{40}N_3O_5$: 594.2890, observed: 594.2999.

***N*-(4-(4-((2′-Chlorobiphenyl-2-yl)methyl)piperazine-1-carbonyl)-benzyl)-2-(3,4,5-trimethoxyphenyl)acetamide (A4)**: Prepared according to general procedure VII from **2d** and **3a** (121 mg, 80%): HPLC: 96.62%, t_R = 1.747 min; ^{1}H NMR (300 Hz, [D$_6$]DMSO): δ = 8.56–8.52 (m, 1H), 7.82 (d, J = 6.9 Hz, 1H), 7.51–7.45 (m, 5H), 7.40–7.31 (m, 5H), 6.59 (s, 2H), 4.31 (d, J = 6.0 Hz, 2H), 3.74 (s, 6H), 3.64 (s, 3H), 3.50 (s, 2H), 3.42 (s, 2H), 3.36 (brs, 4H), 2.52 ppm (brs, 4H); MS (ESI): m/z 628 $[M+H]^+$; HRMS (ESI): m/z $[M]^+$calcd for $C_{36}H_{39}ClN_3O_5$: 627.2500, observed: 627.2511.

***N*-(4-(4-((3′-Chloro-4′-fluorobiphenyl-2-yl)methyl)piperazine-1-carbonyl)benzyl)-2-(3,4,5-trimethoxyphenyl)acetamide (A5)**: Prepared according to general procedure VII from **2e** and **3a** (110 mg, 71%): HPLC: 100%, t_R = 2.246 min; ^{1}H NMR (300 Hz, [D$_6$]DMSO): δ = 8.61–8.59 (m, 1H), 7.55–7.52 (m, 1H), 7.42–7.26 (m, 9H), 6.59 (s, 2H), 4.27 (d, J = 4.5 Hz, 2H), 3.73 (s, 6H), 3.63 (s, 3H), 3.42–3.19 (brs, 6H), 3.16 (brs, 2H), 2.13 ppm (brs, 4H); MS (ESI): m/z 646 $[M+H]^+$; HRMS (ESI): m/z $[M]^+$ calcd for $C_{36}H_{38}ClFN_3O_5$: 645.2406, observed: 645.2417.

***N*-(4-(4-((5-Fluorobiphenyl-2-yl)methyl)piperazine-1-carbonyl)-benzyl)-2-(3,4,5-trimethoxyphenyl)acetamide (A6)**: Prepared according to general procedure VII from **2f** and **3a** (106 mg, 72%): HPLC: 98.55%, t_R = 1.351 min; ^{1}H NMR (300 Hz, [D$_6$]DMSO): δ = 8.55–8.53 (m, 1H), 7.73–7.70 (m, 2H), 7.51–7.40 (m, 5H), 7.34–7.29 (m, 5H), 6.59 (s, 2H), 4.31 (d, J = 5.7 Hz, 2H), 3.74 (s, 6H), 3.69 (s, 3H), 3.63 (s, 2H), 3.53 (s, 2H), 3.49 (brs, 4H), 2.46 ppm (brs, 4H); MS (ESI): m/z 612 $[M+H]^+$; HRMS (ESI): m/z $[M]^+$ calcd for $C_{36}H_{39}FN_3O_5$: 611.2795, observed: 611.2799.

***N*-(4-(4-(Naphthalen-2-ylmethyl)piperazine-1-carbonyl)benzyl)-2-(3,4,5-trimethoxyphenyl)acetamide (A7)**: Prepared according to general procedure VII from **2g** and **3a** (110 mg, 84%): HPLC: 100%, t_R = 1.158 min; ^{1}H NMR (300 Hz, [D$_6$]DMSO): δ = 8.58 (br s, 1H), 8.28 (d, J = 6.9 Hz, 1H), 7.94–7.84 (m, 2H), 7.54–7.45 (m, 4H), 7.35–7.29 (m, 4H), 6.59 (s, 2H), 4.31 (d, J = 5.4 Hz, 2H), 3.92 (s, 2H), 3.74 (s, 6H), 3.69 (s, 3H), 3.46 (s, 2H), 3.42 (br s, 4H), 2.48 ppm (br s, 4H); MS (ESI): *m/z* 568 $[M+H]^+$; HRMS (ESI): *m/z* $[M+H]^+$ calcd for $C_{34}H_{38}N_3O_5$: 568.2733, observed: 568.2741.

***N*-(4-(4-(3,4,5-Trimethoxybenzyl)piperazine-1-carbonyl)benzyl)-2-(3,4,5-trimethoxyphenyl)acetamide (A8)**: Prepared according to general procedure VII from 1-(3,4,5-trimethoxybenzyl)piperazine and **3a** (123 mg, 81%): HPLC: 98.94%, t_R = 0.738 min; ^{1}H NMR (300 Hz, [D$_6$]DMSO): δ = 7.34–7.31 (m, 4H), 6.99 (d, J = 8.4 Hz, 1H), 6.77 (d, J = 9.0 Hz, 1H), 6.59 (s, 2H), 4.31 (d, J = 5.7 Hz, 2H), 3.78 (s, 6H), 3.74 (s, 9H), 3.69 (s, 3H), 3.55 (br s, 4H), 3.55–3.42 (m, 4H), 2.38 ppm (br s, 4H); MS (ESI): *m/z* 608 $[M+H]^+$; HRMS (ESI): *m/z* $[M+H]^+$ calcd for $C_{33}H_{41}N_3O_8$: 608.2794, observed: 608.2799.

***N*-(4-(4-(Biphenyl-2-ylmethyl)piperazine-1-carbonyl)benzyl)-3-(3,4-dimethoxyphenyl)propanamide (A9)**: Prepared according to general procedure VII from **2a** and **3b** (104 mg, 75%): HPLC: 98.39%, t_R = 1.597 min; ^{1}H NMR (300 Hz, CDCl$_3$): δ = 7.52–7.49(m, 1H), 7.39–7.31 (m, 6H), 7.21 (d, J = 8.1 Hz, 2H), 7.06 (d, J = 7.5 Hz, 2H), 7.80–6.71 (m, 5H), 4.34 (d, J = 6.0 Hz, 2H), 3.86 (s, 3H), 3.82 (s, 3H), 3.69 (t, J = 6.9 Hz, 2H), 3.44 (s, 2H), 3.29 (t, J = 6.9 Hz, 2H), 2.92 (t, J = 6.3 Hz, 2H), 2.51 (t, J = 7.2 Hz, 2H), 2.39–2.31 ppm (br, 4H); MS (ESI): *m/z* 578 $[M+H]^+$; HRMS (ESI): *m/z* $[M+H]^+$ calcd for $C_{38}H_{39}N_3O_4$: 578.2941, observed: 578.3046.

***N*-(4-(4-(Biphenyl-3-ylmethyl)piperazine-1-carbonyl)benzyl)-3-(3,4-dimethoxyphenyl)propanamide (A10)**: Prepared according to general procedure VII from **2b** and **3b** (96 mg, 69%): HPLC: 95.88%, t_R = 1.469 min; ^{1}H NMR (300 Hz, [D$_6$]DMSO): δ = 8.39 (m, 1H), 7.64 (m, 4H), 7.45–7.18 (m, 8H), 6.81–6.71 (m, 3H), 4.27 (s, 2H), 3.69 (s, 6H), 3.55 (br s, 4H), 3.17–3.10 (m, 2H), 2.96–2.70 (m, 2H), 2.43 ppm (br, 4H); MS (ESI): *m/z* 578 $[M+H]^+$; HRMS (ESI): *m/z* $[M+H]^+$ calcd for $C_{38}H_{40}N_3O_4$: 578.2941, observed: 578.2956.

***N*-(4-(4-(Biphenyl-4-ylmethyl)piperazine-1-carbonyl)benzyl)-3-(3,4-dimethoxyphenyl)propanamide (A11)**: Prepared according to general procedure VII from **2c** and **3b** (100 mg, 72%): HPLC: 97.05%, t_R = 1.472 min; ^{1}H NMR (300 Hz, [D$_6$]DMSO): δ = 8.38–8.35 (m, 1H), 7.68–7.57 (m, 4H), 7.51–7.28 (m, 7H), 7.18–7.16 (m, 2H), 6.85–6.70 (m, 3H), 4.29 (d, J = 5.4 Hz, 2H), 3.70 (s, 6H), 3.77–3.64 (m, 4H), 3.52 (br s, 2H), 3.18–3.11 (m, 2H), 2.82–2.51 (m, 2H), 2.47–2.42 ppm (br, 4H); MS (ESI): *m/z* 578 $[M+H]^+$; HRMS (ESI): *m/z* $[M+H]^+$ calcd for $C_{38}H_{40}N_3O_4$: 578.2941, observed: 578.2963.

***N*-(4-(4-(Biphenyl-3-ylmethyl)piperazine-1-carbonyl)benzyl)-3-hydroxybenzamide (A12)**: Prepared according to general procedure VII from **2b** and **3c** (83 mg, 68%): HPLC: 98.20%, t_R = 1.126 min; ^{1}H NMR (300 Hz, CDCl$_3$): δ = 8.84 (s, 1H), 7.78 (d, J = 8.7 Hz, 2H), 7.65 (d, J = 7.5 Hz, 2H), 7.58 (s, 2H), 7.54–7.31 (m, 8H), 6.82 (d, J = 8.4 Hz, 2H), 4.47 (d, J = 5.1 Hz, 2H), 3.75–3.58 (br, 4H), 2.51 (s, 2H), 2.43 ppm (br, 4H); MS (ESI): *m/z* 506 $[M+H]^+$; HRMS (ESI): *m/z* $[M+H]^+$ calcd for $C_{32}H_{31}N_3O_3$: 506.2365, observed: 506.2425.

***N*-(4-(4-(Biphenyl-4-ylmethyl)piperazine-1-carbonyl)benzyl)-3-hydroxybenzamide (A13)**: Prepared according to general procedure VII from **2c** and **3c** (75 mg, 62%): HPLC: 97.61%, t_R = 1.154 min; ^{1}H NMR (300 Hz, CDCl$_3$): δ = 8.84 (s, 1H), 7.78 (d, J = 8.4 Hz,2H), 7.65 (t, J = 8.7 Hz, 5H), 7.49–7.36 (m, 7H), 6.81 (d, J = 9.0 Hz, 2H), 4.48 (d, J = 6.0 Hz, 2H), 3.66–3.55 (br, 4H), 2.51 (s, 2H), 2.41 ppm (br, 4H); MS (ESI): *m/z* 506 $[M+H]^+$; HRMS (ESI): *m/z* $[M+H]^+$ calcd for $C_{32}H_{31}N_3O_3$: 506.2365, observed: 506.2330.

3-((4-(4-(Biphenyl-3-ylmethyl)piperazine-1-carbonyl)benzylamino)methyl)benzoic acid (A14): According to the general procedure VII, we obtained the ester intermediate from **3d** and **2c** as crude material. The crude was dissolved in MeOH (10 mL) and 2 N aq NaOH (10 mL) was added. The reaction was stirred for a further 3 h, and then 1 N HCl was added until a white solid formed. The mixture was then filtered, and the solid was dried to give **A14** as a white solid (76 mg, 61%): HPLC: 97.34%, t_R = 1.105 min; ^{1}H NMR (300 Hz, CDCl$_3$): δ = 8.03 (s, 2H), 7.91 (d, J = 7.8 Hz, 2H), 7.62–7.58 (m, 4H), 7.56 (s, 1H), 7.44–7.39 (m, 7H), 7.30 (d, J = 7.2 Hz, 1H), 3.81 (s, 2H), 3.60 (s, 4H), 3.57 (s, 2H), 3.44 (s, 2H), 2.58–2.43 ppm (br, 4H); MS (ESI): *m/z* 518 $[M-H]^-$; HRMS (ESI): *m/z* $[M+H]^+$ calcd for $C_{33}H_{34}N_3O_3$: 520.2522, observed: 520.2531.

3-((4-(4-(Biphenyl-4-ylmethyl)piperazine-1-carbonyl)benzylamino)methyl)benzoic acid (A15): Prepared according to general procedure VII from **3d** and **2b** as described above for **A14**, to **A14** as a white solid (79 mg, 63%): HPLC: 98.53%, t_R = 1.119 min; ^{1}H NMR (300 Hz, CDCl$_3$): δ = 7.78 (d, J = 9.0 Hz, 2H), 7.56 (t, J = 8.7 Hz, 4H), 7.45–7.31 (m, 8H), 7.26 (s, 1H), 6.89 (d, J = 9.0 Hz, 2H), 4.64 (s, 2H), 4.59 (d, J = 6.0 Hz, 2H), 3.79 (br s, 2H), 3.57 (s, 2H), 3.43 (br s, 2H), 2.55–2.41 ppm (br, 4H); MS (ESI): *m/z* 518 $[M-H]^-$; HRMS (ESI): *m/z* $[M+H]^+$ calcd for $C_{33}H_{33}N_3O_3$: 520.2522, observed: 520.2582.

***N*-(4-(4-(Biphenyl-3-ylmethyl)piperazine-1-carbonyl)benzyl)-2-(4-methoxyphenyl)acetamide (A16)**: Prepared according to general procedure VII from **2b** and **3e** (113 mg, 88%): HPLC: 96.31%, t_R = 1.573 min; ^{1}H NMR (300 Hz, [D$_6$]DMSO): δ = 8.53–8.50 (m, 1H), 7.55–7.28 (m, 8H), 7.26–7.17 (m, 7H), 6.88–6.84 (m, 2H), 4.27 (d, J = 4.5 Hz, 2H), 3.72 (s, 3H), 3.56–3.35 (m, 4H), 3.48–3.40 (m, 4H), 3.23 ppm (br s, 4H); MS (ESI): *m/z* 534 $[M+H]^+$; HRMS (ESI): *m/z* $[M+H]^+$ calcd for $C_{34}H_{36}N_3O_3$: 534.2678, observed: 534.2697.

***N*-(4-(4-(Biphenyl-2-ylmethyl)piperazine-1-carbonyl)benzyl)-2-(4-methoxyphenyl)acetamide (A17)**: Prepared according to general procedure VII from **2a** and **3e** (104 mg, 81%): HPLC: 96.55%, t_R = 1.749 min; ^{1}H NMR (300 Hz, [D$_6$]DMSO): δ = 8.51 (m, 1H), 7.55–7.53 (m,1H), 7.47–7.38 (m, 7H), 7.35–7.81 (m, 7H), 6.88–6.85 (m, 2H), 4.28 (d, J = 5.4 Hz, 2H), 3.73 (s, 3H), 3.52 (br s, 6H), 3.41–3.30 (m, 2H), 2.82 ppm (m, 4H); MS (ESI): *m/z* 534 $[M+H]^+$; HRMS (ESI): *m/z* $[M+H]^+$ calcd for $C_{34}H_{36}N_3O_3$: 534.2678, observed: 534.2684.

***N*-(4-(4-(Biphenyl-3-ylmethyl)piperazine-1-carbonyl)benzyl)-2-(4-fluorophenyl)acetamide (A18)**: Prepared according to general procedure VII from **2b** and **3f** (100 mg, 81%): HPLC: 99.72%, t_R = 1.693 min; ^{1}H NMR (300 Hz, [D$_6$]DMSO): δ = 8.64 (m, 1H), 7.68–7.62 (m,4H), 7.50–7.40 (m, 3H), 7.36–7.27 (m, 8H), 7.16–7.10 (m, 2H), 4.30 (d, J = 5.7 Hz, 2H), 3.56 (s, 2H), 3.49 (s, 2H), 3.60–3.49 (m, 4H), 2.51 ppm (br s, 4H); MS (ESI): *m/z* 522 $[M+H]^+$; HRMS (ESI): *m/z* $[M+H]^+$ calcd for $C_{33}H_{33}FN_3O_3$: 522.2749, observed: 522.2757.

***N*-(4-(4-(Biphenyl-3-ylmethyl)piperazine-1-carbonyl)benzyl)-2-(thiophen-3-yl)acetamide (A19)**: Prepared according to general procedure VII from **2b** and **3g** (104 mg, 85%): HPLC: 98.60%, t_R = 1.492 min; ^{1}H NMR (300 Hz, [D$_6$]DMSO): δ = 8.67 (m, 1H), 7.69–7.62 (m, 4H), 7.50–7.30 (m, 10H), 6.98–6.94 (m, 2H), 4.31 (d, J = 5.7 Hz, 2H), 3.73 (s, 2H), 3.52 (s, 2H), 3.60–3.30 (m, 4H), 2.421 ppm (br s, 4H); MS (ESI): *m/z* 510 $[M+H]^+$; HRMS (ESI): *m/z* $[M+H]^+$ calcd for $C_{31}H_{32}N_3O_2S$: 510.2137, observed: 510.2144.

***N*-(4-(4-(Biphenyl-3-ylmethyl)piperazine-1-carbonyl)benzyl)-3-methylbutanamide (A20)**: Prepared according to general procedure VII from **2b** and **3h** (79 mg, 70%): HPLC: 95.13%, t_R = 1.831 min; ^{1}H NMR (300 Hz, [D$_6$]DMSO): δ = 8.33 (m, 1H), 7.52

(m,1H), 7.45–7.38 (m, 7H), 7.35–7.23 (m, 5H), 4.28 (d, J=6.0 Hz, 2H), 3.41 (s, 2H), 3.28 (s, 2H), 2.28 (brs, 4H), 2.03–1.98 (brs, 4H),2.02 (m, 3H), 0.88 ppm (d, J=6 Hz, 6H); MS (ESI): m/z 470 [M+H]$^+$; HRMS (ESI): m/z [M+H]$^+$ calcd for $C_{30}H_{36}N_3O_2$: 470.2729, observed: 470.2739.

Ethyl 2-(3-(4-(4-(biphenyl-3-ylmethyl)piperazine-1-carbonyl)benzylcarbamoyl)phenoxy)acetate (A21): Prepared according to general procedure VII from **2a** and **3i** (92 mg, 65%): HPLC: 98.22%, t_R=2.577 min; ^{1}H NMR (300 Hz, $CDCl_3$): δ=7.59–7.53 (m, 5H), 7.48 (t, J=7.8 Hz, 2H), 7.39 (t, J=7.8 Hz, 3H), 7.29 (t, J=7.2 Hz, 3H), 7.08 (d, J=7.2 Hz, 2H), 6.97 (d, J=8.4 Hz, 2H), 4.49 (d, J=5.7 Hz, 2H), 4.10 (q, J=6.9 Hz, 2H), 3.73 (brs, 2H), 3.36 (s, 2H), 3.37 (brs, 2H), 3.49–3.36 (br, 4H), 2.01 (s, 2H), 1.23 (t, J=6.9 Hz, 3H); MS (ESI): m/z 592 [M+H]$^+$; HRMS (ESI): m/z [M+H]$^+$ calcd for $C_{36}H_{37}N_3O_5$: 592.2733, observed: 592.2768.

Ethyl 2-(3-(4-(4-(biphenyl-4-ylmethyl)piperazine-1-carbonyl)benzylcarbamoyl)phenoxy)acetate (A22): Prepared according to general procedure VII from **2b** and **3i** (97 mg, 68%): HPLC: 97.85%, t_R=1.628 min; ^{1}H NMR (300 Hz, $CDCl_3$): δ=7.77 (d, J=9.3 Hz, 2H), 7.57 (t, J=8.1 Hz, 3H), 7.50–7.39 (m, 4H), 7.37–7.28 (m, 6H), 6.91 (d, J=8.7 Hz, 2H), 4.65 (s, 2H), 4.26 (q, J=6.9 Hz, 2H), 3.78 (brs, 2H), 3.60 (s, 2H), 3.42 (brs, 2H), 2.56–2.41 (br, 4H), 1.75 (s, 2H), 1.29 ppm (t, J=6.9 Hz, 3H); MS (ESI): m/z 592 [M+H]$^+$; HRMS (ESI): m/z [M+H]$^+$ calcd for $C_{36}H_{37}N_3O_5$: 592.2733, observed: 592.2792.

2-(3-(4-(4-(Biphenyl-3-ylmethyl)piperazine-1-carbonyl)benzylcarbamoyl)phenoxy)acetic acid (A23): 2 N NaOH (2 mL) was added to a solution of **A21** in CH_2CH_3OH (2 mL). The reaction mixture was heated at reflux for 2 h, and CH_2CH_3OH was evaporated in vacuo. 1 N HCl was added, and the precipitate was filtrated and washed with H_2O to get **A23** as a white solid (44 mg, 92%): HPLC: 99.12%, t_R=0.429 min; ^{1}H NMR (300 Hz, $CDCl_3$): δ=7.78 (d, J=8.7 Hz, 2H), 7.56 (t, J=8.4 Hz, 5H), 7.25 (s, 1H), 7.45–7.33 (m, 7H), 6.91 (d, J=9.0 Hz, 2H), 4.64 (s, 2H), 4.59 (d, J=6.0 Hz, 2H), 3.79 (brs, 2H), 3.57 (s, 2H), 3.43 (brs, 2H), 3.55–2.41 ppm (br, 4H); MS (ESI): m/z 562 [M−H]$^-$; HRMS (ESI): m/z [M+H]$^+$ calcd for $C_{34}H_{33}N_3O_5$: 564.2420, observed: 564.2483.

2-(3-(4-(4-(Biphenyl-4-ylmethyl)piperazine-1-carbonyl)benzylcarbamoyl)phenoxy)acetic acid (A24): Prepared according to the procedure described for **A23** from **A22** (46 mg, 96%): HPLC: 97.98%, t_R=0.391 min; ^{1}H NMR (300 Hz, $CDCl_3$): δ=7.61–7.55 (m, 5H), 7.50–7.40 (m, 3H), 7.38–7.26 (m, 5H), 7.11 (d, J=8.4 Hz, 2H), 7.00 (d, J=8.7 Hz, 2H), 4.51 (d, J=5.7 Hz, 2H), 3.76 (s, 2H), 3.58 (s, 2H), 3.39 (s, 2H), 2.52–2.39 (br, 4H), 2.04 ppm (s, 2H); MS (ESI): m/z 562 [M−H]$^-$; HRMS (ESI): m/z [M+H]$^+$ calcd for $C_{34}H_{33}N_3O_5$: 564.2420, observed: 564.2456.

***N*-(4-(4-(Biphenyl-2-ylmethyl)piperazine-1-carbonyl)benzyl)-3-(2-bromo-4,5-dimethoxyphenyl)propanamide (A25)**: Prepared according to general procedure VII from **2a** and **3j** (111 mg, 75%): HPLC: 100%, t_R=0.417 min; ^{1}H NMR (300 Hz, $CDCl_3$): δ=7.52–7.49 (m, 1H), 7.41–7.29 (m, 8H), 7.25 (s, 1H), 7.12 (d, J=8.1 Hz, 2H), 6.98 (s, 1H), 6.78 (s, 1H), 5.92 (t, J=6.3 Hz,1H), 4.39 (d, J=6.0 Hz, 2H), 3.83 (s, 3H), 3.80 (s, 3H), 3.71 (t, J=6.6 Hz, 2H), 3.44 (s, 2H), 3.31 (t, J=6.6 Hz, 2H), 3.04 (t, J=7.5 Hz, 2H), 2.52 (t, J=7.5 Hz, 2H), 2.39–2.27 ppm (br, 4H); MS (ESI): m/z 656 [M+H]$^+$; HRMS (ESI): m/z [M+H]$^+$ calcd for $C_{36}H_{38}BrN_3O_4$: 656.2046, observed: 656.2088.

***N*-(4-(4-(Biphenyl-2-ylmethyl)piperazine-1-carbonyl)benzyl)-3-(4′-chloro-4,5-dimethoxybiphenyl-2-yl)propanamide (A26)**: Prepared according to general procedure VII from **2a** and **3k** (117 mg, 72%): HPLC: 100%, t_R=5.011 min; ^{1}H NMR (300 Hz, $CDCl_3$): δ=7.52–7.50 (brs, 2H), 7.39–7.30 (m, 9H), 7.25 (d, J=8.1 Hz, 3H), 7.20 (s, 1H), 7.06 (d, J=7.8 Hz, 2H), 6.82 (s, 1H), 6.67 (s, 1H), 4.31 (d, J=6.0 Hz, 2H), 3.86 (s, 3H), 3.84 (s, 3H), 3.68 (brs, 2H), 3.40 (s, 2H), 3.40–3.32 (br, 2H), 2.91 (t, J=7.2 Hz, 2H), 2.38–2.33 (brs, 4H), 2.30 ppm (t, J=7.5 Hz, 2H); MS (ESI): m/z 688 [M+H]$^+$; HRMS (ESI): m/z [M+H]$^+$ calcd for $C_{42}H_{42}ClN_3O_4$: 688.2864, observed: 688.2908.

2-(2-Bromo-3,4,5-trimethoxyphenyl)-*N*-(3-(4-((4′-chlorobiphenyl-2-yl)methyl)piperazine-1-carbonyl)phenyl)acetamide (B1): Prepared according to general procedure VII from **2h** and **4a** (136 mg, 82%): HPLC: 100%, t_R=0.503 min; ^{1}H NMR (300 Hz, $CDCl_3$): δ=7.87 (s, 1H), 7.62 (d, J=8.1 Hz, 1H), 7.54 (d, J=9.0 Hz, 3H), 7.45 (s, 2H), 7.39 (d, J=8.1 Hz, 3H), 7.30 (t, J=7.5 Hz, 2H), 7.08 (d, J=9.0 Hz, 1H), 4.19 (s, 1H), 4.12 (s, 1H), 3.95 (s, 3H), 3.91 (s, 6H), 3.79 (brs, 2H), 3.60 (s, 2H), 3.48 (brs, 2H), 2.56–2.44 ppm (br, 4H); MS (ESI): m/z 692 [M+H]$^+$; HRMS (ESI): m/z [M+H]$^+$ calcd for $C_{35}H_{36}ClN_3O_5Br$: 692.1527, observed: 692.1537.

2-(2-Bromo-3,4,5-trimethoxyphenyl)-*N*-(3-(4-((4′-chlorobiphenyl-3-yl)methyl)piperazine-1-carbonyl)phenyl)acetamide (B2): Prepared according to general procedure VII from **2i** and **4a** (138 mg, 82%): HPLC: 99.93%, t_R=0.526 min; ^{1}H NMR (300 Hz, $CDCl_3$): δ=7.60 (d, J=7.5 Hz, 4H), 7.50 (d, J=7.5 Hz, 1H), 7.44 (s, 2H), 7.40 (d, J=7.2 Hz, 1H), 7.37–7.29 (m, 4H), 7.10 (t, J=7.5 Hz, 1H), 4.21 (s, 2H), 3.98 (s, 3H), 3.93 (s, 6H), 3.86 (s, 2H), 3.40 (s, 4H), 2.40 (s, 2H), 2.29 ppm (s, 2H); MS (ESI): m/z 692 [M+H]$^+$; HRMS (ESI): m/z [M+H]$^+$ calcd for $C_{35}H_{36}ClN_3O_5Br$: 692.1527, observed: 692.1544.

***N*-(3-(4-(Biphenyl-2-ylmethyl)piperazine-1-carbonyl)phenyl)-2-(4′-chloro-4,5,6-trimethoxybiphenyl-2-yl)acetamide (B3)**: Prepared according to general procedure VII from **2a** and **4b** (136 mg, 82%): HPLC: 100%, t_R=4.226 min; ^{1}H NMR (300 Hz, $CDCl_3$): δ=7.67 (d, J=7.5 Hz, 1H), 7.63–7.61 (m, 3H), 7.53 (d, J=7.5 Hz, 2H), 7.48–7.41 (m, 5H), 7.32 (d, J=8.4 Hz, 3H), 7.23 (d, J=8.4 Hz, 3H), 7.03 (d, J=7.8 Hz, 1H), 4.44 (s, 1H), 4.10 (s, 1H), 3.923 (s, 3H), 3.89 (s, 3H), 3.87 (s, 3H), 3.66 (br, 2H), 3.43 (s, 2H), 3.31–3.27 (br, 2H), 2.38–2.25 ppm (br, 4H); MS (ESI): m/z 690 [M+H]$^+$; HRMS (ESI): m/z [M+H]$^+$ calcd for $C_{41}H_{41}ClN_3O_5$: 690.2735, observed: 690.2749.

***N*-(3-(4-(Biphenyl-2-ylmethyl)piperazine-1-carbonyl)phenyl)-2-(4′-chloro-4,5,6-trihydroxybiphenyl-2-yl)acetamide (B4)**: BBr_3 (2.25 mmol) was added to a solution of **B3** (0.15 mmol) in dry CH_2Cl_2 at −78 °C. After stirring at −78 °C for 12 h, the reaction mixture was diluted, and acidified with 1 N HCl. The mixture was extracted with CH_2Cl_2. The combined organic phases were washed with saturated $NaHCO_3$ and brine, dried over Na_2SO_4, filtered and concentrated in vacuo. The crude compound was purified by chromatography with CH_2Cl_2/CH_3OH (10:1 *v/v*) to afford **B4** as a white solid (68 mg, 70%): HPLC: 95.33%, t_R=1.628 min; ^{1}H NMR (300 Hz, $CDCl_3$): δ=8.31 (s, 1H), 7.43 (d, J=8.4 Hz, 4H), 7.36 (d, J=7.5 Hz, 4H), 7.33–7.26 (m, 5H), 7.18 (d, J=7.5 Hz, 2H), 6.71 (s, 1H), 6.54 (s, 1H), 4.34 (s, 2H), 4.24 (d, J=5.1 Hz, 2H), 4.06–4.00 (br, 2H), 2.60 (s, 2H), 2.26 ppm (t, J=7.2 Hz, 4H); MS (ESI): m/z 562 [M−H]$^-$.

***N*-(3-(4-((3-Fluorobiphenyl-4-yl)methyl)piperazine-1-carbonyl)-phenyl)-3,5-dimethoxybenzamide (B5)**: Prepared according to general procedure VII from **2j** and **4c** (113 mg, 85%): HPLC: 96.42%, t_R=5.870 min; ^{1}H NMR (300 Hz, $CDCl_3$): δ=9.10 (s, 1H), 7.83 (d, J=7.8 Hz, 1H), 7.57 (t, J=8.4 Hz, 3H), 7.45–7.32 (m, 6H), 7.29 (s, 1H), 7.26–7.23 (m, 1H), 7.02 (s, 1H), 6.56 (s, 1H), 3.79 (s, 6H), 3.68 (brs, 2H), 3.62 (s, 2H), 3.45 (brs, 2H), 2.50–2.45 ppm (br, 4H); MS (ESI): m/z 554 [M+H]$^+$.

3,5-Dimethoxy-*N*-(3-(4-((3-methoxybiphenyl-4-yl)methyl)piperazine-1-carbonyl)phenyl)benzamide (B6): Prepared according to general procedure VII from **2k** and **4d** (111 mg, 82%): HPLC:

96.27%, t_R = 0.515 min; ^{1}H NMR (300 Hz, $CDCl_3$): δ = 7.74 (d, J = 8.1 Hz, 1H), 7.59 (s, 1H), 7.40–7.26 (m, 5H), 7.24–7.17 (m, 2H), 6.88 (s, 2H), 6.84–6.80 (m, 1H), 6.60 (s, 1H), 6.50–6.46 (m, 2H), 3.85 (s, 3H), 3.81 (s, 3H), 3.78 (s, 3H), 3.69–3.60 (m, 2H), 3.51 (s, 2H), 3.42 (s, 2H), 2.50–2.38 ppm (br, 4H); MS (ESI): m/z 566 $[M+H]^+$; HRMS (ESI): m/z $[M+H]^+$ calcd for $C_{34}H_{36}N_3O_5$: 566.2655, observed: 566.2679.

2-(3,5-Dimethoxyphenyl)-*N*-(3-(4-((3-methylbiphenyl-4-yl)methyl)piperazine-1-carbonyl)phenyl)acetamide (B7): Prepared according to general procedure VII from **2l** and **4d** (112 mg, 83%): HPLC: 95.27%, t_R = 3.418 min; ^{1}H NMR (300 Hz, $CDCl_3$): δ = 7.77 (s, 1H), 7.57 (d, J = 8.1 Hz, 2H), 7.45–7.38 (m, 4H), 7.32–7.28 (m, 4H), 7.07 (t, J = 7.5 Hz, 1H), 6.46 (s, 2H), 6.42 (s, 1H), 3.79 (s, 6H), 3.74 (s, 1H), 3.64 (s, 2H), 3.52 (s, 1H), 3.42 (s, 2H), 3.01 (s, 1H), 2.94 (s, 1H), 2.55–2.49 (br, 4H), 2.43 ppm (s, 3H); MS (ESI): m/z 564 $[M+H]^+$; HRMS (ESI): m/z $[M+H]^+$ calcd for $C_{35}H_{38}N_3O_4$: 564.2862, observed:564.2869.

2-(3,5-Dimethoxyphenyl)-*N*-(3-(4-((3-methoxybiphenyl-4-yl)methyl)piperazine-1-carbonyl)phenyl)acetamide (B8): Prepared according to general procedure VII from **2k** and **4d** (107 mg, 77%): HPLC: 96.93%, t_R = 4.402 min; ^{1}H NMR (300 Hz, $CDCl_3$): δ = 7.53 (d, J = 8.1 Hz, 1H), 7.40–7.33 (m, 3H), 7.29 (d, J = 8.1 Hz, 4H), 7.17 (d, J = 8.4 Hz, 1H), 7.11 (s, 1H), 7.04 (d, J = 7.2 Hz, 1H), 6.87–6.83 (dd, J = 5.7, 2.4 Hz, 1H), 6.44 (s, 2H), 6.43 (s, 1H), 3.85 (s, 3H), 3.80 (s, 6H), 3.72–3.66 (br, 2H), 3.66 (s, 2H), 3.42 (s, 2H), 3.38–3.32 (br, 2H), 2.40–2.94 ppm (br, 4H); MS (ESI): m/z 580 $[M+H]^+$; HRMS (ESI): m/z $[M+H]^+$ calcd for $C_{35}H_{38}N_3O_5$: 580.2811, observed: 580.2823.

***N*-(3-(4-(Biphenyl-2-ylmethyl)piperazine-1-carbonyl)phenyl)-2-cyclohexylacetamide (B9)**: Prepared according to general procedure VII from **2a** and **4e** (102 mg, 86%): HPLC: 98.56%, t_R = 4.464 min; ^{1}H NMR (300 Hz, $CDCl_3$): δ = 7.68 (s, 1H),7.61 (d, J = 8.4 Hz, 1H), 7.51 (s, 1H), 7.46 (s, 1H), 7.42–7.32 (m, 8H), 7.03 (d, J = 8.1 Hz, 1H), 3.44 (s, 2H), 3.38 (s, 2H), 3.69 (s, 2H), 2.41–2.29 (br, 4H), 2.18 (d, J = 6.9 Hz, 2H), 1.88–1.64 (m, 6H), 1.34–1.12 (m, 3H), 1.03–0.92 ppm (m, 2H); MS (ESI): m/z 496 $[M+H]^+$; HRMS (ESI): m/z $[M+H]^+$ calcd for $C_{32}H_{38}N_3O_2$: 496.2964, observed: 496.2977.

***N*-(3-(4-(Biphenyl-3-ylmethyl)piperazine-1-carbonyl)phenyl)-2-cyclohexylacetamide (B10)**: Prepared according to general procedure VII from **2b** and **4e** (103 mg, 87%): HPLC: 99.17%, t_R = 2.339 min; ^{1}H NMR (300 Hz, $CDCl_3$): δ = 7.62–7.59 (m, 3H), 7.55–7.47 (m, 3H), 7.45–7.34 (m, 4H), 7.31 (s, 1H), 7.28 (s, 1H), 7.08 (d, J = 7.5 Hz, 1H), 3.79 (s, 2H), 3.60 (s, 2H), 3.47 (s, 2H), 3.56–3.43 (br, 4H), 2.19 (d, J = 6.9 Hz, 2H), 1.80–1.68 (m, 4H), 1.30–1.20 (m, 4H), 1.00–0.92 ppm (m, 3H); MS (ESI): m/z 496 $[M+H]^+$; HRMS (ESI): m/z $[M+H]^+$ calcd for $C_{32}H_{38}N_3O_2$: 496.2964, observed: 496.2989.

2-Cyclohexyl-*N*-(3-(4-((3-fluorobiphenyl-4-yl)methyl)piperazine-1-carbonyl)phenyl)acetamide (B11): Prepared according to general procedure VII from **2j** and **4e** (104 mg, 84%): HPLC: 95.63%, t_R = 4.409 min; ^{1}H NMR (300 Hz, $CDCl_3$): δ = 8.59 (s, 1H), 7.69 (d, J = 8.4 Hz, 1H), 7.55 (d, J = 7.5 Hz, 2H), 7.47–7.41 (m, 4H), 7.38–7.33 (m, 2H), 7.29 (s, 1H), 7.02 (d, J = 7.5 Hz, 1H), 3.80 (s, 2H), 3.64 (s, 2H), 3.46 (s, 2H), 2.59–2.45 (br, 4H), 2.16 (d, J = 6.6 Hz, 2H), 1.78–1.66 (m, 5H), 1.27–1.14 (m, 4H), 0.99–0.91 ppm (m, 2H); MS (ESI): m/z 514 $[M+H]^+$; HRMS (ESI): m/z $[M+H]^+$ calcd for $C_{32}H_{37}FN_3O_2$: 514.2870, observed: 514.2881.

***N*-(3-(4-((3-Methoxybiphenyl-4-yl)methyl)piperazine-1-carbonyl)phenyl)-2-naphthamide (B12)**: Prepared according to general procedure VII from **2k** and **4f** (100 mg, 75%): HPLC: 95.13%, t_R = 2.810 min; ^{1}H NMR (300 Hz, $CDCl_3$): δ = 8.64 (s, 1H), 8.39 (s, 1H), 7.92 (s, 2H), 7.87 (t, J = 7.8 Hz, 3H), 7.66 (s, 1H), 7.60–7.51 (m, 3H), 7.36 (d, J = 7.5 Hz, 3H), 7.30 (d, J = 7.8 Hz, 2H), 7.11–7.06 (m, 2H), 6.89–6.84 (m, 1H), 3.82 (s,3H), 3.81 (s, 1H), 3.63 (s, 2H), 3.52 (s, 1H), 3.40 (s, 2H), 2.31 ppm (s, 4H); MS (ESI): m/z 556 $[M+H]^+$; HRMS (ESI): m/z $[M+H]^+$ calcd for $C_{36}H_{34}N_3O_3$: 556.2600, observed: 556.2609.

***N*-(3-(4-(Biphenyl-2-ylmethyl)piperazine-1-carbonyl)phenyl)-2-naphthamide (B13)**: Prepared according to general procedure VII from **2b** and **4f** (93 mg, 75%): HPLC: 96.68%, t_R = 3.510 min; ^{1}H NMR (300 Hz, $CDCl_3$): δ = 8.77 (s, 1H), 8.39 (s, 1H), 7.92–7.82 (m, 5H), 7.63 (s, 1H), 7.56 (t, J = 7.5 Hz, 2H), 7.49–7.47 (m, 1H), 7.39–7.26 (m, 8H), 7.03 (d, J = 7.5 Hz, 1H), 3.59 (s, 2H), 3.40 (s, 2H), 3.40–3.38 (br, 2H), 2.28 ppm (s, 4H); MS (ESI): m/z 526 $[M+H]^+$; HRMS (ESI): m/z $[M+H]^+$ calcd for $C_{35}H_{32}N_3O_2$: 526.2495, observed: 526.2508.

***N*-(3-(4-((3-Methoxybiphenyl-4-yl)methyl)piperazine-1-carbonyl)phenyl)-2-(naphthalen-2-yl)acetamide (B14)**: Prepared according to general procedure VII from **2k** and **4g** (98 mg, 72%): HPLC: 97.34%, t_R = 3.124 min; ^{1}H NMR (300 Hz, $CDCl_3$): δ = 7.89–7.82 (m, 3H), 7.78 (s, 1H), 7.54–7.50 (m, 3H), 7.43–7.35 (m, 6H), 7.29 (d, J = 7.8 Hz, 2H), 7.19 (s, 1H), 7.16 (s, 1H), 7.01 (d, J = 7.5 Hz, 1H), 6.87–6.84 (dd, J = 5.7, 2.4 Hz, 1H), 3.89 (s, 2H), 3.85 (s, 3H), 3.67 (brs, 2H), 3.41 (s, 2H), 3.33 (brs, 2H), 2.39–2.27 ppm (br, 4H); MS (ESI): m/z 570 $[M+H]^+$; HRMS (ESI): m/z $[M+H]^+$ calcd for $C_{37}H_{36}N_3O_3$: 570.2757, observed: 570.2769.

***N*-(3-(4-(Biphenyl-2-ylmethyl)piperazine-1-carbonyl)phenyl)-2-(naphthalen-2-yl)acetamide (B15)**: Prepared according to general procedure VII from **2a** and **4g** (91 mg, 72%): HPLC: 98.67%, t_R = 3.991 min; ^{1}H NMR (300 Hz, $CDCl_3$): δ = 8.09 (s, 1H), 7.82 (d, J = 8.4 Hz, 2H), 7.75 (s, 1H), 7.54 (d, J = 8.1 Hz, 1H), 7.51–7.48 (m, 3H), 7.24 (s, 1H), 7.42–7.37 (m, 5H), 7.33–7.26 (m, 4H), 7.20 (d, J = 7.8 Hz, 1H), 6.93 (d, J = 8.4 Hz, 1H), 3.83 (s, 2H), 3.67 (s, 2H), 3.42 (s, 2H), 3.31 (s, 2H), 2.37–2.25 ppm (br, 4H); MS (ESI): m/z 540 $[M+H]^+$; HRMS (ESI): m/z $[M+H]^+$ calcd for $C_{36}H_{34}N_3O_2$: 540.2651, observed: 540.2667.

***N*-(3-(4-(Biphenyl-3-ylmethyl)piperazine-1-carbonyl)phenyl)-2-(naphthalen-2-yl)acetamide (B16)**: Prepared according to general procedure VII from **2b** and **4g** (92 mg, 70%): HPLC: 95.78%, t_R = 3.412 min; ^{1}H NMR (300 Hz, $CDCl_3$): δ = 7.86 (d, J = 8.1 Hz, 2H), 7.78 (s, 1H), 7.69 (s, 1H), 7.59 (d, J = 7.5 Hz, 2H), 7.54–7.47 (m, 6H), 7.44 (s, 1H), 7.42–7.35 (m, 4H), 7.31 (d, J = 8.1 Hz, 1H), 7.23 (d, J = 7.8 Hz, 1H), 7.02 (d, J = 7.5 Hz, 1H), 3.88 (s, 2H), 3.77 (s, 2H), 3.60 (s, 2H), 3.42 (s, 2H), 2.55–2.41 ppm (br, 2H); MS (ESI): m/z 540 $[M+H]^+$; HRMS (ESI): m/z $[M+H]^+$ calcd for $C_{36}H_{34}N_3O_2$: 540.2651, observed: 540.2647.

***N*-(3-(4-((3-Fluorobiphenyl-4-yl)methyl)piperazine-1-carbonyl)phenyl)-2-(naphthalen-2-yl)acetamide (B17)**: Prepared according to general procedure VII from **2j** and **4g** (95 mg, 71%): HPLC: 96.46%, t_R = 3.510 min; ^{1}H NMR (300 Hz, $CDCl_3$): δ = 8.25 (s, 1H), 7.83–7.75 (m, 5H), 7.62–7.57 (m, 3H), 7.50–7.45 (m, 6H), 7.26–7.19 (m, 3H), 6.96 (d, J = 7.5 Hz, 1H), 3.83 (s, 2H), 3.78 (s, 2H), 3.64 (s, 2H), 3.42 (s, 2H), 2.57–2.43 ppm (br, 4H); MS (ESI): m/z 558 $[M+H]^+$; HRMS (ESI): m/z $[M+H]^+$ calcd for $C_{36}H_{33}FN_3O_2$: 558.2557, observed: 558.2569.

General procedure VIII for the synthesis of C1–C12: **2-(3-((4-((4′-Methoxybiphenyl-2-yl)methyl)piperazin-1-yl)methyl)-1*H*-1,2,3-triazol-1-yl)methyl)phenoxy)acetic acid (C1)**: (+)-Sodium L-ascorbate (0.03 mmol) and $CuSO_4{\cdot}6H_2O$ (0.03 mmol) was added to a solution of **8a** (0.3 mmol) and **9a** (0.3 mmol) in $(CH_3)_3COH$/H_2O.The reaction mixture was stirred at RT for 12 h. The solvent was evaporated in vacuo and the crude product was purified by

chromatography with *n*-pentane/EtOAc (4:1 *v/v*) to afford **C1** as a white solid (132 mg, 80%): HPLC: 99.14%, t_R = 0.506 min; ^{1}H NMR (300 Hz, $CDCl_3$): δ = 7.83 (s, 1H), 7.56 (s, 1H), 7.36–7.33 (m, 2H), 7.25–7.23 (m, 2H), 7.17 (d, J = 8.7 Hz, 2H), 6.94 (d, J = 8.4 Hz, 4H), 6.36 (s, 1H), 5.50 (s, 2H), 4.47 (s, 2H), 4.14 (s, 2H), 3.85 (s, 5H), 3.06 (s, 4H), 2.84 ppm (s, 4H); MS (ESI): *m/z* 526 $[M-H]^-$.

2-(3-((4-((4-((4′-Nitrobiphenyl-2-yl)methyl)piperazin-1-yl)methyl)-1*H*-1,2,3-triazol-1-yl)methyl)phenoxy)acetic acid (C2): Prepared according to general procedure VIII from **8a** and **9b** (82%): HPLC:100%, t_R = 0.462 min; ^{1}H NMR (300 Hz, $CDCl_3$): δ = 8.34 (d, J = 8.4 Hz, 2H), 7.74 (d, J = 8.7 Hz, 2H), 7.62 (s, 2H), 7.48 (t, J = 7.8 Hz, 2H), 7.02–6.83 (m, 5H), 5.56 (s, 2H), 4.62 (s, 1H), 4.48 (s, 2H), 4.30 (s, 1H), 3.87 (s, 2H), 3.18 (br s, 4H), 2.81 ppm (s, 4H); MS (ESI): *m/z* 541 $[M-H]^-$.

2-(3-((4-((4-((4′-Chlorobiphenyl-3-yl)methyl)piperazin-1-yl)methyl)-1*H*-1,2,3-triazol-1-yl)methyl)phenoxy)acetic acid (C3): Prepared according to general procedure VIII from **8a** and **9c** (78%): HPLC: 96.45%, t_R = 3.512 min; ^{1}H NMR (300 Hz, $CDCl_3$): δ = 7.93 (s, 1H), 7.52 (s, 2H), 7.38 (d, J = 8.1 Hz, 4H), 7.22 (d, J = 8.1 Hz, 3H), 6.94 (d, J = 8.1 Hz, 2H), 6.34 (s, 1H), 5.52 (s, 2H), 4.48 (s, 2H), 4.23 (s, 2H), 3.70 (s, 2H), 3.22–2.99 (br, 4H), 2.94–2.82 ppm (br, 4H); MS (ESI): *m/z* 530 $[M-H]^-$.

2-(3-((4-((4-((4′-Fluorobiphenyl-3-yl)methyl)piperazin-1-yl)methyl)-1*H*-1,2,3-triazol-1-yl)methyl)phenoxy)acetic acid (C4): Prepared according to general procedure VIII from **8a** and **9d** (72%): HPLC: 96.83%, t_R = 4.502 min; ^{1}H NMR (300 Hz, $CDCl_3$): δ = 7.55–7.51 (m, 4H), 7.43–7.38 (m, 2H), 7.25–7.23 (m, 1H), 7.14 (t, J = 8.7 Hz, 3H), 7.00–6.91 (dd, J = 11.1, 7.8 Hz, 2H), 6.24 (s, 1H), 5.53 (s, 2H), 4.43 (s, 2H), 4.02 (s, 2H), 3.90 (s, 2H), 2.87–2.82 (br, 4H), 2.82–2.71 ppm (br, 4H); MS (ESI): *m/z* 514 $[M-H]^-$.

2-(3-((4-((4-((4′-Methoxybiphenyl-3-yl)methyl)piperazin-1-yl)methyl)-1*H*-1,2,3-triazol-1-yl)methyl)phenoxy)acetic acid (C5): Prepared according to general procedure VIII from **8a** and **9e** (74%): HPLC: 97.33%, t_R = 2.533 min; ^{1}H NMR (300 Hz, $CDCl_3$): δ = 7.56–7.49 (m, 5H), 7.40 (d, J = 7.8 Hz, 1H), 7.35 (s, 1H), 7.19 (d, J = 7.5 Hz, 1H), 6.98 (d, J = 8.7 Hz, 3H), 6.92 (d, J = 7.5 Hz, 1H), 6.22 (s, 1H), 5.53 (s, 2H), 4.75 (br s, 4H), 4.44 (s, 2H), 4.00 (s, 2H), 3.91 (s, 2H), 3.85 (s, 3H), 2.66 ppm (br s, 4H); MS (ESI): *m/z* 526 $[M-H]^-$.

2-(3-((4-((4-((4′-Nitrobiphenyl-3-yl)methyl)piperazin-1-yl)methyl)-1*H*-1,2,3-triazol-1-yl)methyl)phenoxy)acetic acid (C6): Prepared according to general procedure VIII from **8a** and **9f** (75%): HPLC: 99.08%, t_R = 0.489 min; ^{1}H NMR (300 Hz, $CDCl_3$): δ = 8.32 (d, J = 8.4 Hz, 2H), 7.73 (d, J = 8.7 Hz, 2H), 7.62 (s, 3H), 7.48 (t, J = 8.1 Hz, 1H), 7.33 (t, J = 8.7 Hz, 3H), 6.97 (d, J = 8.7 Hz, 2H), 5.57 (s, 2H), 4.47 (s, 2H), 4.22 (s, 2H), 3.87 (s, 2H), 3.06 ppm (br s, 8H); MS (ESI): *m/z* 541 $[M-H]^-$.

2-(3-((4-((4-((4′-Chlorobiphenyl-2-yl)methyl)piperazin-1-yl)methyl)-1*H*-1,2,3-triazol-1-yl)methyl)phenylamino)acetic acid (C7): Prepared according to general procedure VIII from **8b** and **9g** (69%): HPLC: 97.88%, t_R = 0.465 min; ^{1}H NMR (300 Hz, $CDCl_3$): δ = 7.93 (s, 1H), 7.52 (s, 1H), 7.38 (d, J = 8.1 Hz, 5H), 7.22 (d, J = 8.4 Hz, 3H), 6.93 (d, J = 7.5 Hz, 2H), 6.34 (s, 1H), 5.52 (s, 2H), 4.48 (s, 2H), 4.23 (s, 2H), 3.98 (s, 1H), 3.70 (s, 2H), 2.97 (s, 4H), 2.72 ppm (s, 4H); MS (ESI): *m/z* 529 $[M-H]^-$.

2-(3-((4-((4-((4′-Fluorobiphenyl-2-yl)methyl)piperazin-1-yl)methyl)-1*H*-1,2,3-triazol-1-yl)methyl)phenylamino)acetic acid (C8): Prepared according to general procedure VIII from **8b** and **9h** (66%): HPLC: 99.32%, t_R = 3.131 min; ^{1}H NMR (300 Hz, $CDCl_3$): δ = 7.70 (s, 1H), 7.55 (d, J = 7.5 Hz, 4H), 7.48–7.28 (m, 5H), 6.96 (t, J = 7.2 Hz, 2H), 6.18 (s, 1H), 5.58 (s, 2H), 4.48 (s, 2H), 4.25 (s, 2H), 3.84 (s, 2H), 3.15 ppm (br, 8H); MS (ESI): *m/z* 513 $[M-H]^-$.

2-(3-((4-((4-((4′-Methoxybiphenyl-2-yl)methyl)piperazin-1-yl)methyl)-1*H*-1,2,3-triazol-1-yl)methyl)phenylamino)acetic acid (C9): Prepared according to general procedure VIII from **8b** and **9a** (62%): HPLC: 96.60%, t_R = 2.530 min; ^{1}H NMR (300 Hz, $CDCl_3$): δ = 7.81 (s, 1H), 7.56 (s, 1H), 7.36–7.34 (m, 2H), 7.17 (d, J = 8.1 Hz, 3H), 6.93 (d, J = 8.1 Hz, 5H), 6.33 (s, 1H), 5.51 (s, 2H), 4.47 (s, 2H), 4.15 (s, 2H), 3.86 (s, 5H), 3.06–2.84 ppm (br, 8H); MS (ESI): *m/z* 525 $[M-H]^-$.

2-(3-((4-((4-((4′-Chlorobiphenyl-3-yl)methyl)piperazin-1-yl)methyl)-1*H*-1,2,3-triazol-1-yl)methyl)phenylamino)acetic acid (C10): Prepared according to general procedure VIII from **8b** and **9c** (65%): HPLC: 96.00%, t_R = 0.693 min; ^{1}H NMR (300 Hz, $CDCl_3$): δ = 7.87 (s, 1H), 7.62 (d, J = 8.4 Hz, 1H), 7.52 (d, J = 9.0 Hz, 3H), 7.47–7.37 (m, 5H), 7.31 (d, J = 7.5 Hz, 2H), 6.33 (s, 1H), 5.51 (s, 2H), 4.49 (s, 2H), 4.22 (s, 2H), 4.01 (s, 1H), 3.69 (s, 2H), 3.13 (br s, 4H), 2.81 ppm (s, 4H); MS (ESI): *m/z* 529 $[M-H]^-$.

2-(3-((4-((4-((4′-Methoxybiphenyl-3-yl)methyl)piperazin-1-yl)methyl)-1*H*-1,2,3-triazol-1-yl)methyl)phenylamino)acetic acid (C11): Prepared according to general procedure VIII from **8b** and **9e** (68%): HPLC: 96.58%, t_R = 0.477 min; ^{1}H NMR (300 Hz, $CDCl_3$): δ = 7.56–7.49 (m, 5H), 7.39 (t, J = 7.8 Hz, 1H), 7.35 (s, 1H), 7.19 (d, J = 8.7 Hz, 1H), 6.98 (d, J = 8.7 Hz, 3H), 6.92 (d, J = 7.5 Hz, 1H), 6.22 (s, 1H), 5.53 (s, 2H), 4.81 (s, 1H), 4.44 (s, 2H), 4.00 (s, 2H), 3.91 (s, 2H), 3.85 (s, 3H), 2.83 (s, 4H), 2.60 ppm (s, 4H); MS (ESI): *m/z* 525 $[M-H]^-$.

2-(3-((4-((4-((4′-Nitrobiphenyl-3-yl)methyl)piperazin-1-yl)methyl)-1*H*-1,2,3-triazol-1-yl)methyl)phenylamino)acetic acid (C12): Prepared according to general procedure VIII from **8b** and **9f** (68%): HPLC: 97.13%, t_R = 0.450 min; ^{1}H NMR (300 Hz, $CDCl_3$): δ = 8.33 (d, J = 8.4 Hz, 2H), 7.74 (d, J = 8.7 Hz, 2H), 7.63 (s, 3H), 7.48 (t, J = 8.1 Hz, 1H), 7.33 (t, J = 7.8 Hz, 3H), 6.97 (d, J = 8.4 Hz, 2H), 5.56 (s, 2H), 4.47 (s, 2H), 4.30 (s, 1H), 4.21 (s, 2H), 3.87 (s, 2H), 3.06 (s, 4H), 2.84 ppm (s, 4H); MS (ESI): *m/z* 540 $[M-H]^-$.

General procedure IX for the synthesis of D1–D26: **1-(4-{[2-(4-Chlorophenyl)phenyl]methyl}piperazin-1-yl)-3-(4-methoxyphenyl)propan-1-one (D1)**: HATU (1.5 mmol) and DIPEA (1.5 mmol) was added to a solution of 3-(4-methoxyphenyl)propanoic acid (1.0 mmol) in dry DMF (10 mL). After stirring at −10 °C for 30 min, **2h** (0.8 mmol) was added, and the reaction mixture was stirred at −10 °C for 2 h and then warmed to RT and stirred overnight. The solvent was evaporated in vacuo and the mixture was diluted with H_2O (100 mL) and extracted with CH_2Cl_2. The organic phases were washed with saturated $NaHCO_3$ and brine, dried over Na_2SO_4, filtered and concentrated in vacuo. The crude compound was purified by chromatography with CH_2Cl_2/CH_3OH (30:1 *v/v*) to afford **D1** as a yellow oil (64%): HPLC: 97.89%, t_R = 3.793 min; ^{1}H NMR (400 MHz, $CDCl_3$): δ = 7.46 (d, J = 6.0 Hz, 1H), 7.37 (m, 1H), 7.34–7.36 (m, 2H), 7.33 (t, J = 3.2 Hz, 2H), 7.31 (t, J = 4.0 Hz,1H), 7.22–7.24 (m, 1H), 7.11 (d, J = 8.8 Hz, 2H), 6.81 (d, J = 8.8 Hz, 2H), 3.77 (s, 3H), 3.55 (s, 2H), 3.36 (s, 2H), 3.31 (t, J = 4.4 Hz, 2H), 2.88 (t, J = 7.2 Hz, 2H), 2.55 (t, J = 8.0 Hz, 2H), 2.29 (t, J = 4.8 Hz, 2H), 2.22 ppm (s, 2H); MS (ESI): *m/z* 449 $[M+H]^+$; HRMS (ESI): *m/z* $[M+H]^+$ calcd for $C_{27}H_{29}ClN_2O_2$: 449.1918, observed: 449.2013.

1-(4-{[2-(4-Chlorophenyl)phenyl]methyl}piperazin-1-yl)-3-(3,4,5-trimethoxyphenyl)propan-1-one (D2): Prepared according to general procedure IX from 3-(3,4,5-trimethoxyphyl)propanoic acid (70%): HPLC:97.10%, t_R = 2.307 min; ^{1}H NMR (400 MHz, $CDCl_3$): δ = 7.38–7.48 (m, 1H), 7.25–7.38 (m, 6H), 7.23–7.24 (m, 1H), 6.78 (d,

J=8.8 Hz, 2H), 3.86 (s, 6H), 3.85 (s, 3H), 3.56 (t, J=4.8 Hz, 2H), 3.37 (s, 2H), 3.32 (t, J=5.4 Hz, 2H), 2.90 (t, J=7.5 Hz, 2H), 2.57 (t, J=7.2 Hz, 2H), 2.30 (t, J=5.1 Hz, 2H), 2.24 ppm (t, J=4.8 Hz, 2H); MS (ESI): m/z 509 $[M+H]^+$; HRMS (ESI): m/z $[M+H]^+$ calcd for $C_{29}H_{33}ClN_2O_4$: 509.2129, observed: 509.2226.

1-(4-{[2-(4-Chlorophenyl)phenyl]methyl}piperazin-1-yl)-2-(3,4,5-trimethoxyphenyl)ethan-1-one (D3): Prepared according to general procedure IX from 2-(3,4,5-trimethoxyphenyl)acetic acid (62%): HPLC: 97.09%, t_R=1.879 min; ^{1}H NMR (400 MHz, $CDCl_3$): δ=7.46–7.43 (m, 1H), 7.38–7.34 (m, 3H), 7.33–7.28 (m, 3H), 7.23–7.20 (m, 1H), 6.42 (s, 2H), 3.83 (s, 3H), 3.82 (s, 6H), 3.64 (s, 2H), 3.58 (t, J=5.6 Hz, 2H), 3.40–3.38 (br, 2H), 3.36 (s, 2H), 2.31 (t, J=5.2 Hz, 2H), 2.20 ppm (t, J=5.2 Hz, 2H); MS (ESI): m/z 495 $[M+H]^+$; HRMS (ESI): m/z $[M+H]^+$ calcd for $C_{28}H_{31}ClN_2O_4$: 495.1917, observed: 495.2023.

1-(4-{[2-(4-Fluorophenyl)phenyl]methyl}piperazin-1-yl)-3-(3,4,5-trimethoxyphenyl)propan-1-one (D4): Prepared according to general procedure IX from 3-(3,4,5-trimethoxyphyl)propanoic acid and **2s** (70%): HPLC: 98.71%, t_R=1.637 min; ^{1}H NMR (400 MHz, $CDCl_3$): δ=7.46 (s, 1H), 7.31–7.35 (m,4H), 7.22–7.24 (m, 1H), 7.07 (t, J=8.8 Hz, 2H), 6.41 (s, 2H), 3.83 (s, 6H), 3.80 (s, 3H), 3.56 (s, 2H), 3.35 (m, 4H), 2.88 (t, J=7.2 Hz, 2H), 2.57 (t, J=8.4 Hz, 2H), 2.29 (s, 2H), 2.24 ppm (s, 2H); MS (ESI): m/z 493 $[M+H]^+$; HRMS (ESI): m/z $[M+H]^+$ calcd for $C_{29}H_{33}FN_2O_4$: 493.2424, observed: 493.2494.

1-(4-{[2-(3-Fluorophenyl)phenyl]methyl}piperazin-1-yl)-3-(3,4,5-trimethoxyphenyl)propan-1-one (D5): Prepared according to general procedure IX from 3-(3,4,5-trimethoxyphyl)propanoic acid and **2t** (65%): HPLC: 97.18%, t_R=1.711 min; ^{1}H NMR (400 MHz, $CDCl_3$): δ=7.47 (s, 1H), 7.33–7.38 (m,3H), 7.25–7.27 (m, 1H), 7.19 (m, 1H), 7.13 (dt, J=1.2, 7.2 Hz, 1H), 7.03–7.07 (m,1H), 6.41 (s, 2H), 3.84 (s, 6H), 3.81 (s, 3H), 3.58 (s, 2H), 3.38 (d, J=3.6 Hz, 4H), 2.89 (t, J=6.8 Hz, 2H), 2.58 (t, J=8.4 Hz, 2H), 2.32 (s, 2H), 2.27 ppm (s, 2H); MS (ESI): m/z 493 $[M+H]^+$; HRMS (ESI): m/z $[M+H]^+$ calcd for $C_{29}H_{33}FN_2O_4$: 493.2424, observed: 493.2470.

1-(4-{[2-(3-Chloro-4-fluorophenyl)phenyl]methyl}piperazin-1-yl)-3-(3,4,5-trimethoxyphenyl)propan-1-one (D6): Prepared according to general procedure IX from 3-(3,4,5-trimethoxyphyl)propanoic acid and **2e** (62%): HPLC: 96.99%, t_R=2.493 min; ^{1}H NMR (400 MHz, $CDCl_3$): δ=7.69 (dd, J=2.0, 7.2 Hz, 1H), 7.38 (s,1H), 7.33–7.35 (m, 2H), 7.22–7.25 (m, 2H), 7.17 (t, J=8.8 Hz, 1H), 6.43 (s, 2H), 3.85 (s, 6H), 3.82 (s, 3H), 3.60 (s, 2H), 3.38 (t, J=4.0 Hz, 2H), 3.32 (s, 2H), 2.90 (t, J=7.6 Hz, 2H), 2.60 (t, J=8.4 Hz, 2H), 2.35 (s, 2H), 2.29 ppm (s, 2H); MS (ESI): m/z 527 $[M+H]^+$; HRMS (ESI): m/z $[M+H]^+$ calcd for $C_{29}H_{32}ClFN_2O_4$: 527.2035, observed: 527.2108.

1-{4-[(2-Phenylphenyl)methyl]piperazin-1-yl}-3-(3,4,5-trimethoxyphenyl)propan-1-one (D7): Prepared according to general procedure IX from 3-(3,4,5-trimethoxyphyl)propanoic acid and **2a** (68%): HPLC: 98.83%, t_R=1.664 min; ^{1}H NMR (400 MHz, $CDCl_3$): δ=7.52 (m, 1H), 7.39 (m,1H), 7.38 (m, 1H), 7.34–7.35 (m, 3H), 7.31–7.33 (m, 2H), 7.25–7.27 (m, 1H), 6.41 (s, 2H), 3.83 (s, 6H), 3.80 (s, 3H), 3.66 (s, 2H), 3.43 (s, 2H), 3.34 (t, J=4.4 Hz, 2H), 2.88 (t, J=7.2 Hz, 2H), 2.57 (t, J=8.0 Hz, 2H), 2.30 (t, J=4.8 Hz, 2H), 2.25 ppm (t, J=4.8 Hz, 2H); MS (ESI): m/z 475 $[M+H]^+$; HRMS (ESI): m/z $[M+H]^+$ calcd for $C_{29}H_{34}N_2O_4$: 475.2519, observed: 475.2579.

1-{4-[(3-Phenylphenyl)methyl]piperazin-1-yl}-3-(3,4,5-trimethoxyphenyl)propan-1-one (D8): Prepared according to general procedure IX from 3-(3,4,5-trimethoxyphyl)propanoic acid and **2b** (78%): HPLC: 98.37%, t_R=1.515 min; ^{1}H NMR (400 MHz, $CDCl_3$): δ=7.61 (m, 1H), 7.59 (m, 1H), 7.54 (m, 1H), 7.50 (d, J=7.6 Hz, 1H), 7.44 (t, J=7.2 Hz, 2H), 7.40 (t, J=7.6 Hz, 1H), 7.35 (m, 1H), 7.28 (d, J=7.6 Hz, 1H),6.43 (s, 2H), 3.84 (s, 6H), 3.82 (s, 3H), 3.66 (t, J=4.8 Hz, 2H), 3.56 (s, 2H), 3.41 (t, J=4.8 Hz, 2H), 2.91 (t, J=7.2 Hz, 2H), 2.61 (t, J=8.4 Hz, 2H), 2.44 (t, J=4.8 Hz, 2H), 2.35 ppm (t, J=4.8 Hz, 2H); MS (ESI): m/z 475 $[M+H]^+$; HRMS (ESI): m/z $[M+H]^+$ calcd for $C_{29}H_{34}N_2O_4$: 475.2519, observed: 475.2595.

1-(4-{[3-(4-Fluorophenyl)phenyl]methyl}piperazin-1-yl)-3-(3,4,5-trimethoxyphenyl)propan-1-one (D9): Prepared according to general procedure IX from 3-(3,4,5-trimethoxyphyl)propanoic acid and **2p** (72%): HPLC: 97.27%, t_R=1.482 min; ^{1}H NMR (400 MHz, $CDCl_3$): δ=7.56 (t, J=2.8 Hz, 1H), 7.54 (t, J=2.8 Hz, 1H), 7.50 (s, 1H), 7.46 (dt, J=1.2, 7.6 Hz, 1H), 7.39 (t, J=8.4 Hz, 1H), 7.28 (t, J=7.6 Hz, 1H), 7.12 (t, J=8.8 Hz, 2H), 6.43 (s, 2H), 3.84 (s, 6H), 3.82 (s, 3H), 3.67 (s, 2H), 3.57 (s, 2H), 3.42 (t, J=4.8 Hz, 2H), 2.91 (t, J=7.2 Hz, 2H), 2.61 (t, J=8.4 Hz, 2H), 2.46 (t, J=4.8 Hz, 2H), 2.36 ppm (s, 2H); MS (ESI): m/z 493 $[M+H]^+$; HRMS (ESI): m/z $[M+H]^+$ calcd for $C_{29}H_{33}FN_2O_4$: 493.2424, observed: 493.2476.

1-(4-{[3-(4-Chlorophenyl)phenyl]methyl}piperazin-1-yl)-3-(3,4,5-trimethoxyphenyl)propan-1-one (D10): Prepared according to general procedure IX from 3-(3,4,5-trimethoxyphyl)propanoic acid and **2o** (61%): HPLC: 98.48%, t_R=2.122 min; ^{1}H NMR (400 MHz, $CDCl_3$): δ=7.53 (m, 1H), 7.51 (m, 2H), 7.46 (d, J=7.6 Hz, 1H), 7.41 (s, 1H), 7.39 (s, 1H), 7.37 (s, 1H), 7.30 (d, J=7.6 Hz, 1H), 6.42 (s, 2H), 3.84 (s, 6H), 3.82 (s, 3H), 3.66 (s, 2H), 3.55 (s, 2H), 3.41 (t, J=4.8 Hz, 2H), 2.91 (t, J=7.2 Hz, 2H), 2.61 (t, J=8.0 Hz, 2H), 2.44 (t, J=4.8 Hz, 2H), 2.35 ppm (t, J=4.8 Hz, 2H); MS (ESI): m/z 509 $[M+H]^+$; HRMS (ESI): m/z $[M+H]^+$ calcd for $C_{29}H_{33}ClN_2O_4$: 509.2129, observed: 509.2238.

3-(3,4-Dihydroxyphenyl)-1-{4-[(3-phenylphenyl)methyl]piperazin-1-yl}propan-1-one (D11): Prepared according to general procedure IX from 3-(3,4-dihydroxyphenyl)propanoic acid and **2b** (63%): HPLC: 98.38%, t_R=1.010 min; ^{1}H NMR (400 MHz, $CDCl_3$): δ=7.60 (m, 1H), 7.57 (m, 1H), 7.53 (s, 1H), 7.50 (d, J=8.0 Hz, 1H), 7.44 (t, J=7.2 Hz, 2H), 7.39 (t, J=7.6 Hz, 1H), 7.34 (tt, J=1.2, 7.6 Hz, 1H), 7.28 (d, J=7.6 Hz, 1H), 6.76 (d, J=8.0 Hz, 1H), 6.73 (d, J=1.6 Hz, 1H), 6.55 (dd, J=1.6, 8.0 Hz, 1H), 3.63 (s, 2H), 3.55 (s, 2H), 3.37 (t, J=4.4 Hz, 2H), 2.82 (t, J=7.6 Hz, 2H), 2.59 (t, J=7.2 Hz, 2H), 2.44 (s, 2H), 2.26 (s, 2H), 2.18 ppm (s, 1H); MS (ESI): m/z 417 $[M+H]^+$; HRMS (ESI): m/z $[M+H]^+$ calcd for $C_{26}H_{28}N_2O_3$: 417.2100, observed: 417.2173.

3-(3,4-Dimethoxyphenyl)-1-{4-[(3-phenylphenyl)methyl]piperazin-1-yl}propan-1-one (D12): Prepared according to general procedure IX from 3-(3,4-dimethoxyphenyl)propanoic acid and **2b** (72%): HPLC: 98.51%, t_R=1.548 min; ^{1}H NMR (400 MHz, $CDCl_3$): δ=7.60 (m, 1H), 7.58–7.59 (m, 1H), 7.54 (m, 1H), 7.49–7.52 (dt, J=1.2, 8.8 Hz, 1H), 7.43–7.46 (m, 2H), 7.40 (m, 1H), 7.33–7.37 (m, 1H), 7.29 (d, J=7.6 Hz, 1H), 6.79 (d, J=8.8 Hz, 1H), 6.74–6.76 (m, 2H), 3.86 (s, 3H), 3.85 (s, 3H), 3.65 (t, J=4.4 Hz, 2H), 3.55 (s, 2H), 3.39 (t, J=5.2 Hz, 2H), 2.92 (t, J=7.2 Hz, 2H), 2.60 (t, J=8.0 Hz, 2H), 2.44 (t, J=4.8 Hz, 2H), 2.34 ppm (t, J=5.2 Hz, 2H); MS (ESI): m/z 445 $[M+H]^+$; HRMS (ESI): m/z $[M+H]^+$ calcd for $C_{28}H_{32}N_2O_3$: 445.2413, observed: 445.2470.

4-Oxo-4-{4-[(3-phenylphenyl)methyl]piperazin-1-yl}-*N*-(3,4,5-trimethoxyphenyl)butanamide (D13): Prepared according to general procedure IX from **10c** and 3,4,5-trimethoxyaniline (78%): HPLC: 96.44%, t_R=1.268 min; ^{1}H NMR (400 MHz, $CDCl_3$): δ=8.58 (s, 1H), 7.61 (s, 1H), 7.58 (s, 1H), 7.54 (s, 1H), 7.50 (d, J=7.6 Hz, 1H), 7.45 (m, 2H), 7.40 (d, J=6.0 Hz, 1H), 7.37 (d, J=7.6 Hz, 1H), 7.27 (d, J=6.0 Hz, 1H), 6.83 (s, 2H), 3.82 (s, 6H), 3.78 (s, 3H), 3.66 (s, 2H), 3.58 (s, 2H), 3.51 (t, J=6.4 Hz, 2H), 2.72 (d, J=4.6 Hz, 4H), 2.47 ppm (br s, 4H); MS (ESI): m/z 518 $[M+H]^+$; HRMS (ESI): m/z $[M+H]^+$ calcd for $C_{30}H_{35}N_3O_5$: 518.2577, observed: 518.2630.

4-(4-{[3-(4-Chlorophenyl)phenyl]methyl}piperazin-1-yl)-4-oxo-*N*-(3,4,5-trimethoxyphenyl)butanamide (D14): Prepared according to general procedure IX from **10b** and 3,4,5-trimethoxyaniline (63%): HPLC: 100%, t_R = 1.728 min; ^{1}H NMR (400 MHz, $CDCl_3$): δ = 9.06 (s, 1H), 7.52–7.53 (m, 1H), 7.50–7.51 (m, 2H), 7.45–7.47 (d, J = 7.6 Hz, 1H), 7.41 (m, 2H), 7.37–7.39 (m, 1H), 7.29–7.31 (d, J = 7.6 Hz, 1H), 6.83 (s, 2H), 3.77 (s, 6H), 3.76 (s, 3H), 3.64 (s, 2H), 3.56 (s, 2H), 3.53 (t, J = 4.8 Hz, 2H), 2.74–2.76 (m, 4H), 2.47 (t, J = 4.8 Hz, 2H), 2.42 ppm (t, J = 4.8 Hz, 2H); MS (ESI): m/z 552 $[M+H]^+$; HRMS (ESI): m/z $[M+H]^+$ calcd for $C_{30}H_{34}ClN_3O_5$: 552.2187, observed: 552.2278.

4-(4-{[3-(4-Fluorophenyl)phenyl]methyl}piperazin-1-yl)-4-oxo-*N*-(3,4,5-trimethoxyphenyl)butanamide (D15): Prepared according to general procedure IX from **10a** and 3,4,5-trimethoxyaniline (78%): HPLC: 100%, t_R = 1.237 min; ^{1}H NMR (400 MHz, $CDCl_3$): δ = 8.83 (s, 1H), 7.52–7.55 (m, 2H), 7.48 (s, 1H), 7.45 (dt, J = 1.2, 7.6 Hz, 1H), 7.38 (t, J = 7.6 Hz, 1H), 7.27 (d, J = 7.6 Hz, 1H), 7.11 (t, J = 8.8 Hz, 2H), 6.81 (s, 2H), 3.70 (s, 6H), 3.76 (s, 3H), 3.64(s, 2H), 3.56 (s, 2H), 3.52 (t, J = 4.8 Hz, 2H), 2.73 (m, 4H), 2.48 (s, 2H), 2.43 ppm (t, J = 4.8 Hz, 2H); MS (ESI): m/z 536 $[M+H]^+$; HRMS (ESI): m/z $[M+Na]^+$ calcd for $C_{30}H_{34}FN_3O_5$: 558.2482, observed: 558.2343.

5-Oxo-5-{4-[(3-phenylphenyl)methyl]piperazin-1-yl}-*N*-(3,4,5-trimethoxyphenyl)pentanamide (D16): Prepared according to general procedure IX from **10d** and 3,4,5-trimethoxyaniline (76%): HPLC: 99.49%, t_R = 1.338 min; ^{1}H NMR (400 MHz, $CDCl_3$): δ = 8.39 (s, 1H), 7.63 (d, J = 1.6 Hz, 1H), 7.59 (m, 1H), 7.55 (m, 1H), 7.51–7.53 (m, 1H), 7.43–7.47 (m, 2H), 7.41 (t, J = 7.6 Hz, 1H), 7.34–7.38 (m, 1H), 7.30 (d, J = 7.6 Hz, 1H), 6.89 (s, 2H), 3.84 (s, 6H), 3.81 (s, 3H), 3.67 (s, 2H), 3.60 (s, 2H), 3.51 (t, J = 5.2 Hz, 2H), 2.43–2.51 (m, 8H), 1.99–2.06 ppm (m, 2H); MS (ESI): m/z 532 $[M+H]^+$; HRMS (ESI): m/z $[M+H]^+$ calcd for $C_{31}H_{37}N_3O_5$: 532.2733, observed: 532.2834.

5-(4-{[3-(4-Chlorophenyl)phenyl]methyl}piperazin-1-yl)-5-oxo-*N*-(3,4,5-trimethoxyphenyl)pentanamide (D17): Prepared according to general procedure IX from **10e** and 3,4,5-trimethoxyaniline (52%): HPLC: 99.10%, t_R = 1.810 min; ^{1}H NMR (400 MHz, $CDCl_3$): δ = 8.52 (s, 1H), 7.53 (m, 1H), 7.51 (m, 2H), 7.46–7.48 (m, 1H), 7.41 (m, 2H), 7.38–7.40 (m, 1H), 7.30–7.32 (d, J = 7.6 Hz, 1H), 6.90 (s, 2H), 3.83 (s, 6H), 3.80 (s, 3H), 3.66 (s, 2H), 3.58 (s, 2H), 3.51 (t, J = 4.8 Hz, 2H), 2.43–2.50 (m, 8H), 1.99–2.06 ppm (m, 2H); MS (ESI): m/z 566 $[M+H]^+$; HRMS (ESI): m/z $[M+H]^+$ calcd for $C_{31}H_{36}ClN_3O_5$: 566.2343, observed: 566.2427.

***N*-(2,4-Dimethoxyphenyl)-5-oxo-5-{4-[(3-phenylphenyl)methyl]piperazin-1-yl}pentanamide (D18)**: Prepared according to general procedure IX from **10d** and 2,4-dimethoxyaniline (64%): HPLC: 99.13%, t_R = 1.650 min; ^{1}H NMR (400 MHz, $CDCl_3$): δ = 8.11 (d, J = 3.2 Hz, 1H), 7.92 (s, 1H), 7.61 (m, 1H), 7.59 (s, 1H), 7.54 (s, 1H), 7.50 (d, J = 7.6 Hz, 1H), 7.44 (t, J = 7.2 Hz, 2H), 7.39 (t, J = 7.6 Hz, 1H), 7.32–7.36 (m, 1H), 7.29 (d, J = 7.6 Hz, 1H), 6.77 (d, J = 8.8, 1 Hz), 6.54–6.57 (dd, J = 2.8, 8.8 Hz, 1H), 3.81 (s, 3H), 3.76 (s, 3H), 3.64 (t, J = 4.4 Hz, 2H), 3.56 (s, 2H), 3.47 (t, J = 5.2 Hz, 2H), 2.50 (t, J = 6.8 Hz, 2H), 2.42–2.45 (m, 6H), 2.01–2.08 ppm (m, 2H); MS (ESI): m/z 502 $[M+H]^+$; HRMS (ESI): m/z $[M+H]^+$ calcd for $C_{30}H_{35}N_3O_4$: 502.2628, observed: 502.2711.

***N*-(3-Methoxyphenyl)-5-oxo-5-{4-[(3-phenylphenyl)methyl]piperazin-1-yl}pentanamide (D19)**: Prepared according to general procedure IX from **10d** and 3-methoxyaniline (72%): HPLC: 100%, t_R = 1.644 min; ^{1}H NMR (400 MHz, $CDCl_3$): δ = 8.74 (s, 1H), 7.58–7.60 (m, 2H), 7.53 (s, 1H), 7.50 (d, J = 8.0 Hz, 1H), 7.43 (t, 2H), 7.37 (t, J = 7.6 Hz, 1H), 7.32–7.36 (m, 2H), 7.28 (d, J = 7.6 Hz, 1H), 7.16 (m, 1H), 7.04 (d, J = 8.0 Hz, 1H), 6.61 (dd, J = 2.4, 8.0 Hz, 1H), 3.75 (s, 3H), 3.63 (t, J = 4.4 Hz, 2H), 3.55 (s, 2H), 3.46 (t, J = 4.8 Hz, 2H), 2.42–2.45 (m, 8H), 1.97–2.04 ppm (m, 2H); MS (ESI): m/z 472 $[M+H]^+$; HRMS (ESI): m/z $[M+H]^+$ calcd for $C_{29}H_{33}N_3O_3$: 472.2522, observed: 472.2584.

***N*-(3-Hydroxyphenyl)-4-oxo-4-{4-[(3-phenylphenyl)methyl]piperazin-1-yl}butanamide (D20)**: Prepared according to general procedure IX from **10c** and 3-hydroxyaniline (62%): HPLC: 97.38%, t_R = 1.030 min; ^{1}H NMR (400 MHz, $CDCl_3$): δ = 9.83 (s, 1H), 9.35 (s, 1H), 7.66 (d, J = 7.6 Hz, 2H), 7.57 (d, J = 9.6 Hz, 2H), 7.47 (m, 2H), 7.42 (d, J = 7.6 Hz, 1H), 7.38 (d, J = 7.2 Hz, 1H), 7.32 (d, J = 7.2 Hz, 1H), 7.19 (s, 1H), 7.04 (t, J = 8.1 Hz, 1H), 6.95 (d, J = 8.0 Hz, 1H), 6.42 (dd, J = 1.2, 7.6 Hz, 1H), 3.56 (s, 2H), 3.46 (d, J = 3.6 Hz, 4H), 2.60 (d, J = 5.2 Hz, 2H), 2.52 (m, 2H), 2.40 (s, 2H), 2.34 ppm (s, 2H); MS (ESI): m/z 444 $[M+H]^+$; HRMS (ESI): m/z $[M+H]^+$ calcd for $C_{27}H_{29}ClN_3O_3$: 444.2209, observed: 444.2294.

***N*-[(3,5-Dimethoxyphenyl)methyl]-4-oxo-4-{4-[(3-phenylphenyl)-methyl]piperazin-1-yl}butanamide (D21)**: Prepared according to general procedure IX from **10c** and (3,5-dimethoxyphehyl)methanamine (71%): HPLC: 99.01%, t_R = 1.505 min; ^{1}H NMR (400 MHz, $CDCl_3$): δ = 7.61 (s, 1H), 7.59 (s, 1H), 7.54 (s, 1H), 7.51 (d, J = 8.0 Hz, 1H), 7.44 (m,2H), 7.41 (d, J = 6.4 Hz, 1H), 7.36 (d, J = 7.6 Hz, 1H), 7.29 (d, J = 7.6 Hz, 1H), 6.81 (t, J = 7.2 Hz, 1H), 6.41 (d, J = 2.0 Hz, 2H), 6.32 (t, J = 2.8 Hz, 1H), 4.35 (d, J = 6.0 Hz, 2H), 3.74 (s, 6H), 3.52–3.56 (m, 4H), 3.47 (t, J = 6.8 Hz, 2H), 2.66 (t, J = 8.4 Hz, 2H), 2.56 (t, J = 7.6 Hz, 2H), 2.44 (t, J = 6.8 Hz, 2H), 2.38 ppm (t, J = 6.4 Hz, 2H); MS (ESI): m/z 502 $[M+H]^+$; HRMS (ESI): m/z $[M+H]^+$ calcd for $C_{30}H_{35}N_3O_4$: 502.2628, observed: 502.2734.

***N*-[(2-Methoxyphenyl)methyl]-4-oxo-4-{4-[(3-phenylphenyl)methyl]piperazin-1-yl}butanamide (D22)**: Prepared according to general procedure IX from **10c** and (2-methoxyphehyl)methanamine (64%): HPLC: 98.63%, t_R = 1.616 min; ^{1}H NMR (400 MHz, $CDCl_3$): δ = 7.61 (m, 1H), 7.58 (m, 1H), 7.54 (s, 1H), 7.50 (dt, J = 1.2, 7.6 Hz, 1H), 7.43 (td, J = 1.6, 7.2 Hz, 2H), 7.39 (t, J = 7.6 Hz, 1H), 7.34 (tt, J = 1.2, 7.2 Hz, 1H), 7.29 (d, J = 7.6 Hz, 1H), 7.23 (m, 2H), 6.89 (td, J = 0.8, 7.6 Hz, 1H), 6.84 (d, J = 8.0 Hz, 1H), 6.56 (s, 1H), 4.41 (d, J = 6.0 Hz, 2H), 3.82 (s, 3H), 3.58 (t, J = 4.8 Hz, 2H), 3.56 (s, 2H), 3.46 (t, J = 4.8 Hz, 2H), 2.64 (t, J = 6.8 Hz, 2H), 2.52 (t, J = 6.8 Hz, 2H), 2.44 (t, J = 4.8 Hz, 2H), 2.40 ppm (t, J = 5.2 Hz, 2H); MS (ESI): m/z 472 $[M+H]^+$; HRMS (ESI): m/z $[M+H]^+$ calcd for $C_{29}H_{33}N_3O_3$: 472.2522, observed: 472.2568.

***N*-[(2,5-Dimethoxyphenyl)methyl]-5-oxo-5-{4-[(3-phenylphenyl)-methyl]piperazin-1-yl}pentanamide (D23)**: Prepared according to general procedure IX from **10d** and (2,5-dimethoxyphehyl)methanamine (62%): HPLC: 99.01%, t_R = 1.574 min; ^{1}H NMR (400 MHz, $CDCl_3$): δ = 7.61 (m, 1H), 7.58 (m, 1H), 7.54 (s, 1H), 7.50 (dt, J = 1.2, 7.6 Hz, 1H), 7.43 (t, J = 7.2 Hz, 2H), 7.39 (m, 1H), 7.32–7.36 (m, 1H), 7.29 (d, J = 7.6 Hz, 1H), 6.83 (d, J = 2.8 Hz, 1H), 6.71–6.76 m, 2H), 6.36 (s, 1H), 4.38 (d, J = 5.6 Hz, 2H), 3.77 (s, 3H), 3.71 (s, 3H), 3.59 (t, J = 4.8 Hz, 2H), 3.56 (s, 2H), 3.42 (t, J = 4.8 Hz, 2H), 2.41 (t, J = 4.8 Hz, 4H), 2.35 (t, J = 7.2 Hz, 2H), 2.26 (t, J = 7.2 Hz, 2H), 1.90–1.97 ppm (m, 2H); MS (ESI): m/z 516 $[M+H]^+$; HRMS (ESI): m/z $[M+H]^+$ calcd for $C_{31}H_{37}N_3O_4$: 516.2784, observed: 516.2839.

***N*-[(2-Methoxyphenyl)methyl]-5-oxo-5-{4-[(3-phenylphenyl)methyl]piperazin-1-yl}pentanamide (D24)**: Prepared according to general procedure IX from **10d** and (2-methoxyphehyl)methanamine (75%): HPLC: 98.80%, t_R = 1.631 min; ^{1}H NMR (400 MHz, $CDCl_3$): δ = 7.61 (m, 1H), 7.58–7.59 (m, 1H), 7.54 (m, 1H), 7.49–7.51 (dt, J = 2.8, 7.6 Hz, 1H), 7.44 (t, J = 8.0 Hz, 2H), 7.39 (t, J = 7.6 Hz, 1H), 7.32–7.37 (m, 1H), 7.28 (d, J = 7.6 Hz, 1H), 7.23–7.25 (m, 1H), 7.20–7.22 (m, 1H), 6.86–6.90 (m, 1H), 6.83 (d, J = 8.0 Hz, 1H), 6.32 (t, J = 8.0 Hz, 1H), 4.42 (d, J = 6.0 Hz, 2H), 3.82 (s, 3H), 3.59 (t, J = 4.8 Hz, 2H), 3.56 (s, 2H), 3.41 (t, J = 4.8 Hz, 2H), 2.41 (t, J = 4.8 Hz,

4H), 2.34 (t, $J=7.2$ Hz, 2H), 2.25 (t, $J=6.8$ Hz, 2H), 1.89–1.96 ppm (m, 2H); MS (ESI): *m/z* 486 $[M+H]^+$; HRMS (ESI): *m/z* $[M+H]^+$ calcd for $C_{30}H_{35}N_3O_3$: 486.2678, observed: 486.2785.

General procedure X for the synthesis of D25–D26: **2-({4-[(3-Phenylphenyl)methyl]piperazin-1-yl}carbonyl)-*N*-(3,4,5-trimethoxyphenyl)benzamide (D25)**: Isobenzofuran-1,3-dione (1.1 mmol) was added to a mixture of **2b** (1.0 mmol) in CH_2Cl_2 (3 mL). After heating to 40 °C overnight, the starting material disappeared as monitored by TLC. The reaction mixture was concentrated in vacuo to give crude compound **6**. HATU (1.5 mmol) and DIPEA (1.5 mmol) was added to a solution of **6** (1 mmol) in dry DMF. After stirring at −10 °C for 30 min, 3,4,5-trimethoxyaniline (1.2 mmol) was added, and the reaction mixture was stirred at −10 °C for 2 h and then warmed to RT and stirred overnight. The solvent was evaporated in vacuo and the mixture was diluted with H_2O (100 mL) and extracted with CH_2Cl_2. The organic phases were washed with saturated $NaHCO_3$ and brine, dried over Na_2SO_4, filtered and concentrated in vacuo. The crude compound was purified by chromatography with CH_2Cl_2/CH_3OH (30:1 *v/v*) to afford **D25** as a yellow oil (414 mg, 72%): HPLC: 100%, $t_R=1.615$ min; ^{1}H NMR (400 MHz, $CDCl_3$): $\delta=$ 8.97 (s, 1H), 7.88 (d, $J=5.6$ Hz, 1H), 7.58 (s, 1H), 7.55 (s, 1H), 7.49–7.50 (m, 2H), 7.48 (m,2H), 7.43 (m, 2H), 7.32–7.39 (m, 2H), 7.21–7.23 (m, 2H), 6.96 (s, 2H), 3.88 (s, 6H), 3.83 (s, 3H), 3.47 (s, 2H), 3.23 (s, 2H), 2.35 (br s, 4H), 1.59 ppm (s, 2H); MS (ESI): *m/z* 566 $[M+H]^+$; HRMS (ESI): *m/z* $[M+H]^+$ calcd for $C_{34}H_{35}N_3O_5$: 566.2577, observed: 566.2650.

***N*-(2,4-Dimethoxyphenyl)-2-({4-[(3-phenylphenyl)methyl]piperazin-1-yl}carbonyl)benzamide (D26)**: Prepared according to general procedure X from 2,4-dimethoxyaniline (60%): HPLC: 100%, $t_R=$ 2.192 min; ^{1}H NMR (400 MHz, $CDCl_3$): $\delta=8.71$ (s, 1H), 8.23 (d, $J=$ 3.2 Hz, 1H), 7.78–7.81 (dd, $J=1.6$, 7.2 Hz, 1H), 7.56–7.59 (m, 2H), 7.51–7.54 (m, 2H), 7.48 (d, $J=1.2$ Hz, 2H), 7.43–7.46 (d, $J=7.2$ Hz, 2H), 7.41 (t, $J=8.4$ Hz, 1H), 7.31–7.36 (m, 3H), 6.82 (d, $J=8.8$ Hz, 1H), 6.61–6.65 (dd, $J=3.2$, 9.2 Hz, 1H), 3.84 (s, 3H), 3.83 (s, 3H), 3.47 (s, 2H), 3.25 (t, $J=6.0$ Hz, 2H), 2.37 (t, $J=6.8$ Hz, 4H), 1.57 ppm (s, 2H); MS (ESI): *m/z* 536 $[M+H]^+$; HRMS (ESI): *m/z* $[M+H]^+$ calcd for $C_{33}H_{33}N_3O_4$: 536.2471, observed: 536.2511.

^{1}H NMR spectra of all target compounds, that is, **A1**–**A26**, **B1**–**B17**, **C1**–**C12**, and **D1**–**D26**, are given in the Supporting Information.

Binding assay

A fluorescence polarization (FP)-based assay was employed in this study to measure the binding affinities of small-molecule compounds to three antiapoptotic Bcl-2 family proteins, including Mcl-1, Bcl-x_L, and Bcl-2. A 26-residue peptide truncated from the BH3 domain of the Bid protein (QEDIIRNIARHLAQVGDSMDRSIPPG) was modified by adding 5-carboxyfluorescein (5-FAM) on the N terminus, which was used as the fluorescence tracer in this assay. In each measurement, the target protein was incubated with the Bid-BH3 peptide first, and then the competitive binding of the given compound was characterized quantitatively by monitoring the changes in FP signals upon the addition of the compound at different doses. This assay has been applied successfully in our previous studies on Bcl-2 family protein inhibitors.[48,49] Details on the preparation of the protein samples and experimental settings used in FP measurement can be found in our recent publication.[49]

In this study, each compound was initially screened at three concentrations (i.e., 1 μM, 10 μM, and 50 μM), against all three target proteins (Mcl-1, Bcl-x_L, and Bcl-2). At each concentration, the average fluorescence polarization value (*FP* in mP units) of three parallel measurements was used to compute the inhibition ratio using Equation (1).

$$\text{Inhibition}(\%) = \frac{FP_{max} - FP_{test}}{FP_{max} - FP_{NC}} \quad (1)$$

Here, FP_{max} refers to the *FP* value detected when the protein was incubated with the Bid-BH3 peptide, FP_{NC} refers to the *FP* value detected from the negative control, that is, the Bid-BH3 peptide alone, and FP_{test} refers to the *FP* value detected when the test compound was added at a certain concentration. If the test compound showed obvious dose-dependent competitive binding to the target protein and achieved an inhibition ratio over 50% at 50 μM, it was further tested at seven different concentrations (i.e., 1 nM, 10 nM, 100 nM, 1 μM, 10 μM, 50 μM and 100 μM) to obtain a complete dose-dependent binding curve. The binding curve was derived through nonlinear fitting using GraphPad Prism software (version 5). The concentration of the given compound at which 50% of the bound peptide was displaced (IC_{50}) was derived from the binding curve. The competitive inhibition constant (K_i) of the test compound was calculated with a mathematical equation developed by Wang et al.[50] assuming that it formed a binary complex with the target protein.

Heteronuclear single quantum coherence (HSQC) NMR

The Bcl-x_L protein used for this purpose was a special truncated construction of the full-length protein, with deletion of residues 45–84 on a long-loop region and residues 210–233 at the C terminus. An 8×His tag was added to the N terminus. The corresponding sequence was cloned into the pSJ2 vector (a modified vector based on pET28a) at the EcoRI and XhoI sites, using the following oligonucleotides: 5′-TCTCGAATTCATGTCTCAGAGCAACCGGGA-3′ and 5′-GGTCCTCGAGTCAGCGTTCCTGGCCCTTTCG-3′. The protein was expressed in *E. coli* BL21(DE3) cells. Cells were grown at 37 °C in M9 medium containing ^{15}N-NH_4Cl and ampicillin (1 mM) to an OD_{600} 0.6. Protein expression was induced by IPTG (0.4 mM) at 20 °C for 16 h. Cells were lysed in Tris-HCl (25 mM, pH 7.0) containing NaCl (100 mM) and PMSF (0.1 mg mL^{-1}). ^{15}N-labeled His-TEV-Bcl-x_L protein was purified from the soluble fraction using Ni-NTA resin (Qiagen). The ^{15}N-labeled His-TEV-Bcl-x_L protein was further cleaved by TEV protease (0.5 mg mL^{-1}, 4 °C, 12 h) to obtain ^{15}N-labeled Bcl-x_L protein. Then, the ^{15}N-labeled Bcl-x_L protein was purified on Superdex75 (GE Healthcare) in phosphate-buffered saline (PBS).

^{15}N-Heteronuclear single quantum correlation (HSQC) NMR spectra were recorded on a Bruker DMX 600 MHz NMR spectrometer at 25 °C with samples containing 200–500 μM of the ^{15}N-labeled protein. The ratio of each tested compound and the Bcl-x_L protein in the sample was 1:1. The resulting NMR spectra were processed with the nmrPipe software and analyzed with the Spark software (version 3). The HSQC spectrum of free Bcl-x_L, which is publicly available from the Biological Magnetic Resonance Data Bank (http://www.bmrb.wisc.edu/, BMRB ID: 18250), was adopted as the reference for assignment of chemical shifts.

In this study, compound **D11** was selected to be tested using the protocols described above. ABT-737, which is known to bind to the BH3 binding groove on Bcl-x_L, was also tested as a reference.

Fragment-based design and molecular modeling

We recently developed a computational algorithm for mining the so-called characteristic interaction patterns (CIPs) on protein–pro-

tein binding interfaces.[46] By definition, such a pattern is a cluster of four interacting residues, which is conserved across different protein–protein complexes. Our survey revealed that such patterns are related to the "hot spot" regions with a significant probability. Based on such information, small-molecule binders to a protein–protein binding interface can be designed through a fragment-based strategy. It can be done by finding protein-ligand complexes sharing the same CIPs with the given target protein–protein complex. For a pair of matched CIPs, the binding partner in the former case (i.e., a chemical fragment) resembles the binding partner in the latter case, that is, an amino acid residue (the "anchor"). If multiple CIPs exist on the given protein–protein binding interface, assembling matched chemical fragments will yield complete ligand molecules (Figure 2).

To achieve this goal, an extensive library of protein–ligand and protein–protein complex structures is needed. The Protein Data Bank (PDB)[47] is a good resource for this purpose. We downloaded the entire PDB (a total of 78235 structures as released in January 2012) from the RCSB web site (http://www.rcsb.org/), which includes over 25000 valid protein–ligand complex structures. To reduce redundancy, these protein–ligand complexes were clustered by sequence alignment of the protein molecules in them. The sequence similarity cutoff used in clustering was set to 90%. Then, the ligand molecule in each complex was dissected into fragments with an in-house computer program. The rules in fragmentation were as follows: (1) a substructure containing a single ring or fused rings was defined as a fragment; (2) four continuous heavy atoms on a chain were defined as a fragment; (3) any isolated atom or group was merged into the nearest fragment. All of the resulting fragments were further filtered by the "rules of three", that is, molecular weight $\leq$300, number of hydrogen-bond donors $\leq$3, number of hydrogen-bond acceptors $\leq$3 and computed log*P* value $\leq$3, to keep the valid ones. At the next stage, the pattern mining algorithm developed by us was applied to all remaining fragments in the protein–ligand complex library to detect their interacting residues on the protein side. If the interacting residues found for a certain fragment match a certain CIP on the given protein–protein binding interface, that fragment was retrieved as a candidate.

Bcl-2 family proteins execute their biological functions in apoptosis through binding to BH3-only proteins. In order to identify the CIPs on their binding interfaces, a number of complex structures formed between Bcl-x_L or Mcl-1 protein and BH3-only peptides were analyzed. As for the complexes formed between Bcl-x_L and BH3-peptides, PDB IDs 1PQ1, 2BZW, 2P1L, 2XA0, 2YJ1, 2YQ6, 2YQ7, 3FDL, 3IO8, 3P17, and 3R85 were considered; whereas for the complexes formed between Mcl-1 and BH3-peptides, PDB IDs 2NL9, 2PQK, 3D7V, 3IO9, 3KJ0, 3KJ1, 3KJ2, 3KZ0, 3MK8, 3PK1, and 4G35 were considered. All of the CIPs identified on the protein–protein binding interfaces in these complexes were used as queries to search our library of protein–ligand complexes. All fragment-residue interaction patterns included in this library were compared to the CIP queries with computer programs, by which they were superimposed with the CIP queries in pairs, and the root-mean-square deviation (RMSD) values between them were calculated. The hits for each query were sorted by their RMSD values in an ascending order. The top 30 hits for each query were examined visually. If a chemical fragment matched in terms of both spatial and chemical properties with the "anchor" residue in the given CIP query, it was considered as an appropriate candidate. Because we divided the binding groove on Bcl-x_L or Mcl-1 into three subsites, that is, P-site, Q-site, and L-site (Figure 3), those candidate fragments were assigned to these subsites according to their partner residues in related hot-spot regions. Finally, four series of molecules were manually designed by adding some synthetically feasible "linkers" to connect the selected fragments for each subsite (Figure 4).

Molecular docking and molecular dynamics (MD) simulation were employed to derive the possible binding modes to Bcl-x_L and Mcl-1 for the active compounds described in this study. Several compounds, including **A1**, **A15**, **D11**, and **D12**, were selected for this purpose because their chemical structures are representative, and they exhibit good binding affinities and interesting selectivities to Mcl-1. Note that Bcl-2 has a very similar binding site to that of Bcl-x_L, and thus extra modeling targeting Bcl-2 was not performed in our study.

Molecular docking was employed first to derive a rough binding mode of the selected compounds to Bcl-x_L and Mcl-1. The complex structure formed by human Bcl-x_L and ABT-737 (PDB ID: 2YXJ) and the complex structure formed between human Mcl-1 and the Bim-BH3 peptide (PDB ID: 2PQK) was used in this task. The molecular structures of compound **A1**, **A15**, **D11**, and **D12** were sketched with the SYBYL software (version 8.1), and optimized with the MMFF94 force field. Automatic docking of each molecule to Bcl-x_L or Mcl-1 was performed by using the GOLD software (version 5.1, released by Cambridge Crystallographic Data Centre). In each case, a rough binding pose given by manual docking was provided as the input. The binding site considered in docking for Bcl-x_L protein was defined as all amino acid residues within 10 Å from the reference ligand ABT-737. For Mcl-1 protein, the binding site was defined as the amino acid residues within 10 Å from Thr266 in the binding pocket. The GOLD software employs a genetic algorithm (GA) to conduct the docking process. In our study, the key parameters for docking were as follows: the whole population was placed on five separate islands with 100 individuals on each island; total number of GA operations = 100000; probabilities for crossover, mutation and migration operations = 95, 95 and 10, respectively; scoring function = ChemScore. A total of 50 final binding poses were generated for input molecule. These binding poses were further clustered with a RMSD cutoff of 2.0 Å using the "rms_analysis" tool included in the GOLD software package. Among the binding poses with the highest binding score in each cluster, one reasonable binding pose was selected after visual examination. This selection was made also by referring to the known binding mode of ABT-737, since the ^{15}N-HSQC NMR spectrum of compound **D11** suggested that our compounds adopt a binding mode similar to ABT-737.

Binding modes of the selected compounds to Bcl-x_L and Mcl-1 proteins produced by molecular docking were further evaluated by MD simulations using the AMBER program (version 9, released by University of California San Francisco, USA). Each MD simulation was performed in explicit water for 3 ns. To set up each job, the force field parameters applied to the small-molecule ligand were prepared by applying the Antechamber module in AMBER. Atomic partial charges on the small-molecule ligand were derived with the RESP method based on the HF/6-31G* computation results given by the Gaussian software (version 09, released by the Gaussian Inc.). Atoms on the protein were assigned the PARM99 template charges implemented in AMBER, and all ionizable residues were set at the default protonation states at a neutral pH. The complex structure was soaked in a box of TIP3P water molecules with a margin of 10 Å along each dimension. An appropriate number of counter ions were added to neutralize the whole system.

After these preparations, the complex structure was first relaxed by 100 cycles of steepest descent minimization, followed by 4900 cycles of conjugated gradient minimization. After that, the systems were gradually heated up with the Berendsen algorithm from 0 K to 300 K in 100 ps. Then, 3 ns long MD simulation was performed for each complex at a constant temperature of 300 K and a constant pressure of 1 atm. Electrostatic interactions were calculated with the particle mesh Ewald (PME) algorithm. The distance cutoff of nonbonded interactions was set as 12 Å. The SHAKE algorithm was applied to fix the lengths of all chemical bonds connecting hydrogen atoms. All MD simulations were performed on an Intel Xeon 5345-based Linux cluster. The RMSD fluctuations for both the ligand and the entire complex during MD simulation are given in the Supporting Information, where one can see that the binding mode of the given complex had reached a quasi-stable state in most cases after 3 ns simulation. This is perhaps attributed to the fact that our simulation started with a reasonable binding mode. Thus, longer MD simulations were not attempted in our study.

On each resulting MD trajectory, 3000 conformations were retrieved at an interval of 1 ps. The MMTSB tool implemented in the AMBER package was used to group these conformations into several clusters based on the mass-weighted RMSD values. The cluster cutoff was set as 1.2 Å. Finally, the conformation closest to the cluster center in the largest cluster was selected as the representative binding mode. The final binding modes of the selected compounds to Bcl-x_L and Mcl-1 are shown in Figure 6 and 7. Other renders of the same set of binding modes are given in the Supporting Information.

Acknowledgements

We gratefully acknowledge financial support from the National Natural Science Foundation of China (Grant No. 91229204 and 81025017 to Prof. Liu and Grant No. 81172984, 21072213, and 21002117 to Prof. Wang). We also thank Prof. Chunyang Cao's group at the Shanghai Institute of Organic Chemistry for their technical supports in obtaining the ^{15}N-HSQC spectra reported in this study.

Keywords: apoptosis · bcl-2 family proteins · protein–protein interactions · selective inhibitors

[1] J. C. Reed, *Nat. Rev. Drug Discovery* **2002**, *1*, 111 – 121.
[2] S. W. Fesik, *Nat. Rev. Cancer* **2005**, *5*, 876 – 885.
[3] M. H. Andersen, J. C. Becker, P. T. Straten, *Nat. Rev. Drug Discovery* **2005**, *4*, 399 – 409.
[4] A. Vazquez, E. E. Bond, A. J. Levine, G. L. Bond, *Nat. Rev. Drug Discovery* **2008**, *7*, 979 – 987.
[5] T. G. Cotter, *Nat. Rev. Cancer* **2009**, *9*, 501 – 507.
[6] S. Cory, J. M. Adams, *Nat. Rev. Cancer* **2002**, *2*, 647 – 656.
[7] G. Lessene, P. E. Czabotar, P. M. Colman, *Nat. Rev. Drug Discovery* **2008**, *7*, 989 – 1000.
[8] A. Ashkenazi, *Nat. Rev. Drug Discovery* **2008**, *7*, 1001 – 1012.
[9] T. Oltersdorf, S. W. Elmore, A. R. Shoemaker, R. C. Armstrong, D. J. Augeri, B. A. Belli, M. Bruncko, T. L. Deckwerth, J. Dinges, P. J. Hajduk, *Nature* **2005**, *435*, 677 – 681.
[10] C.-M. Park, M. Bruncko, J. Adickes, J. Bauch, H. Ding, A. Kunzer, K. C. Marsh, P. Nimmer, A. R. Shoemaker, X. Song, *J. Med. Chem.* **2008**, *51*, 6902 – 6915.
[11] C. Tse, A. R. Shoemaker, J. Adickes, M. G. Anderson, J. Chen, S. Jin, E. F. Johnson, K. C. Marsh, M. J. Mitten, P. Nimmer, *Cancer Res.* **2008**, *68*, 3421 – 3428.
[12] S. Kitada, M. Leone, S. Sareth, D. Zhai, J. C. Reed, M. Pellecchia, *J. Med. Chem.* **2003**, *46*, 4259 – 4264.
[13] B. Becattini, S. Kitada, M. Leone, E. Monosov, S. Chandler, D. Zhai, T. J. Kipps, J. C. Reed, M. Pellecchia, *Chem. Biol.* **2004**, *11*, 389 – 395.
[14] M. Nguyen, R. C. Marcellus, A. Roulston, M. Watson, L. Serfass, S. M. Madiraju, D. Goulet, J. Viallet, L. Bélec, X. Billot, *Proc. Natl. Acad. Sci. USA* **2007**, *104*, 19512 – 19517.
[15] J.-L. Wang, D. Liu, Z.-J. Zhang, S. Shan, X. Han, S. M. Srinivasula, C. M. Croce, E. S. Alnemri, Z. Huang, *Proc. Natl. Acad. Sci. USA* **2000**, *97*, 7124 – 7129.
[16] A. Degterev, A. Lugovskoy, M. Cardone, B. Mulley, G. Wagner, T. Mitchison, J. Yuan, *Nat. Cell Biol.* **2001**, *3*, 173 – 182.
[17] G. Wang, Z. Nikolovska-Coleska, C.-Y. Yang, R. Wang, G. Tang, J. Guo, S. Shangary, S. Qiu, W. Gao, D. Yang, *J. Med. Chem.* **2006**, *49*, 6139 – 6142.
[18] G. Tang, Z. Nikolovska-Coleska, S. Qiu, C.-Y. Yang, J. Guo, S. Wang, *J. Med. Chem.* **2008**, *51*, 717 – 720.
[19] L. Wang, D. T. Sloper, S. N. Addo, D. Tian, J. W. Slaton, C. Xing, *Cancer Res.* **2008**, *68*, 4377 – 4383.
[20] J. Wei, S. Kitada, M. F. Rega, J. L. Stebbins, D. Zhai, J. Cellitti, H. Yuan, A. Emdadi, R. Dahl, Z. Zhang, *J. Med. Chem.* **2009**, *52*, 4511 – 4523.
[21] J. Wei, J. L. Stebbins, S. Kitada, R. Dash, W. Placzek, M. F. Rega, B. Wu, J. Cellitti, D. Zhai, L. Yang, *J. Med. Chem.* **2010**, *53*, 4166 – 4176.
[22] Y. Feng, X. Ding, T. Chen, L. Chen, F. Liu, X. Jia, X. Luo, X. Shen, K. Chen, H. Jiang, *J. Med. Chem.* **2010**, *53*, 3465 – 3479.
[23] Z. Zhang, G. Wu, F. Xie, T. Song, X. Chang, *J. Med. Chem.* **2011**, *54*, 1101 – 1105.
[24] B. E. Sleebs, P. E. Czabotar, W. J. Fairbrother, W. D. Fairlie, J. A. Flygare, D. C. Huang, W. J. Kersten, M. F. Koehler, G. Lessene, K. Lowes, *J. Med. Chem.* **2011**, *54*, 1914 – 1926.
[25] H. Zhou, A. Aguilar, J. Chen, L. Bai, L. Liu, J. L. Meagher, C.-Y. Yang, D. McEachern, X. Cong, J. A. Stuckey, *J. Med. Chem.* **2012**, *55*, 6149 – 6161.
[26] J. Chen, H. Zhou, A. Aguilar, L. Liu, L. Bai, D. McEachern, C.-Y. Yang, J. L. Meagher, J. A. Stuckey, S. Wang, *J. Med. Chem.* **2012**, *55*, 8502 – 8514.
[27] H. L. Perez, P. Banfi, J. Bertrand, Z.-W. Cai, J. W. Grebinski, K. Kim, J. Lippy, M. Modugno, J. Naglich, R. J. Schmidt, *Bioorg. Med. Chem. Lett.* **2012**, *22*, 3946 – 3950.
[28] A. Friberg, D. Vigil, B. Zhao, R. N. Daniels, J. P. Burke, P. M. Garcia-Barrantes, D. Camper, B. A. Chauder, T. Lee, E. T. Olejniczak, S. W. Fesik, *J. Med. Chem.* **2013**, *56*, 15 – 30.
[29] A. Aguilar, H. Zhou, J. Chen, L. Liu, L. Bai, D. McEachern, C.-Y. Yang, J. Meagher, J. Stuckey, S. Wang, *J. Med. Chem.* **2013**, *56*, 3048 – 3067.
[30] G. Lessene, P. E. Czabotar, B. E. Sleebs, K. Zobel, K. N. Lowes, J. M. Adams, J. B. Baell, P. M. Colman, K. Deshayes, W. J. Fairbrother, J. A. Flygare, P. Gibbons, W. J. A. Kersten, S. Kulasegaram, R. M. Moss, J. P. Parisot, B. J. Smith, I. P. Street, H. Yang, D. C. S. Huang, K. G. Watson, *Nat. Chem. Biol.* **2013**, *9*, 390 – 397.
[31] M. F. van Delft, A. H. Wei, K. D. Mason, C. J. Vandenberg, L. Chen, P. E. Czabotar, S. N. Willis, C. L. Scott, C. L. Day, S. Cory, *Cancer Cell* **2006**, *10*, 389 – 399.
[32] L. Fu, Y.-A. Kim, X. Wang, X. Wu, P. Yue, S. Lonial, F. R. Khuri, S.-Y. Sun, *Cancer Res.* **2009**, *69*, 8967 – 8976.
[33] M. Konopleva, R. Contractor, T. Tsao, I. Samudio, P. P. Ruvolo, S. Kitada, X. Deng, D. Zhai, Y.-X. Shi, T. Sneed, *Cancer Cell* **2006**, *10*, 375 – 388.
[34] C. Skoda, B. M. Erovic, V. Wachek, L. Vormittag, F. Wrba, H. Martinek, G. Heiduschka, P. Kloimstein, E. Selzer, D. Thurnher, *Oncol. Rep.* **2008**, *19*, 1499 – 1503.
[35] W. Sieghart, D. Losert, S. Strommer, D. Cejka, K. Schmid, S. Rasoul-Rockenschaub, M. Bodingbauer, R. Crevenna, B. P. Monia, M. Peck-Radosavljevic, *J. Hepatol.* **2006**, *44*, 151 – 157.
[36] R. J. Youle, A. Strasser, *Nat. Rev. Mol. Cell Biol.* **2008**, *9*, 47 – 59.
[37] D. J. Veis, C. M. Sorenson, J. R. Shutter, S. J. Korsmeyer, *Cell* **1993**, *75*, 229 – 240.
[38] N. Motoyama, F. Wang, K. A. Roth, H. Sawa, K.-i. Nakayama, K. Nakayama, I. Negishi, S. Senju, Q. Zhang, S. Fujii, *Science* **1995**, *267*, 1506 – 1510.
[39] J. L. Rinkenberger, S. Horning, B. Klocke, K. Roth, S. J. Korsmeyer, *Gene Dev.* **2000**, *14*, 23 – 27.
[40] K. L. Loveland, L. Gibson, T. Meehan, A. Stylianou, N. Wreford, D. de Kretser, D. Metcalf, F. Köntgen, J. M. Adams, S. Cory, *Proc. Natl. Acad. Sci. USA* **1998**, *95*, 12424 – 12431.

[41] B. A. Quinn, R. Dash, B. Azab, S. Sarkar, S. K. Das, S. Kumar, R. A. Oyesanya, S. Dasgupta, P. Dent, S. Grant, *Expert Opin. Invest. Drugs* **2011**, *20*, 1397 – 1411.
[42] M. R. Arkin, J. A. Wells, *Nat. Rev. Drug Discovery* **2004**, *3*, 301 – 317.
[43] L. Zhao, J. Chmielewski, *Curr. Opin. Struct. Biol.* **2005**, *15*, 31 – 34.
[44] J. A. Wells, C. L. McClendon, *Nature* **2007**, *450*, 1001 – 1009.
[45] V. Azzarito, K. Long, N. S. Murphy, A. J. Wilson, *Nat. Chem.* **2013**, *5*, 161 – 173.
[46] Y. Li, Z. Liu, L. Han, C. Li, R. Wang, *J. Chem. Inf. Model.* **2013**, *53*, 2437 – 2447.
[47] H. M. Berman, J. Westbrook, Z. Feng, G. Gilliland, T. Bhat, H. Weissig, I. N. Shindyalov, P. E. Bourne, *Nucleic Acids Res.* **2000**, *28*, 235 – 242.
[48] B. Zhou, X. Li, Y. Li, Y. Xu, Z. Zhang, M. Zhou, X. Zhang, Z. Liu, J. Zhou, C. Cao, *ChemMedChem* **2011**, *6*, 904 – 921.
[49] Y. Xu, M. Zhou, Y. Li, C. Li, Z. Zhang, B. Yu, R. Wang, *ChemMedChem* **2013**, *8*, 1345 – 1352.
[50] Z. Nikolovska-Coleska, R. Wang, X. Fang, H. Pan, Y. Tomita, P. Li, P. P. Roller, K. Krajewski, N. G. Saito, J. A. Stuckey, *Anal. Biochem.* **2004**, *332*, 261 – 273.

Received: July 19, 2013
Published online on October 9, 2013